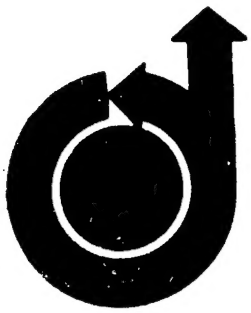

80-0431

Effects of Wind Tunnel Disturbances on Boundary-Layer Transition with Emphasis on Radiated Noise: A Review

Samuel R. Pate, *ARO, Inc., AEDC Division*
Arnold Air Force Station, Tennessee

11th AERODYNAMIC TESTING CONFERENCE

Colorado Springs, Colorado/March 18-20, 1980

EFFECTS OF WIND TUNNEL DISTURBANCES ON BOUNDARY-LAYER TRANSITION WITH EMPHASIS ON RADIATED NOISE: A REVIEW*

(Invited Paper)

Samuel R. Pate**
ARO, Inc., AEDC Division
A Sverdrup Corporation Company
Arnold Air Force Station, Tennessee 37389

Abstract

Effects of wind tunnel free-stream disturbances on boundary-layer transition are reviewed. Experimental results show that free-stream disturbances dominate the transition process as determined by the experimentally measured transition Reynolds numbers on simple geometries (flat plates and sharp cones). Principal modes of disturbance are turbulence ($\tilde{u}/U_\infty$) and acoustic sound ($\tilde{p}/q_\infty$) at subsonic speeds; hole/slot acoustic resonance at transonic speeds ($\tilde{p}/q_\infty$); and tunnel wall turbulent-boundary-layer radiated noise at supersonic-hypersonic speeds ($\tilde{p}/q_\infty$). Data correlations and resulting empirical equations that show the direct relationship between transition Reynolds numbers and free-stream disturbance levels are presented and discussed.

1.0 Introduction

Figure 1 illustrates overall publication levels and trends of transition research during the last 40 years. Studies into the basic mechanisms contributing to boundary-layer instability and transition have been reported in Refs. 1 through 10. Experimental studies of transition Reynolds numbers at subsonic-transonic, supersonic-hypersonic Mach numbers have been reported in Refs. 7 through 39. Correlation and semi-empirical methods for predicting the occurrence of transition have been reported in Refs. 5 and 6, 14 through 18, 22 through 28, and 37 through 50.

The widespread interest in transition research can be attributed to two basic scientific and engineering groups: (1) academia and (2) developers of flight vehicles. The complex mathematical and fluid-mechanics process inherent in the boundary-layer transition process offers a challenge unsurpassed in the history of fluid mechanics. From the practical viewpoint of aircraft and missile design, the location of transition (as illustrated in Fig. 2) is a major factor that can often have a first order effect on skin-friction drag, surface heat-transfer rates, flow separation and surface pressure distributions, extent of shock boundary-layer interactions, flow separation and control effectiveness, unsteady flow phenomena, vehicle stability and control, surface pressure fluctuations, structural fatigue, acoustic noise, and others.

Although the boundary-layer transition phenomenon has received widespread attention, the transition process is still not completely understood. Specifically, today, there is no single theoretical or empirical method that will predict the onset of transition under typical conditions that exist in flight or in ground test facilities. A. M. O. Smith (1972)[51] commented on the current state of being able to predict, in general, the occurrence of boundary-layer transition. Presented in Fig. 3 is Smith's qualitative assessment of the percentage of time that a prediction would be about 90 to 95% correct. Note that in 1972 (after 90 years of transition research), the understanding of the transition process rated only about 15% on predictability as compared to the laminar-turbulent boundary-layer understanding level of about 85 to 90%. Even today, the curve of Smith can only be extended a modest amount as suggested by the dashed extension in Fig. 3. Figure 3 provides some appreciation for the complexity of the transition process.

As indicated in Fig. 1, the study of boundary-layer transition, particularly at high speeds, has been an area of very active research during the last 25 years. Beginning in the late 1960's and continuing into the late 1970's, studies of free-stream disturbance effects on the boundary-layer transition Reynolds numbers has been the focal point of transition research.

In particular, the effects of free-stream disturbances on boundary-layer transition at transonic-supersonic-hypersonic Mach numbers have been of world wide interest in recent years.

The purpose of this paper is to provide a general review and summary of the effects of free-stream disturbance on boundary-layer transition Reynolds numbers (Re_t) in wind tunnels. Types of free-stream disturbances in wind tunnels (subsonic-transonic-supersonic and hypersonic) will be discussed with special attention devoted to radiated acoustic noise disturbance levels in supersonic and hypersonic wind tunnels. Dominance of free-stream disturbances on the transition process will be shown. Correlation of transition Reynolds numbers (Re_t) with disturbance levels will be reviewed, and various Re_t prediction techniques (including limitations and application) will be discussed. Recent transonic-supersonic flight data published by Dougherty[26] are also included.

Most of the material presented in this paper was published by the author in Ref. 50. Indepth discussion, definitions, and descriptions of test models, test apparatus, test techniques, and test facilities are included in Ref. 50. Much of the transition and disturbance data included in Ref. 50 are presented in chronological format and grouped according to contributing nations and organizations.

*The research reported herein was performed by the Arnold Engineering Development Center (AEDC), Air Force Systems Command (AFSC). Work and analysis for this research was conducted by personnel of ARO, Inc., a Sverdrup Corporation Company, operating contractor of AEDC. Further reproduction is authorized to satisfy needs of the U. S. Government.

**Director, Propulsion Wind Tunnel Facility (PWT).

REPORT DOCUMENTATION PAGE

Form Approved OMB No. 0704-0188

1. REPORT DATE *(DD-MM-YYYY)*	2. REPORT TYPE	3. DATES COVERED *(From - To)*
01/03/1980	Conference Paper	

4. TITLE AND SUBTITLE
Effects of Wind Tunnel Disturbances on Boundary-Layer Transition with Emphasis on Radiated Noise: A Review

5a. CONTRACT NUMBER

5b. GRANT NUMBER

5c. PROGRAM ELEMENT NUMBER

6. AUTHOR(S)
Samuel R. Pate

5d. PROJECT NUMBER

5e. TASK NUMBER

5f. WORK UNIT NUMBER

7. PERFORMING ORGANIZATION NAME(S) AND ADDRESS(ES)
ARO, Inc., AEDC Division
Arnold Air Force Station,
Tennessee

8. PERFORMING ORGANIZATION REPORT NUMBER
AIAA Paper 80-0431

9. SPONSORING / MONITORING AGENCY NAME(S) AND ADDRESS(ES)
Air Force Systems Command

10. SPONSOR/MONITOR'S ACRONYM(S)

11. SPONSOR/MONITOR'S REPORT NUMBER(S)

12. DISTRIBUTION / AVAILABILITY STATEMENT
unclassified, distribution unlimited

13. SUPPLEMENTARY NOTES
This AIAA Paper missed the usual archiving. Supplied by S.P. Schneider, Purdue Univ., 9/00, from a copy provided by Ken Stetson, one of the meeting organizers.

14. ABSTRACT
Effects of wind tunnel free-stream disturbances on boundary layer transition are reviewed. Experimental results show that free-stream disturbances dominate the transition process as determined by the experimentally measured transition Reynolds numbers on simple geometries (flat plates and sharp cones). Principal modes of disturbance are turbulence and acoustic sound at subsonic speeds; hole/slot acoustic resonance at transonic speeds; and tunnel wall turbulent-boundary-layer radiated noise at supersonic-hypersonic speeds. Data correlations and resulting empirical equations that show direct relationship between transition Reynolds numbers and free-stream disturbance levels are presented and discussed.

15. SUBJECT TERMS
transonic supersonic hypersonic wind tunnels, laminar-turbulent transition

16. SECURITY CLASSIFICATION OF:			17. LIMITATION OF ABSTRACT	18. NUMBER OF PAGES	19a. NAME OF RESPONSIBLE PERSON
a. REPORT unclassified	b. ABSTRACT unclassified	c. THIS PAGE unclassified	none	46	S.P. Schneider
					19b. TELEPHONE NUMBER *(include area code)* 765-494-3343

2.0 Wind Tunnel Disturbances

Kovasznay (1953)[52] theoretically identified three possible disturbance sources in wind tunnels: (a) vorticity fluctuations (turbulence), $\tilde{u}$; (b) entropy fluctuations (or temperature spottiness), $\tilde{T}$; and (c) sound waves, $\tilde{p}$. Vorticity and entropy fluctuations are essentially covected along streamlines and are traceable to conditions in the settling chamber. Sound disturbances can travel across streamlines and consequently can originate in the stilling chamber and from the boundaries of the test section. The turbulent boundary layer (shear layer) on the tunnel wall is also a source for radiating sound (acoustic noise) disturbances. The three fundamental and distinctly different types of free-stream disturbance modes can exist independently in compressible flow wind tunnel facilities as illustrated in Fig. 4. The disturbances are propagated into the free stream, sustained in their original mode form and then transmitted by the test gas over the test article. Vorticity ($\tilde{u}$) and acoustic noise ($\tilde{p}$ disturbances are present, at varying intensity levels, in all wind tunnels. Disturbances $\tilde{u}$ and $\tilde{p}$ can be of significant magnitude, depending on the Mach number range, to cause first order effects, and in many cases a dominating effect on the transition process and transition Reynolds number (Re_t) on wind tunnel test models. There are no data to date, to the author's knowledge, that establish entropy fluctuations ($\tilde{T}$) as having a significant (first-order) effect on the transition process.

This section will discuss the spectra and intensity levels of the three disturbance modes ($\tilde{u}$, $\tilde{p}$, $\tilde{T}$) in subsonic, transonic, and supersonic-hypersonic wind tunnels. Correlations of boundary-layer transition with disturbance intensities will be presented in Section 5.0.

Subsonic Tunnel Disturbances

Free-stream disturbances in subsonic aerodynamic wind tunnels are typically of two general types: (1) turbulence (velocity fluctuations) ($\tilde{u}$) and/or (2) acoustic sound ($\tilde{p}$), Figs. 4 through 7.

Velocity fluctuations (turbulence) ($\tilde{u}$) are generated in the stilling chamber as a result of inlet mass flow separated regions, wakes from flow straightens (honeycombs, screens), support braces, etc., and then convected along streamlines over the test model as illustrated in Fig. 4. Research by Dryden (1936),[53] Hall (1938),[54] Schubauer and Skramstad (1947),[8] Boltz et al. (1960),[55] Spangler and Wells (1968),[56] and Hall and Gibbings (1972),[48] have shown that turbulence intensities ($\tilde{u}/U_\infty$) can be expected to vary from 0.1 to 3.0%, as illustrated in Fig. 5. By proper selection and placing of damping screens in the stilling chamber, the turbulence ($\tilde{u}/U_\infty$) levels can be reduced to values below 0.1%.

Acoustical disturbances can be of the standing wave (organ pipe) type caused by resonance in the test section or traveling acoustic waves (acoustical noise) caused by fan noise, sound generators, etc. Schubauer and Skramstad (1947)[8] found in their wind tunnel studies that for disturbance levels ($\tilde{u}/U_\infty$) less than 0.05%, 90% of the energy was acoustic energy generated by the fan; this is confirmed by the spectra shown in Fig. 6 taken from Ref. 8. The total intensity ($\tilde{u}/U_\infty$) of 0.033% corresponded to a flow velocity of 80 fps. These studies indicated that acoustical sound can account for essentially all the disturbance present in subsonic wind tunnels having very low intensity levels ($\tilde{u}/U_\infty \leq 0.1\%$).

Spangler and Wells (1968)[56] studied the spectra and intensity levels associated with acoustic noise generated by a discrete frequency air-driven rotating-wave sound generator. Intensity levels ($\tilde{u}/U_\infty$) from 0.03 to 0.32% at various fundamental frequencies ranging from 27 to 82 cps were generated.* Typical noise and turbulence spectra for $\tilde{u}/U_\infty = 0.09\%$ (from Ref. 56) are shown in Fig. 6. The presence of the fundamental frequency and several harmonics should be noted in the noise spectra. Turbulence generated by the grid mesh in the stilling chamber produced no discrete frequencies.

The studies of Refs. 8 and 56 have established that the intensity levels of either turbulence ($\tilde{u}$) and/or acoustic noise ($\tilde{p}$) can be significant in subsonic tunnels. To properly identify the free-stream disturbances mode, measurements of intensity and spectra must be made. With proper wind tunnel design, the free-stream disturbance levels can be reduced to intensities less than 0.05%. The effects of discrete frequencies at the same intensity level on boundary-layer transition will be discussed in Section 3.0.

Transonic Tunnel Disturbances

As shown by Uberoi (1956)[57] flow expansion in a wind tunnel nozzle significantly reduces stilling chamber turbulence ($\tilde{u}$), as shown in Fig. 8.

Velocity fluctuations could be significant in a transonic tunnel, but little information has been published to date.

Noise ($\tilde{p}$) attributable to wall hole/slot resonance in porous and/or slotted wall transonic wind tunnels is the dominant source of free-stream disturbance as illustrated by Varner (1973),[58] Fig. 9, and measured by Credle (1970, 1971),[59,60] Dougherty (1974, 1980),[35,36] Owen (1979),[61] and Mabey (1976).[62] These studies documented the intensity levels and spectra from many tunnels located in the USA and Western Europe. Typical transonic aerodynamic noise spectra and intensity measured in a porous wall test section using a microphone mounted on a cone test model are presented in Fig. 10 as taken from Ref. 35.

In general, porous/slotted-wall transonic wind tunnels are classified as very noisy compared to well-designed solid-wall subsonic tunnels. Correlations of Re_t with transonic wind tunnel noise intensity ($\tilde{p}/q_\infty$) will be presented in Section 5.0.

Supersonic-Hypersonic Tunnel Disturbances

Kovasznay (1953)[52] showed that the hot-wire anemometer could be operated in a supersonic flow

---

*Noise levels measured with a microphone (prms) can be converted to equivalent hot-wire measured $\tilde{u}/U_\infty$ values.[55] At U_∞ = 100 fps, a noise level of 105 decibels is equivalent to a turbulence level of 0.028% (u = 0.028 fps), $\tilde{u}/U_\infty = \tilde{p}/\gamma p_\infty M_\infty = 10^{(0.05\ db\ -\ 3.7)}/\gamma pM$.

and the three disturbance modes (vorticity, entropy, and sound) could be represented by the rms output of a hot wire operated at different temperatures. He conducted hot-wire experiments and showed that all three disturbances could be present in supersonic wind tunnels. The presence of entropy fluctuations (temperature spottiness) was confirmed using mode diagram analysis and from direct stilling chamber and free-stream measurements using various types of tunnel air-heating apparatus. A fluctuating pressure field (sound waves) was generated using a weak shock emanating from the leading edge of a sharp flat plate. The oscillating flow field generated by the weak waves produced the proper sound wave mode diagram. Thus the experimental data obtained at $M_\infty = 1.7$ and the analytical models developed by Kovasznay supported his three-mode theory.

Morkovin (1957)[63] discussed the possible sources of free-stream disturbance in supersonic wind tunnels. Following Kovasznay,[52] Morkovin discussed the sources that could produce free-stream disturbances: (1) vorticity fluctuations, (2) entropy fluctuations, and (3) sound waves. He further classified sound waves as: (1) radiation from the wall turbulent boundary layer, (2) shimmering Mach waves from wall roughness or waviness, (3) wall vibrations, and (4) diffraction and scattering of otherwise steady pressure gradients. Morkovin further stated that any of the three principal modes or any of the four specific sound sources could promote early transition if the disturbance levels were high enough. Morkovin (1959)[64] commented further on wind tunnel disturbances. He discussed ways to effectively reduce vorticity fluctuations and entropy fluctuations by proper stilling chamber design. However, he stated that the sound from the turbulent boundary layer would probably be the major disturbance. Morkovin stated that this type of disturbance was very difficult to measure or to predict theoretically. Furthermore, he stated that seemingly little could be done to appreciably reduce its intensity level.

The following paragraphs will discuss in some detail the three possible disturbance modes in supersonic wind tunnels.

Vorticity (turbulence fluctuations) ($\tilde{u}$) will be greatly reduced by the nozzle contraction and resulting flow expansion as shown in Fig. 8. The effects of turbulence ($\tilde{u}$) on transition were investigated at Mach numbers from 1.7 to 4 by Laufer and Marte (1955)[11] by varying the turbulence level in the stilling chamber from 0.6 to 7%. In the low Mach number flow, $M_\infty \lesssim 2.5$, the stilling chamber level was found to have a strong effect on sharp-cone boundary-layer-transition Reynolds numbers; however, no significant effect was noted for $M_\infty \gtrsim 2.5$. Similar experiments were conducted at Mach 1.76 by Morkovin (1957),[63] and no measurable shift in flat-plate transition Reynolds number resulted when the settling chamber turbulence was raised from 0.7 to 4.6%. Van Driest and Boison (1957)[16] also showed that for $M_\infty \gtrsim 2.5$, the stilling chamber turbulence level had no significant effect on sharp-cone transition Reynolds numbers. These data are consistent with the results of Uberoi[57] presented in Fig. 8. Vorticity fluctuations measured at supersonic Mach numbers by Laufer (1961)[65] and Donaldson (1971)[66] have shown that at $M_\infty = 4$, $\tilde{u}/U_\infty$ fluctuations in the test section are only one tenth the value of radiated noise ($\tilde{p}/p_\infty$). The measurements of Donaldson are shown in Fig. 18. Therefore, it is concluded that for $M_\infty \gtrsim 1.0$, velocity fluctuations will have a negligible effect on transition data in well-designed wind tunnels.

Entropy fluctuations (temperature spottiness), $\tilde{T}$, that are present in the test section are traceable to the settling chamber and farther upstream. In the test section, the temperature fluctuations are related isentropically to those in the stilling chamber. Effective means such as the use of mixing sections and screens in the supply passage are used to reduce temperature to small levels in supersonic tunnels as reported by Kovasznay (1953),[52] Laufer (1961,[65] and Donaldson (1971).[66] The measurements of Donaldson are presented in Fig. 18, and the low level of $\tilde{T}/T_\infty$ in a $M_\infty = 4$ wind tunnel should be noted.

Limited studies of the effects of temperature fluctuations on transition locations have been conducted by Brinich (1956)[67] and Ross (1973).[68] Brinich changed T_o from 52° to 176°F at $M_\infty = 3.1$ and found that the transition location on a flat plate was essentially unchanged. Transition measurements were conducted by Ross at $M_\infty = 4$ where T_o was varied from 295 to 434°K, keeping the unit Reynolds number constant, and he found no appreciable change in Re_t data obtained with a hollow-cylinder model. Thus, it is concluded that in well-designed supersonic wind tunnels (i.e., a stilling chamber equipped with proper mixing screens), entropy fluctuations will have a negligible effect on transition data. There is a possibility that in shock tunnels, arc tunnels, and "combustion" type tunnels that the temperature fluctuations ($\tilde{T}$) can affect mean boundary-layer properties and transition. However, transition data from arc tunnels are consistent with conventional tunnel data (see Ref. 50).

Pressure fluctuations ($\tilde{p}$) (radiated aerodynamic noise) is the third type of unsteady disturbance present in supersonic-hypersonic tunnels. Radiated noise is generated by the turbulent boundary layer on the nozzle and test section walls. This disturbance is the major factor affecting transition in supersonic and hypersonic wind tunnels for $M_\infty \gtrsim 2.5$.

Laufer (1961)[69] pointed out the startling fact that fluctuations at the high Mach numbers were 50 times greater than fluctuations measured in a low turbulence subsonic wind tunnel.

Through the use of hot-wire measurements and mode diagram analysis (e.g., Refs. 65 and 69), Laufer ruled out vorticity ($\tilde{u}$) and entropy ($\tilde{T}$) fluctuations as the cause of the measured hot-wire fluctuations. Laufer also argued on physical grounds that vorticity and entropy could be ruled out. Since no temperature fluctuations had been measured in the stilling chamber and since temperature fluctuations are convected along streamlines, then if they are negligible in the stilling chamber they will be negligible in the test section. He also argued that the large contraction ratio in the JPL tunnel (40 at $M_\infty = 1.6$ and 1,500 at $M_\infty = 5$) diminished the stilling chamber velocity fluctuations to such a low value that they could not be the source of the disturbance (see Fig.8). Following

Kovasznay,[52] Laufer provided the experimental data (hot-wire mode designs) and the appropriate analytical expressions to demonstrate positively that the measured fluctuating field was a pure sound field in which the isentropic relationships between the fluctuating quantities would hold.

Based on the results from his very thorough experimental investigation and supporting analytical analysis, Laufer proved that the source of free-stream disturbances was the sound field (aerodynamic noise) emanating from the tunnel wall turbulent boundary layer. Laufer pointed out, however, that direct measurements of the sound field were not yet available. Laufer further cautioned that stability and transition studies in supersonic wind tunnels would be handicapped by the presence of the sound field.

The radiated noise levels as determined by Laufer using hot-wire theoretical equations and mode analysis of hot-wire measurements are presented in Fig. 11. Laufer's classical work is considered to have been the "star in the evening" that opened the way for others to study the effects of noise on wind tunnel data.

Continuing studies conducted in the JPL wind tunnels on aerodynamic noise radiated by supersonic turbulent boundary layers was reported in January 1961.[70] In Ref. 70, it was pointed out that previous JPL studies[69] had shown that: (a) the amplitude of pressure fluctuations increased with Mach number, (b) the intensity was uniform in the flow field, and (c) the pressure field manifested a certain directionality. Reference 70 presented results showing that the $\tilde{p}/p_\infty$ fluctuations could be correlated with the tunnel wall boundary-layer displacement thickness (δ^*).

Kistler and Chen (1963)[71] reported on pressure fluctuations that were made under a turbulent boundary layer on the sidewalls of the JPL 18- by 20-in. supersonic wind tunnel at M_∞ = 1.3 to 5.0. Two findings of particular importance were (1) the normalized pressure fluctuation ($\tilde{p}/\tau_w$) on the surface of a flat plate was found to correlate with Re^*_δ, and (2) the tunnel wall root-mean-square ($\tilde{p}$) of the pressure fluctuation was found to be proportional to the tunnel wall turbulent skin friction as shown in Fig. 12.

Laufer (1964)[72] discussed the radiation field generated by a supersonic turbulent boundary layer at Mach numbers from 1.5 to 5 and compared the hot-wire results with those obtained by Kistler and Chen[71] using microphones positioned in the tunnel wall. In each of these tests, the wall and free-stream pressure fluctuations were found to scale with the mean wall shear for all Mach numbers, as shown in Fig. 12. In addition, it was noted that the intensity of the radiated pressure fluctuations was an order of magnitude less than the pressure fluctuations on the wall. By operating the JPL 18- by 20-in. supersonic tunnel at low pressures, the boundary layer was maintained laminar on all four walls. Then by tripping the boundary layer on one wall, Laufer showed that the intensity of the radiated pressure fluctuations was proportional to the size of the test section. For example, radiation from one wall was approximately equal to one-fourth the radiation measured from four walls. Also, the measured values were constant across the test section, once the hot wire was one to two boundary-layer thicknesses away from the wall.

Phillips (1960)[73] proposed a theory to describe the generation of sound by turbulence at high Mach numbers. Laufer (1964),[72] in commenting on Phillips' theory, noted that it is based on the premise that the sound-generating mechanism consists of a moving, spatially random, virtually wavy wall formed by an eddy pattern that is convected supersonically with respect to the free-stream and is consistent with the principal features of the sound field found in experiments. Using this view, Laufer derived an expression for the pressure fluctuation intensity that is a function of the mean skin-friction coefficient, wall boundary-layer thickness, lengths that scale with the boundary-layer thickness, convection speed, angle of the radiated disturbance, and free-stream Mach number. This theory was found to be in partial agreement with experimental data at Mach numbers from 1.5 to 3.5 and considerably below experimental data at Mach 5.

Williams reported in 1965[74] that the sound field in supersonic flows would be dominated by eddy Mach waves. He stated that the efficiency of radiation increases with Mach number as a result of the turbulent "eddies" moving supersonically with respect to the mean flow and creating Mach waves. Also the waves were highly directional and had their fronts aligned near the Mach angle as pointed out by Phillips.[73]

Williams commented that Phillips (1960)[73] was the first to make a thorough, theoretical attack on the supersonic shear-radiated wave problem. Williams[74] developed an analytical equation [Eq. (1)] for estimating the Mach wave radiation from a supersonic turbulent shear layer based on a description of the pressure fluctuation in the wall boundary layer. Basic in his derivation was the assumption that turbulent pressures scale with the wall boundary-layer thickness.

$$\frac{\tilde{p}}{\tau_w} = \frac{\tilde{p}_w}{\tau_w} \left\{ \frac{5\varepsilon}{24\pi^2} \int_1^{M_\infty} \frac{(M^2 - 1)^{1/2}\, dM}{M^m \{1 + 0.2\, M^2\}^2} \right\}^{1/2} \qquad (1)$$

The radiated noise intensities as computed by Williams using Eq. (1) and the measured wall $\tilde{p}_w$ of Kistler are shown in Fig. 15. Excellent agreement exists between the computed values of Williams and the free-stream measurements of Laufer.

Kendall (1970, 1975)[29,30] continued the outstanding work begun by Laufer at JPL and published additional experimental hot-wire data on wind tunnel free-stream disturbances. Before beginning his flat-plate boundary-layer stability-transition studies (which were directed toward providing experimental confirmation of Mack's stability theory[5]), Kendall demonstrated that the fluctuations picked up by the hot wire located in the laminar boundary layer on the flat plate were the result of forcing by the tunnel free-stream sound field that emanated from the tunnel wall boundary. Data taken from Kendall and published by Morkovin[1] are shown in Fig. 13. These data represent free-stream hot-wire measurements obtained when the JPL tunnel wall boundary

layer was laminar and then turbulent. By operating the JPL tunnel at low pressures, a laminar boundary layer could be maintained on all four walls. Then by tripping the flow on one wall and then rotating the flat plate, Kendall showed the hot-wire response was greatest when facing the turbulent wall, as shown in Fig. 14. The data shown in Figs. 13 and 14 remove any doubts as to the intensity of the radiated aerodynamic noise. Kendall also found that the free-stream pressure fluctuations were amplified one to two orders of magnitude by the laminar boundary layer on a flat plate as shown in Fig. 15. This amplification has significance when comparing surface microphone ($\widetilde{p}$) and free-stream hot-wire ($\widetilde{p}$) measurements as will be discussed in Section 3.0.

Donaldson and Wallace (1971)[66] reported on hot-wire anemometry measurements made in the AEDC-VKF 12-in. supersonic wind tunnel to determine the level of flow fluctuations in the test section free stream. Donaldson and Wallace analyzed the hot-wire data using the mode diagram concept of Kovasznay[52] and the data reduction technique of Morkovin (1956)[71] following the assumption used by Laufer.[69] Their results supported the hypothesis of Laufer that the disturbance was a fluctuating pressure field (aerodynamic noise) that radiated from the tunnel wall boundary layer. The radiated noise (rms pressure fluctuation) data measured by Donaldson and Wallace are presented in Fig. 16 and compared with Laufer's data.[69] Note that both sets of $\widetilde{p}$ data have been divided by two (i.e., p^{-2} divided by 4) to correspond to the radiation from one wall only. The power spectral density for the three unit Reynolds numbers investigated by Donaldson[66] are shown in Fig. 17. The experimental boundary-layer thickness (δ) obtained from Ref. 76 was used to normalize the data. Using mode diagrams along with the assumption that the fluctuating field was a pure sound field, then the hot-wire rms voltage equation was used to estimate the fluctuating quantities of pressure, mass flow density, temperature, velocity, and total temperature. Results of these calculations taken from Ref. 66 are shown in Fig. 18 (note the low level of $\widetilde{u}/U$ and $\widetilde{T}/T$ disturbances as compared to $\widetilde{p}/p_\infty$ intensities).

Hypersonic free-stream disturbance measurements have been reported by Demetriades (1975).[78] Donaldson (1976)[77] provided information on equipment and techniques used in the hot-wire experiments conducted at $M_\infty = 6$ and 8.

Wagner, Maddalon, Weinstein, and Henderson (1970)[79,80] reported on the first of a long series of investigations conducted at NASA/LRC* on the influence of free-stream disturbances on boundary-layer transition at hypersonic speeds. Using an approach similar to Laufer's[69] they found that the mode diagrams were linear with a positive slope for all pressure levels investigated in the $M_\infty = 20$, 22-in.-diam helium tunnel. Analysis of the mode diagrams led to the conclusion that the disturbance was radiated noise as described by Laufer.[69] They found that when the tunnel flow was laminar (22-in. tunnel at $P_\infty < 3$ mw/m^2), the free-stream fluctuations were lowest and when the nozzle flow was transitional, they were highest (see Fig. 19).

Fischer and Wagner (1972)[81] reported on hot-wire measurements conducted in the NASA-LRC 22-in.-diam and 60-in.-diam helium tunnels at $M_\infty = 20$ and 18, respectively. Using the mode diagram method of analysis, they found the free-stream fluctuation disturbances to be consistent with the radiated noise hypothesis. Radiated noise disturbances measured in two helium hypersonic tunnels, 22-in.-diam ($M_\infty = 20$) and 60-in.-diam ($M_\infty = 18$), are shown in Fig. 19. Selected spectra are shown in Fig. 20.

Further measurements by Stainback and Wagner (1972)[82,83] showed that a pitot probe instrumented with a flush-mounted pressure transducer could be used to measure the free-stream pressure fluctuations in hypersonic wind tunnels. The flush-mounted pitot pressure transducer gave direct measurements at radiated noise intensities ($\widetilde{p}/p_\infty$) and were consistent with the $\widetilde{p}/p_\infty$ value deduced from hot-wire measurements.

From the now classical experimental work of Laufer[65,69,72] and the follow-on work of Kendall[4,29], Wagner, et al.,[80-82] Donaldson and Wallace[66] and the theoretical work of Kovasznay,[52] Phillips,[73] and Williams,[74] it is definitely concluded that the dominant source of free-stream disturbance in a well-designed supersonic-hypersonic wind tunnel will be the pressure fluctuating field (radiated noise) emanating from the tunnel wall turbulent boundary layer.

Harvey (1978)[47] summarized published free-stream disturbance intensities. Harvey's correlation of disturbance intensity ($\widetilde{p}$) with Mach number is shown in Fig. 21. He presented the free-stream disturbance data in two basic nondimensionalized forms, $\widetilde{p}/p_\infty$ versus M_∞ and $\widetilde{p}/q_\infty$ versus M_∞.

Dougherty (1980)[36] published a similar correlation of $\widetilde{p}/q_\infty$ data from several wind tunnels and compared the results to flight measurements as shown in Fig. 22. The similarity of the two correlations, Figs. 21b and 22, are to be noted.

The significance of radiated noise disturbances on hypersonic boundary-layer properties has been recognized by NASA and a major effort has been underway since 1970 to design and construct a $M_\infty = 5$ wind tunnel free from radiated noise disturbances.[33,84-88] as illustrated in Fig. 23.

The effects of turbulence $\widetilde{u}/U_\infty$ and radiated noise disturbances ($\widetilde{p}/q_\infty$) on boundary-layer transition will be discussed in Section 3.0. Free-stream disturbance can also have a significant effect on other boundary-layer characteristics, i.e., C_F, θ, H, etc. These experimental and analytical results will not be discussed in this paper, and the reader is referred to Refs. 89 through 97.

3.0 Effects of Free-Stream Disturbance Levels on Transition

The free-stream disturbance modes and intensity levels that can be present in wind tunnels

*National Aeronautics and Space Administration (NASA) Langley Research Center (LRC), Hampton, Virginia.

were discussed in Section 2.0. Results presented in this section will show that free-stream disturbance intensities have a dominating effect on the transition process as reflected in the experimentally measured boundary-layer transition Reynolds number. As was shown in Fig. 4, the type disturbance that will be present depends on the physics of the flow as reflected in wind tunnel type and Mach number range. The following table identifies the type disturbances that will be addressed in this section.

Type Tunnel	M_∞ Range	Type Disturbance	Source
Subsonic	0 to 0.3	Turbulence ($\tilde{u}$)	Stilling Chamber
		Acoustic ($\tilde{p}$)	Standing Waves (Organ Pipe Resonance)
			Traveling Waves (Fan Noise, Sound Generator)
Transonic	0.4 to 1.5	Acoustic ($\tilde{p}$)	Porous (Holes) Wall (Edge Tone Discrete Frequency)
			Slotted Wall (Resonance)
Supersonic-Hypersonic	~2 to ~20	Radiated Sound ($\tilde{p}$)	Wall Turbulent Boundary Layers

Subsonic

The classical transition-noise data published by Schubauer-Skramstad (1947)[8] are presented in Fig. 24. These data showed that boundary-layer transition Reynolds number could be correlated directly with free-stream disturbance levels ($\tilde{u}/U_\infty$). Data obtained by Spangler and Wells (1968)[56] are also included in Fig. 24 and show a strong dependence of Re_t on frequency at the low disturbance levels ($\tilde{u}/U_\infty < 0.3\%$). Based on Tollmien-Schlichting linear stability theory,[113] the significant variation of Re_t within the frequency range tested is to be expected at the test conditions used. It should be noted that for pure turbulence (i.e., true random fluctuations), the disturbance spectra will not exhibit discrete frequencies, and the correlation of Re_t with intensity level, without exhibiting a dependence on frequency, is to be expected.

Transonic Wind Tunnels

Dougherty and Steinle (1974)[35] peformed and/or coordinated extensive measurements of free-stream disturbance levels and corresponding transition locations on a 5-deg, half-angle cone in 22 wind tunnels located in the USA and Western Europe. Results from four of these tunnels are shown in Figs. 25 through 28. Data taken in the AEDC-PWT 16- by 16-ft tunnel are presented in Fig. 25. The primary free-stream disturbance was acoustic noise produced by edge-tone resonance generated by the porous (60-deg inclined holes) walls as discussed in Section 2.0. As shown in Fig. 25, there was "fair" correlation of Re_t with $\tilde{p}/q_\infty$ values. Note that with the holes taped the lowest noise level and highest Re_t values were obtained.

Presented in Fig. 26 are data from the NASA-ARC 8-ft slotted wall tunnel. The correlation of Re_t with $\tilde{p}/q_\infty$ is fairly good. The acoustic noise disturbance was generated by a combination of discrete frequencies from slot resonance, the fan harmonics, and broad-band noise, as discussed in Ref. 35.

Transition data from the NASA-ARC 11-ft wind tunnel, Fig. 27, exhibited a fairly good correlation with disturbance intensity. The acoustic disturbance was dominated by two discrete acoustic frequencies generated by the test section wall slots. The variation in a $\tilde{p}/q_\infty$ with axial location was the result of increased fan noise as the model moved aft. The lowest acoustic noise levels and highest transition Re_t values were measured by Dougherty[35] in the NASA-LRC 16-ft slotted wall tunnel. The spectra were generally broad-band noise except for discrete frequency disturbances generated by the fan at $M_\infty = 0.3$ to 0.4. A good correlation of Re_t with $\tilde{p}/q_\infty$ is seen to exist.

Dougherty and Fisher (1980)[36] continued their investigation of transition and free-stream disturbances to include extensive flight experiments. The 5-deg, half-angle cone used in his tunnel experiments was flown mounted from the nose of an F-15 aircraft. (Fig. 29). The cone Re_t values and noise intensities measured in flight are presented in Figs. 30 and 31. Of particular significance is the fact that a measurable disturbance level was present in flight, and there appears to be a direct correspondence of Re_t (Fig. 31) with the $\tilde{p}/q_\infty$ levels (Fig. 30).

A general summary of free-stream disturbance levels ($\tilde{p}/q_\infty$) measured in transonic and supersonic wind tunnels and flight is shown in Figs. 32 and 33. By making direct comparisons of Re_t with $\tilde{p}/q_\infty$ levels, a fairly good correlation exists over a very wide Mach number range (i.e., as the disturbance level goes down, Re_t goes up and vice versa.)

Supersonic-Hypersonic Tunnels

Pate and Schueler (1967)[26] conducted the first experiments that provided positive proof that the radiated noise from a tunnel wall turbulent boundary would significantly and adversely affect model boundary-layer-transition location. Details of these experiments can be found in Refs. 26, 27, and 50. Results from these studies are presented in Figs. 34 through 36. The objective of the experiment was to expose a hollow-cylinder "planar" transition model and subsequently a flat-plate "planar" microphone model to various levels of radiated noise. The approach was to control the state of the boundary layer (laminar or turbulent) on the inside wall of the long shroud over a range of test conditions (i.e., various Mach numbers and unit Reynolds numbers).

The tests were conducted in the AEDC-VKF Tunnel A 40- by 40-in. supersonic wind tunnel at $M_\infty = 3$, 4, and 5. Baseline data were obtained in Tunnel A with the shroud removed. It should be noted in Figs. 34a and b that the transition Reynolds number increased as the unit Reynolds number increased with the accompanying decrease in the radiated noise disturbance level, $\tilde{p}/q_\infty$. By increasing the unit Reynolds number and/or by placing a boundary-layer trip at the shroud leading edge (see Refs. 26 and 50 for details), the shroud inner wall boundary-layer-transition location (i.e., length of turbulent flow) could be positioned from very near the shroud leading edge to downstream of the flat-plate and hollow-cylinder models. With

the shroud installed and at a test condition of $M_\infty = 3.0$ and low unit Reynolds numbers (Re/in. $\lesssim 0.1 \times 10^6$), the boundary layer on the shroud inner wall was maintained laminar. Consequently, no radiated noise was generated and the pressure disturbance $\tilde{p}/q_\infty$ was lower than the baseline data, i.e., shroud removed. This also suggests that the shroud provided some shielding effect from the tunnel wall noise.

As the boundary layer on the shroud inner wall changed from laminar to turbulent, the transition Reynolds numbers decreased (Fig. 34c) and the radiated noise levels increased (Fig. 34d). It should be noted that the test was repeated and the noise measurements duplicated in the second test program.

Fourier analysis of the three data points identified in Fig. 34d as ① , ② , and ③ are presented in Fig. 35. The spectra data follow the same qualitative trend as exhibited by the overall rms ($\tilde{p}/q_\infty$) data presented in Fig. 34d. The pressure fluctuations at low frequencies were quite large. Two spikes appeared in all these sets of data at approximately 7 and 14 kHz. These were probably mechanically induced vibrational effects.

Similar Re_t and $\tilde{p}/q_\infty$ results were obtained at $M_\infty = 4$ and 5. The $M_\infty = 5$ data are presented in Fig. 36 and the transition Reynolds number is seen to also have a direct inverse correlation with the measured radiated noise levels ($\tilde{p}/q_\infty$).

The shroud experiments of Pate and Schueler[26] provided positive proof that the boundary-layer transition location and transition Reynolds numbers on simple flat-plate models will be dominated by aerodynamic noise that radiates from the tunnel wall turbulent boundary layer.

Pate (1967, 1971, and 1977)[26,27,50] investigated the effects of radiated noise ($\tilde{p}$) on boundary-layer transition using a hollow-cylinder model and a 5-deg, half-angle sharp-cone model in various wind tunnels ranging in size from 1 ft to 16 ft.

The transition Reynolds number measured in the same two tunnels on the sharp-leading-edge hollow-cylinder model and 5-deg half-angle sharp cone are shown in Fig. 37. The transition Reynolds number data measured in the 40-in. tunnel were significantly higher than the 12-in. tunnel results. Of particular significance is the fact that the increase in Re_t between the two tunnels for both the hollow cylinder and sharp cone were about the same. This suggests that radiated noise effects on the transition process for simple geometries will be about the same.

The microphone data by Pate[50] obtained at $M_\infty = 4$ are compared with data measured at $M_\infty = 4$ by Donaldson and Wallace[66] using the same model. There are several points to note in this figure: (1) at Re/in. $= 0.025 \times 10^6$, the Tunnel D $\tilde{p}/q_\infty$ values were very low. This corresponds to a laminar boundary layer on the tunnel wall as determined from boundary-layer data published in Ref. 72; (2) at Re/in. $\approx 0.05 \times 10^6$, the wall boundary layer was estimated to be transitional and the measured high peak is in agreement with the findings of Vrebalovich (1960),[98] Laufer (1961),[69] and Wagner, et al. (1969);[20] (3) the microphone $\tilde{p}/q_\infty$ measurements in Tunnel D were significantly higher than the free-stream hot-wire data. These results are as expected, if the findings of Kendall (1970)[29] are considered. Using a hot wire, Kendall found that the free-stream disturbance ($\tilde{p}$) was amplified by the laminar boundary layer on a flat plate by as much as a factor of one to two orders of magnitude, as previously shown in Fig. 15. The data presented in Fig. 38 are consistent with the results of Kendall; and (4) the most significant result obtained from Fig. 38 is that the Tunnel D (12 in.) $\tilde{p}/q_\infty$ data, flat plate and hot wire, are significantly higher than the Tunnel A (40 in.) data. Correspondingly, Tunnel D Re_t data are significantly lower than the Tunnel A data, Fig. 37. These results are in good agreement with the results in Figs. 34 and 36, the higher the free-stream disturbance level (i.e., the noise intensity), the lower the transition Reynolds number.

Power spectral density plots as measured using the flat-plate microphone model in Tunnel D by Donaldson and Wallace[66] are shown in Fig. 39. Donaldson and Wallace concluded that the peaks must be mechanically introduced by the microphone or mounting system since no such peaks appeared in the free-stream hot-wire data.

Recent data published by Beckwith (1975)[84] support the present assumption that a microphone mounted on the surface of a model will measure significantly higher pressure fluctuation intensities than a hot-wire or flush-mounted microphone-pitot tube positioned in the free stream at certain supersonic-hypersonic Mach numbers. Presented in Fig. 40 are Beckwith's data taken from Ref. 84. There are two significant factors to note: (1) Pressure-fluctuating rms levels measured on the surface of a model may not be strongly dependent on the model boundary layer provided the model boundary layer is fully turbulent or fully laminar, as shown in Fig. 40. This conclusion was also reached by Dougherty[35] for low supersonic and transonic test conditions; and (2) the model microphones measured a significantly higher pressure fluctuation intensity, Fig. 40b. This result supports statement three above. Beckwith also concluded that the amplification of the free-stream radiated noise by the laminar boundary layer as reported by Mack[5] and Kendall[29] might be the reason.

A paper by Bergstrom (1972)[99] compared wind tunnel free-stream disturbance measurements from several sources and commented on the large scatter in the data. The data used for the comparison included free-stream hot-wire and model surface microphone data. Bergstrom noted that the model surface microphone data were significantly higher than the hot-wire data and concluded that additional studies need to be directed toward resolving this apparent discrepancy. It is proposed that a significant part of the differences in the data are the result of the free-stream radiated noise disturbance being amplified by the model laminar boundary layer and producing the higher microphone rms levels. Other possibilities are mechanical and microphone resonance frequencies that are not properly filtered.

Wagner, Maddalon, and Weinstein (1969)[20] reported on one of the most fundamental and informative of the NASA-LRC transition studies. They used a $M_\infty = 20$ helium flow tunnel (test section diameter = 20 in.) to investigate radiated aerodynamic

noise disturbances in the tunnel free-stream when the tunnel wall boundary changed from laminar to turbulent. They used a hot-wire positioned in the free stream to determine the type and magnitude of the free-stream disturbances using the Kovasznay-type model diagram and the analysis developed by Laufer as discussed in Section 2.0. Presented in Fig. 41 are the rms pressure fluctuations measured in the test section free stream (Station 139) of the $M_\infty = 20$ helium tunnel. Note that below a unit Reynolds number of $\approx 0.15 \times 10^6$, there was a sharp drop in the $\tilde{p}/p_\infty$ data, and this was the result of a laminar boundary developing on the tunnel wall.[80] Boundary-layer transition Reynolds numbers were measured on a sharp-leading edge, 10-deg inclined wedge positioned in the test section, as shown in Fig. 41a. Included in Fig. 41b are the measured free-stream radiated pressure fluctuation data. Although there were no transition data obtained below (Re/in.) $\lesssim 0.15 \times 10^6$ (transition off the back of the model), it can be seen that the changes in Re_t data varied inversely with the $\tilde{p}/q_\infty$ values.

The shroud results obtained by Pate and Schueler (1967),[26] presented in Figs. 34 and 36, and the NASA studies (1969),[80] given in Fig. 41 produced essentially the same results using completely independent methods.

Fischer and Wagner (1972)[81] extended the NASA-LRC transition studies to include the study of transition on sharp cones and the measurement of the free-stream radiated noise levels in two helium tunnels ($M_\infty = 20$, 22-in.-diam tunnel and the $M_\infty = 18$, 60-in.-diam tunnel). These data are presented in Fig. 42. The transition Reynolds numbers found varied inversely with the measured noise levels as reported earlier in Ref. 80 and provided additional confirmation of the strong effects of radiated noise on transition.

Additional summary discussion on the many NASA transition-noise experiments can be found in Refs. 33 and 50.

As evident from results presented in this section, the radiated aerodynamic noise ($\tilde{r}$) inherent in conventional supersonic-hypersonic wind tunnels ($M_\infty \gtrsim 3$) will have a severe adverse effect (if not the dominating effect) on boundary-layer transition on simple geometries, i.e., flat plates and sharp cones at zero incidence.

4.0 Variation of Supersonic-Hypersonic Transition Reynolds Number with Tunnel Size

It has been established in Sections 2.0 and 3.0 that free-stream disturbances present in subsonic, transonic, and supersonic-hypersonic wind tunnels will have a dominating effect on the transition process as reflected in the experimentally measured boundary-layer transition Reynolds number (Re_t). It was also shown that Re_t values could be correlated with disturbance levels ($\tilde{u}/U_\infty$, $\tilde{p}/p_\infty$). The subsonic-transonic disturbance modes (turbulence, $\tilde{u}'/U_\infty$ and acoustic sound, $\tilde{p}/q_\infty$) are related to inlet flow conditions, stilling chamber design, porous/slotted configurations, fan-drive and diffuser noise. These sources of disturbances are unique to each facility. Consequently, the disturbance levels must be obtained by direct measurement as discussed in Section 2.0. The radiated aerodynamic noise disturbance mode present in conventional supersonic-hypersonic tunnels is generated by the tunnel wall turbulent boundary layer. This is a unique characteristic that allows the radiated noise level to be related to tunnel size and flow condition.

The direct relationship and variation of Re_t with tunnel size was first demonstrated by Pate and Schueler (1967)[26] for $M_\infty = 3$ to 5. These studies were part of their extensive research program conducted to confirm the correlation of Re_t with radiated noise. The systematic variation of Re_t with tunnel size was later confirmed by additional and independent studies in the USA, Russia, England, and The Netherlands.

Results presented in Figs. 34 and 36 (the shroud experiments by Pate) provided conclusive evidence that radiated noise can dominate the transition process. Free-stream pressure fluctuation data measured in the AEDC-VKF Tunnel A (40- by 40-in. test section) and the AEDC-VKF Tunnel D (12- by 12-in. test section) presented in Figs. 37 and 38 have shown that higher noise levels and lower transition Reynolds numbers are associated with small tunnels. Furthermore, the radiated noise intensities can be directly related to the properties (τ_w, δ^*) of the turbulent boundary layer on the tunnel walls (Fig. 12 and Ref. 70).

Pate (1967, 1971, 1977)[26,27,50] reported on extensive experimental transition programs conducted to verify that the transition location was dependent on tunnel size (or radiated noise levels). The location of transition was measured in five different AEDC supersonic-hypersonic wind tunnels using planar (flat-plate and hollow-cylinder) and sharp-cone models as described in Refs. 26, 27, and 50. Three of these tunnels are shown in Fig. 43.

Transition Reynolds numbers measured by Pate and Schueler (1967)[26] at $M_\infty = 3.0$ on hollow-cylinder models in three AEDC wind tunnels having test sections ranging in size from 1 to 16 ft are presented in Fig. 44. Sharp-cone transition data obtained by Pate[27] at $M_\infty = 4.0$ in two different sizes of AEDC wind tunnels are also presented. The large increase in transition Reynolds numbers with increasing tunnel size is attributed to the decrease in radiated aerodynamic noise levels as discussed in Sections 2.0 and 3.0. Details of the experiments can be found in Refs. 26, 27, and 50.

Ross (1974)[100] conducted an experimental transition program in two supersonic blowdown wind tunnels (Netherlands). The transition model was the 2-in.-diam hollow-cylinder model used by LaGraff (1970).[101] The transition location was determined using a surface pitot probe. Ross found a large variation in Re_t with tunnel size as shown in Fig. 45. These results were in agreement with the findings of Pate and Schueler[26] and provided independent confirmation of the strong variation of Re_t data with tunnel size.

Studies were conducted in the USSR by Struminskiy, Kharitonov, and Chernykh (1972)[102] to establish if unit Reynolds number effects and tunnel size effects at $M = 3$ and 4 as reported by Pate and Schueler[26] existed at higher unit

Reynolds numbers. Two wind tunnels were used (Tunnel T-313, 23.6 by 23.6 in., and Tunnel T-325, 7.9 by 7.9 in. Transition locations were determined using the surface pitot probe end-of-transition technique (see Ref. 50). Values of Re_t for an effective zero leading-edge bluntness was obtained by extrapolation (see Ref. 50). Presented in Fig. 46 are the basic transition data from Ref. 102. The significant increase in Re_t with increasing tunnel size should be noted. An attempt was made in Ref. 102 to correlate the Re_t data for a given Mach number using a Reynolds number based on the test section diameter. For the $M_\infty = 3$ data, fair agreement was obtained by correlating Re_t with $Re_{\infty,D}$.

In 1975, Kharitonov and Chernykh[103] extended their research to include pressure fluctuation measurements on the walls of Tunnels T-325 and T-313 at $M_\infty = 3$ and 4. Their studies established a change in Re_t levels with a change in acoustic levels. They concluded that the change in Re_t with a change in unit Reynolds number (Re/in.) was the result of the acoustic perturbations (aerodynamic noise) present in the test section. They reasoned that the scale of turbulence was related to the tunnel wall turbulent boundary-layer displacement thickness. Using the theory that Re_t was related to the intensity ($\tilde{u}/u$), the scale of turbulence ($\ell = \delta^*$), and a characteristic length ($L = d$), they obtained a correlation of $Re_t = F\,(\tilde{u}/u)(L/\ell)^{1/n}$ for $n = 0.25$ and $M_\infty = 2.5$ to 6. The scatter for flat-plate transition data obtained in six wind tunnels was ±15%. They used their data and data from AEDC-VKF Tunnels A and D and AEDC-PWT Tunnel 16S as taken from Ref. 26.

LaGraff (1970)[101] reported on a series of supersonic transition studies conducted using a hollow-cylinder model. He stated that as a result of the paper by Pate and Schueler (1967)[26] a test program was initiated at Oxford University, England to investigate the dependence of transition on facility-generated disturbances. Four research groups from Great Britain and Sweden participated in the study as listed in Table 4.[50] The two sets of data that can be compared directly are the Oxford University data for $M_\infty = 6.95$ and the Aerodynamic Research Institute of Sweden data for $M_\infty = 7.15$. These gun tunnel data are presented in Fig. 47 and show the effects of tunnel size similar to the results shown in Figs. 45 through 46. Results from two different types of tunnels are presented in Fig. 47 and provide added confirmation of the increase in Re_t with increasing tunnel size.

Bergstrom, et al. analyzed three sets of gun tunnel flat-plate transition data (1971)[104] in addition to his transition studies conducted at $M_\infty = 7.0$ in the Loughborough University of Technology gun tunnel. Using the Pate-Schueler aerodynamic noise correlation[26] developed for conventional wind tunnels (see Section 4.0), he correlated gun tunnel Re_t data and concluded that transition data obtained in hypersonic gun tunnels were influenced essentially by the aerodynamic noise present in the test section. He further concluded that many of the discrepancies in gun tunnel transition data could be explained on this basis. The transition data from the four gun tunnels displayed good overall correlation with aerodynamic noise and tunnel size parameters according to the method of Pate and Schueler.[26] For a given Mach number, Bergstrom et al.[104] also found that transition Reynolds numbers correlated very well against the free-stream rms pressure fluctuations ratioed to free-stream static ($\tilde{p}_{rms}/p_\infty$) as calculated using the method of Williams and Maidanik[74] (Eq. 1) for a wide range of tunnel sizes.

Composite plots comparing the variation of Re_t with tunnel size as measured by different researchers in several countries are presented in Figs. 48 through 52.

Transition Reynolds number data measured at $M_\infty = 3$ on flat plates and hollow cylinders in six different sizes of wind tunnels having test section sizes varying from 7.9 to 16 ft are shown in Fig. 48. The systematic variation with tunnel size and unit Reynolds number should be noted. Note also that the long shroud "simulated tunnel" data from Fig. 34 falls at about the expected location.

Similar trends with tunnel size are exhibited by two sets of Re_t data obtained at $M_\infty = 8$ in the AEDC 50-in. and the NASA/LRC 18.3-in. tunnels, Fig. 49.

Several sets of flat-plate and sharp-cone Re_t data ($M_\infty = 3$) are presented in Fig. 50 and show a systematic variation with tunnel size when presented as a function of nozzle length. Presented in Figs. 51 and 52 are summary plots of cone and planar Re_t data plotted as a function of tunnel size (circumference). The tunnel test section sizes varied from 5.0 to 50 in. in height for the sharp-cone experiments and from 7.9 in. to 16 ft for the planar model experiments. The variations in Re_t with tunnel size are very similar for both planar and sharp-cone models for Mach numbers 3, 5, and 8.

The results presented in this section have shown conclusively that supersonic-hypersonic ($M_\infty = 3$) transition Reynolds number measured on cones and planar models in conventional wind tunnels will increase with increasing tunnel size in a systematic and monatonic manner.

5.0 Boundary-Layer Transition Correlations and Prediction Techniques

Because of the absence of a readily available, easily used, and successful theoretical transition model, researchers and designers have, from necessity, pursued the traditional path of attempting to develop data correlations that allow reasonable estimates to be made. These correlations have been and still are the basis on which most transition locations on aircraft and missiles are estimated and wind tunnel and flight test programs are planned.

Various published techniques will be reviewed in this section. Special emphasis will be devoted to the supersonic-hypersonic Re_t-radiated noise correlations.

Methods that have been used for predicting boundary-layer transition can be grouped into five general classifications:

1. Data correlations based on local flow conditions and observed trends in experimental data.
2. Three-dimensional (cross-flow) instability methods.

3. Linear stability theory with specified amplification rates.

4. Kinetic energy of turbulence approach.

5. Correlations and semi-empirical methods based on free-stream disturbance intensities.

(NOTE: Methods 3, 4, and 5 incorporate free-stream disturbance intensities.)

Reviews of smooth body transition prediction methods have been given by Gazley (1953),[9] Deem et al. (1965),[39] Morkovin (1969),[2] Granville (1974),[40] Kistler (1971),[108] Shamroth and McDonald (1972),[49] Tetervin (1973),[109] Smith and Gamberoni (1956),[41] Reshotko (1969),[110] Hanner and Schmitt (1970),[111] Michel (1973),[89] Hall and Gibbings (1972),[48] and Mack (1977).[46] White (1974)[112] also gives a good review of many of the older well-known methods and some of the more recent methods. Of course, the interested person will want to read the sections on stability and transition by Schlichting.[113]

Linear stability theory and the kinetic energy of turbulence approach offers perhaps the best possibility of eventually modeling and predicting the onset of the boundary-layer transition, even though to date they have not yet been very successful. However, these methods will probably not be widely used (at least not for many years) by the design engineer, wind tunnel experimentalists, or the aeronautical engineer involved in trying to predict the occurrence of transition on his aircraft or missile of interest. The linear stability and kinetic energy theories are very sophisticated, both in the concepts involved and the numerical and analytical mathematics required. Years of experience are required in developing and using the complicated computer programs. Vehicle configurations, particularly in the preliminary design stage, often change faster than the theory can be modified and/or the geometry is too complicated to be modeled.

Semi-empirical methods and correlations based on physical concepts and/or free-stream disturbance intensities have, to date, been the most successful in correlating and predicting boundary-layer transition at subsonic-transonic-supersonic Mach numbers.

Since it is not the purpose of this paper to present a critical review of the many published papers and methods, only a few of the techniques will be presented to illustrate types of methods, the correlation parameters used, and some of the typical results obtained.

As might be expected, special attention will be devoted to those transition correlation techniques based on the theory of free-stream disturbance domination.

6.0 Data Correlations Based on Local Flow Conditions and Observed Trends in Experimental Data

These correlations can be divided into two general areas: (1) tripped flows and (2) smooth body flows.

Tripped Flow

Results from three of these methods are briefly discussed to illustrate the correlation parameters used.

At subsonic speeds, Dryden (1953)[15] successfully correlated the effectiveness of two-dimensional elements (wires) and cylindrical roughness elements in promoting early boundary-layer transition. This correlation is shown in Fig. 53.

Van Driest, et al. (1960-1968)[18,114,115] conducted a systematic experimental and analytical program and successfully correlated the location of the "effective" transition location for spherical roughness heights, and the effects of roughness in conjunction with wall cooling and Mach number ($0 < M_\infty < 4$) on flat plates and sharp cones. The resulting correlation is presented in Fig. 54.

The trip correlation developed by Potter and Whitfield (1962,1969)[23,116] is shown in Fig. 55 for flat plates and sharp cones. This trip correlation is, to this author's knowledge, the most comprehensive of any published to date and incorporates the effects of trip size, wall cooling, and local Mach number ($0 < M_\delta < 10$). This correlation also predicts the trip size required to move transition from its smooth body location to the trip location or any point in between.

Other extensive experimental studies using different trip geometries at hypersonic conditions have been performed and reported by Whitehead (1969).[22]

The problem of roughness effects on transition is always a current problem, as illustrated by wind tunnel tests conducted by Pate and Eaves (1973)[117] and Stalmach and Goodwich (1976)[118] to establish the effective roughness of the thermal insulating tiles on the space shuttle orbiter.

An obvious question relative to "tripped" transition is whether the transition location will be trip dominated or whether the free-stream disturbance level will be an influencing factor. None of the trip correlations discussed included free-stream, disturbance levels in the correlation.

Research was conducted by Pate (1971, 1978)[28,50] to determine if free-stream disturbance levels were a significant factor in tripped transition results. The model was exposed to significantly different levels of radiated free-stream disturbance intensities by conducting tests in the AEDC-VKF 12-in. and 40-in. supersonic tunnels (see Figs. 37 and 38).

Presented in Fig. 56 are comparisons of the 12-in. and 40-in. tunnel results obtained using the identical cone model under identical M_∞ and $(Re/in.)_\infty$ conditions. As discussed in Section 3.0 (Fig. 37), the smooth-wall transition locations are significantly higher in the 40-in. tunnel because the radiated noise levels are significantly lower as shown in Fig. 38.

It is seen that the "effective point" location as defined by van Driest and Blumer[18] was essentially the same in both tunnels. This indicates that when the transition process is trip dominated, "i.e., X_t is at the effective points, then the influence of free-stream disturbances can be considered negligible." Therefore, the method of van Driest (and presumably the method of Dryden) can be used "with reasonable confidence" without having to consider the smooth-body transition location or the tunnel disturbance level.

The method of Potter and Whitfield[23,116] requires the smooth-body transition Reynolds number as input data. Consequently, the tunnel turbulence level must be considered. Results computed using the method of Potter and Whitfield and the proper smooth-wall transition location are shown in Fig. 56a. Reasonable agreement is seen to exist.

The studies by Pate (1971)[28] have verified that the "effective point" location defined by van Driest[17] is trip disturbance dominated and essentially independent of the tunnel disturbance levels at supersonic speeds.

Smooth-Body Flows

In correlations of transition Reynolds numbers on smooth-wall, two-dimensional models (flat plates or hollow cylinders) at supersonic speeds the effects of Mach number, leading-edge bluntness, wall cooling, unit Reynolds number, and leading-edge sweep have been considered. The studies by Deem, et al. (1965)[39] considered all five of these parameters and is perhaps the most extensive in scope of these types of correlations. Their correlation did not include the effects of free-stream disturbance and consequently often provides only qualitative predictions. In Ref. 119 the analytical expressions developed by Deem et al. have been presented in graphical form for rapidly estimating the transition location for flat-plate wind tunnel models with supersonic leading edges at zero angle of attack. Deem et al. also compared the estimated Re_t for each data point used in developing their correlation, and the result is shown in Fig. 57. The standard deviation was 33%.

Beckwith and Bertram (1972)[33] developed supersonic-hypersonic transition correlations using boundary-layer parameters such as $Re_{\delta*}$ and local flow conditions M_e and h_e and the wall parameter h_w. Their correlations were developed using a digital computer to define functional relationships and corresponding coefficients that produced the smallest standard deviation σ. An example of one correlation developed for wind tunnel data is presented in Fig. 58. Correlations for ballistic range and free-flight data were also developed and are published in Ref. 33. The results presented in Ref. 33 are the most comprehensive published to date and represent several years of effort by researchers at the NASA Langley Research Center. The standard deviation for wind tunnel sharp-cone transition data is between 29 and 41%, as illustrated in Fig. 58. These correlations can only be judged to be fair in their ability to provide reasonable predictions of transition Reynolds numbers.

Fehrman and Masek (1972)[38] attempted to correlate high Mach number transition Reynolds number measured on the windward centerline of the NASA orbiter at angle of attack using Re_θ, M_e, and the local unit Reynolds number (Re_e/ft) as the correlating parameters. The correlation from Ref. 38 is shown in Fig. 59, and the scatter in the correlation of the data is seen to be quite large.

Other correlation methods that account for nose bluntness and severe nose roughness on blunted-cone geometry have been reported by Stetson (1979),[37] Boudreau (1978),[120] and Reda (1979).[121]

A summary of transition research conducted at AEDC is given in Ref. 122.

In general, it can be stated that the "tripped methods" have been successfully and widely used. The smooth-body fully empirical methods have filled a void and fulfilled a need, but their general applications and usefulness have been limited.

Three-Dimensional-Crossflow Instability Method

The laminar boundary-layer profile in a three-dimensional viscous flow, such as a swept wing or cylinder, will have a twisted profile that can be resolved into tangential (u) and normal (w) velocity components as illustrated in Fig. 60. Owen and Randall (1952)[14] found that the instantaneous jump of transition from the trailing edge to near the leading edge of subsonic swept wings could be correlated with a critical crossflow Reynolds number. This critical crossflow Reynolds number is a function of the maximum crossflow velocity (normal component) and a thickness defined as nine-tenths the boundary-layer thickness as shown in Fig. 60. This type of transition process can be related physically to the instability of the boundary layer as a result of the inflection point in the crossflow profile. The crossflow concept was investigated initially at subsonic speeds by Owen and Randall,[14] at supersonic conditions by Chapman (1961)[24] using swept cylinders, and by Pate (1965)[25] using supersonic swept wings.

Adams (1973)[43] extended this concpt to supersonic sharp cones at incidence. Adams and Martindale[44] explained high heating rates on the NASA space shuttle at incidence using the crossflow concept.

This technique is classified as semi-empirical since it requires a theoretical solution of the three-dimensional laminar boundary, and transition is then predicted to occur when the crossflow Reynolds number (χ) reaches a value of 150 to 175. This empirical constant appears to hold for subsonic and supersonic flow regimes and for all types of geometries, as shown by the correlation presented in Fig. 60.

Free-stream disturbances will probably have a negligible effect on the crossflow criteria, since mean flow laminar boundary-layer velocity profiles are not strongly affected (at least not to the first order) by free-stream disturbances.

Linear Stability Theory with Specified Amplification Rates

The stability of fluid flow was first considered by Raleigh for incompressible, inviscid flows.[112,113] He found that an inflection point in the velocity profile was a necessary requirement for instabilities to occur. Prandtl extended linear stability theory to include the destabilizing effects of the fluid viscosity.[112,113] A detailed theory of stability for incompressible, viscous flows was developed by Tollmien and Schlichting.[113] The confirmation of the existence of the Tollmien-Schlichting type waves was provided by the classical experiments of Schubauer and Skramstad (1947).[8] Extension of the linear stability theory to compressible flows was accomplished by Lees and Lin (1946).[134] Experimental verification of this theory was provided by Laufer and Vrebalovich (1960).[135] Mack (1969,1975)[5,46] extended linear stability theory to higher Mach numbers, identified and studied the presence of higher modes* of disturbance, and showed that the destabilizing effects of viscosity begin to decrease above $M_\infty \approx 3$. Kendall (1970,1975)[4,30] provided experimental verification for many of Mack's theoretical predictions. One particularly significant finding of the Mack-Kendall research at JPL was the prediction and experimental confirmation that free-stream radiated noise disturbance, independent of a critical frequency, is amplified by the laminar boundary layer. This amplification begins at the leading edge of a flat plate and continues downstream until transition occurs. Mack-Kendall showed that a laminar boundary layer at $M_\infty = 3$ and 4 can amplify the free-stream disturbance by an order of magnitude as shown in Fig. 15. The fact that all free-stream disturbances are amplified and can be an order of magnitude higher in the laminar boundary layer than in the free stream were discussed in Section 2.0 with regard to surface microphone measurements.

The use of linear stability theory to predict the onset of boundary-layer transition as opposed to just predicting the onset of amplification of small disturbance waves has been studied by Smith and Gamberoni (1956)[41]; Jaffe, Okamura, and Smith (1969)[6]; Mack (1975)[5]; and Reshotko (1969).[3] This approach is based on the observation by Michel (1951)[42] that the location of transition occurred at a constant value ($\approx e^9$) of the amplification of the Tollmien-Schlichting type sinusoidal disturbances. Presented in Figs. 61, 62, and 63 are results computed by Smith and Gamberoni[41]; Jaffe, Okamura, and Smith[6]; and Mack[5]; and comparisons are made with experimental data.

The theoretical results presented in Figs. 61, 62, and 63 have limited application because of the following reasons. The theory of Smith, et al.[6,41] is applicable only to incompressible, low turbulence flows. The subsonic data presented in Figs. 61 and 62 were obtained in very low turbulence wind tunnels where the free-stream disturbance levels were negligible. The supersonic results of Mack[5] (Fig. 63) made the assumptions that: (a) the initial disturbance amplitude (A_o), at a reference Mach number ($M = 1.3$), varied as the square of the Mach number ratio; (b) the disturbances in the boundary layer are proportional in amplitude to the free-stream radiated sound; and (c) the disturbance spectrum in the boundary layer is flat with respect to frequency and independent of axial location.

Of particular significance is the fact that those methods considered free-stream disturbance levels and the method of Mack required the radiated noise disturbance level as a direct impact.

Kinetic Energy of Turbulence Approach

In recent years, kinetic energy of turbulence model equations, as investigated by Shamroth and McDonald (1972),[49] have been used to investigate transition as shown in Fig. 64. This method consideres a particular type of free-stream disturbance that is introduced into the laminar boundary layer and follows the disturbance until transition occurs. One objection to this approach, at least by the proponents of linear stability theory, is the absence of a critical frequency in the theory and only a requirement that the free-stream disturbance amplitude (or energy) be specified. This technique has also been used with some success in predicting the occurrence of transition and of relaminarization of turbulent boundary layers subjected to strong favorable pressure gradients. Of particular significance to the present research is the fact that pressure fluctuations (aerodynamic noise) as presented in Sections 2.0 and 3.0 are considered by Shamroth and McDonald[49] as the primary source of the free-stream disturbances that they incorporated into their kinetic energy of turbulence formulation. Shamroth and McDonald[49] reported that only a small amount ($\approx$1%) of acoustic energy absorption is required to trigger transition. Presented in Fig. 64 are computed results of Shamroth and McDonald[49] compared with experimental heat-transfer data. It is important to note that the acoustic energy loss (absorbed) must be specified. Therefore, for the data presented in Fig. 63 it is not known a priori which disturbance level should be used to predict the location of transition.

Correlations and Semi-Empirical Methods Based on Free-Stream Disturbance Intensities

Michel (1951)[42] was successful in correlating low turbulence wind tunnel transition Reynolds number data obtained on smooth surface wings having varying pressure gradients in subsonic incompressible flow. Michel used the momentum thickness Reynolds number (Re_θ) as the correlating parameter. His correlation is shown in Fig. 61. Granville (1974)[40] using Michel's hypothesis that the transition Reynolds number (Re_t) was related to a momentum thickness Reynolds number (Re_θ) successfully correlated low-speed flows using the parameter ($Re_t - Re_{cr}$) with Re_θ. (Below Re_{cr}, all small disturbances are damped.)

Van Driest and Blumer[17] used Liepman's hypothesis (1943)[136] that transition will occur at a critical Reynolds number (Re_{cr}) that is equal to the ratio of the turbulent shear stress (Reynolds stress) $\overline{\rho u' u'}$ and the viscous stress $\mu(du/dy)$, i.e., $Re_{cr} = \overline{\rho u' v'}/[\mu(du/dy)]$. By evaluating the

*The Tollmien-Schlichting type of modes was defined as the primary mode.

Reynolds stress using Prandtl's mixing length hypothesis and using the Pohlhausen velocity profile to determine du/dy, van Driest developed a semi-empirical equation for transition Reynolds number in incompressible flow that accounts for the effect of free-stream turbulence through the effect of the pressure fluctuation on the pressure gradient and consequently the velocity profile through the Pohlhausen shape factor. Presented in Fig. 65 are some of the classical subsonic data plotted versus free-stream vorticity disturbance (or velocity fluctuation). Included in Fig. 65 is van Driest's semi-empirical equation with the constants adjusted to match the older data. Note that the more recent data of Spangler and Wells (1968)[56] are much higher than the older Schubauer-Skramstad data (1948).[8] Wells[45] developed a new expression using the new data, and this equation is also shown in Fig. 65. Benek and High (1974)[137] followed the approach used by van Driest et al. and developed a semi-empirical expression for compressible transonic and low supersonic flow that successfully predicts transition on sharp slender cones. Typical results are shown in Fig. 66.

Hall and Gibbings (1972)[48] continued the study of the influence of free-stream turbulence on boundary-layer transition in incompressible, zero pressure gradient flows. Their correlation of Re_{θ_t} as a function of $\tilde{u}/U_\infty$ is shown in Fig. 67. Empirical equations developed in Ref. 48 for the beginning and end of the transition region are included in Fig. 67. Note that the curve developed from the empirical method of van Driest and Blumer (1963)[17] (see Fig. 65) is included in Fig. 67.

Dougherty (1974,1980)[36,61] conducted extensive wind tunnel and flight experiments on boundary-layer transition and free-stream disturbances. The test model was a 5-deg, half-angle sharp cone instrumented with surface microphones and a traversing pitot probe. A correlation of transition Reynolds numbers measured in 21 transonic wind tunnels and in flight with the measured free-stream disturbance intensities normalized by the free-stream dynamic pressure was successfully developed by Dougherty (1980)[36] as shown in Fig. 68. The type of acoustic disturbances present in the various wind tunnels and some of the basic Re_t and $\tilde{p}/\tilde{p}_\infty$ data were discussed in Sections 2.0 and 3.0, Figs. 25 through 33. The experiments by Dougherty were the first to obtain Re_t and disturbance measurements on the same model in wind tunnels and in flight. The data obtained in flight indicated that significant disturbance were present in the free stream at the model location. These disturbances emanated from either the atmospheric environment or were generated by the F-15 aircraft. These data have provided one more significant piece of information that indicates the transition process as reflected by the experimentally measured transition Reynolds number is dominated by the free-stream disturbance intensity.

Harvey (1978)[47] developed correlations of Re_t on flat plates and sharp cones as a function of measured $\tilde{p}/\tilde{q}_\infty$ free-stream disturbance levels for a wide range of Mach numbers. Considerable improvement was made by normalizing $\tilde{p}$ with the free-stream dynamic pressure (q_∞) as compared to previous correlation using $\tilde{p}/\tilde{p}_\infty$ (see Refs. 81, 82, and 84). Figure 69 does not reflect the difference in Re_t values on a cone at $M_\infty = 4$ and a sharp plate as presented in Fig. 38. The accuracy of the correlation shown in Fig. 69 will probably be on the order ±20 to ±30%.

Theoretical and experimental studies contributing to the basic understanding of the radiated pressure field (aerodynamic noise) generated by a turbulent boundary layer were reviewed in Section 2.0. Results were presented that identified the tunnel wall turbulent-boundary-layer mean shear and displacement thickness as major parameters influenced the radiated pressure fluctuations ($\tilde{p}/\tilde{q}_\infty$).

Attempts at correlating Re_t data directly with measured $\tilde{p}/\tilde{q}_\infty$ data are hampered by inconsistencies in the measured $\tilde{p}/\tilde{p}_\infty$ data and experimental scatter (nonrepeatable) in pressure fluctuation data. There are also basic differences in the absolute levels of intensity measured using a flat plate equipped with microphones and hot-wire anemometers positioned in the free stream as discussed in Section 3.0 (Fig. 38).

Because of the inherent difficulties in obtaining radiated noise measurements and because most previously published transition data did not record the free-stream disturbance level, Pate (1967,1971,1977)[26,27,50] developed correlations of Re_t as a function of radiated noise parameters. These parameters were the tunnel-wall turbulent-boundary-layer mean parameters (C_F and δ^*) and tunnel test section size (parameter C).

Beginning with the hypothesis that $Re_t = f(C_F, \delta^*, C)$, Pate successfully developed correlation parameters for planar and sharp cone models. The details of these correlation developments can be found in Refs. 26, 27, and 50.

Presented in Fig. 70 is Pate's[50] correlations of sharp-cone and planar model transition Reynolds numbers as a function of radiated noise parameters (C_F, δ^*, and c). The sharp, flat-plate correlation represents transition Reynolds number data from 13 supersonic-hypersonic wind tunnels and covered the Mach number range from 3 to 8 and tunnel sizes from 7.9-in. to 16-ft test sections. The sharp-cone correlation represents transition Reynolds number data from 16 supersonic-hypersonic facilities and covered the Mach number range from 3 to 20 and tunnel sizes from 5- to 54-in.-diam test sections. The tunnel wall turbulent skin friction was computed using the method of van Driest II (1956)[123] and includes nonadiabatic tunnel wall effects. The tunnel wall turbulent-boundary-layer displacement thickness (δ^*) was obtained from experimental data or semi-empirical methods as discussed in Ref. 50. Tables 5 and 6 in Ref. 50 provide detailed information on test conditions, tunnel size, method of transition measurement, amounts of adjustment in Re_t values, source for δ^* values, and identify the sources for all the data presented in Fig. 70. The following empirical equations [Eqs. (2) and (3)] were developed from the correlations in Fig. 70:*

*The correlations shown in Fig. 70 are discussed in detail in Ref. 50. Slight differences exist in these equations as compared to the original correlations developed by Pate in 1967 (planar) and 1971) (cone). The constant 0.0126 in Eq. (2) was originally 0.0141 in Ref. 26 (1967). All other constants in Eqs. (2) and (3) have remained the same. The size parameter ($\bar{C}$) was modified to be $\bar{C} = 1.0$ for $C_i/C > 1.0$ as discussed in Ref. 50.

$$(Re_{t_\delta})_{\substack{\text{flat}\\\text{plates}}} = \frac{0.0126\ (C_{F_{II}})^{-2.55}\ (\bar{C})}{\sqrt{\frac{\delta^*}{C}}} \qquad (2)$$

$$(Re_{t_\delta})_{\text{cone}} = \frac{48.5\ (C_{F_{II}})^{-1.40}\ (\bar{C})}{\sqrt{\frac{\delta^*}{C}}} \qquad (3)$$

Essentially all of the data included in Fig. 70 are for model adiabatic wall conditions (T_w/T_{aw} = 1). The few data points for $T_w/T_{aw} < 1$ were for $M_\infty > 6$. It is well known that the model wall temperature (T_w/T_{aw}) can have a significant effect on the location of transition at supersonic speeds ($M_\infty \lesssim 5$).[2,18,112] Tables 5 and 6 in Ref. 50 provide a tabulation of the T_w/T_{aw} value for each data set. Based on the experimental results of Deem et al.,[39] Rhudy,[124] and Kendall,[4] it is assumed that planar and cone transition data are not a function of T_w/T_{aw} for $M_\infty \gtrsim 6$. Therefore, all the transition data included in Fig. 70 are assumed to represent adiabatic wall values.

The reader is reminded that the transition Reynolds number correlations cannot be applied to ballistic ranges, atmospheric free flight, or any test environment other than a conventional wind tunnel ($M_\infty \gtrsim 3$) because of the obvious restrictions imposed by the aerodynamic-noise-dominance hypothesis and the correlating parameters, C_F, δ^*, and C. Similarly, since the correlation was developed for finite-size wind tunnels, the proper boundary conditions for free flight are not included.

At first glance, Eqs. (2) and (3) appear to be fairly simple. However, computation of the tunnel wall turbulent-boundary-layer displacement thickness (δ^*), tunnel wall skin-friction coefficient ($C_{F_{II}}$), along with the tunnel free-stream unit Reynolds number and flow properties at the surface of an inviscid cone, become a fairly involved and lengthy process. In order to provide a systematic method for solving Eqs. (2) and (3) and to provide a completely analytical technique that can be used for adequately predicting transition locations on sharp planar and cone models at zero angle of attack, Pate (1977)[50] developed a math model and computer code to solve Eqs. (2) and (3). The only required input data are model geometry (planar or cone), axial location of model in tunnel, tunnel test section perimeters (C), tunnel wall temperature (T_w), and test conditions, P_o, T_o, or $(Re/ft)_\infty$.

The algorithms developed to solve the aerodynamic-noise-transition empirical equations for a sharp flat plate, Eq. (2), and sharp slender cone, Eq. (3) at zero angle of attack are presented in detail in Appendix C of Ref. 50. The FORTRAN program listing, operational instructions, and check cases are included in Ref. 50.

Pate[50] made extensive comparisons between the experimental data and calculations from the radiated nose-transition correlation, Eqs. (2) and (3), and the corresponding math models and FORTRAN IV Computer Code. Comparisons between the math model results of Ref. 50 and experimental transition Reynolds number data obtained on sharp flat plates (and hollow cylinders) and sharp slender-cones at zero incidence in wind tunnels varying in size (test section height) from 5 in. to 16 ft, for Mach numbers from 3 to 14, over a unit Reynolds number range from 0.1×10^6 to 2.5×10^6 per in. are presented in Figs. 71 through 80.

Variations of Re_t with Tunnel Size

Experimental data illustrating the large variation of transition Reynolds numbers on sharp flat plates and sharp slender cones with tunnel size are presented in Fig. 71 for a Mach number from 3 to 12 and $(Re/in.)_\infty = 0.20 \times 10^6$. The predicted variations of $(Re_t)_\delta$ with tunnel size and $(Re/in.)_\infty = 0.20 \times 10^6$ for a Mach number ranging from 3 to 16 are included in Fig. 71. The experimental data and the calculated results clearly illustrate the significant and monatonic increase in Re_t with increasing tunnel size. The agreement between the computed results and the experimental data is considered good. It should be noted that the computed data correspond to the correct tunnel wall temperature ratio (T_w/T_{aw}) tunnel geometry and model location as indicated in Fig. 71. Results presented in Fig. 71 show that the variation of $(Re_t)_\delta$ with tunnel size is significant for all Mach numbers ($M_\infty \gtrsim 3$). This variation must be considered when comparing $(Re_t)_\delta$ data or transition-sensitive aerodynamic data from different facilities, developing new Re_t correlations, verifying $(Re_t)_\delta$ theories, or planning wind tunnel test programs where the location of transition on the model could affect the data.

Figure 72a shows the variation in Re_t data obtained on planar models in five $M_\infty = 3$ wind tunnels having test section heights varying from 7.7 in. to 16 ft. Data obtained in the USSR by Struminsky, Kharitonau, and Cherhykh (1972)[102] have provided Re_t values at considerably higher unit Reynolds numbers than were reported in Refs. 26 and 50. It should be noted that the increase in Re_t with increasing Re/in. values appears to continue, at least up to Re/in. $\approx 2 \times 10^6$. The predicted results from the computer code are in good agreement with the experimental data and correctly predict the effects of tunnel size and unit Reynolds number.

Transition Reynolds numbers obtained in four $M_\infty \approx 8$ wind tunnels are shown in Fig. 72b. The $M_\infty = 7.5$ data obtained by Pate[50] is, to the author's knowledge, the highest unit Reynolds number wind tunnel Re_t data published. As was the case at $M_\infty = 3$, the values of $(Re_t)_\delta$ continue to increase with increasing (Re/in.) values and increasing tunnel size. The computed values are in good agreement with the experimental data.

Additional experimental data published by Pate in Ref. 50, with results from the Radiated Noise Transition Computer Code, for M_∞ = 4.5, 5.0, and 8.0 showed that variations in model axial positions within a test section will produce insignificant changes in model transition locations.

Re_t Trends with Mach Number and Unit Reynolds Number

Presented in Figs. 73 and 74 are plots of planar and cone model Re_t data as a function of unit

Reynolds numbers $(Re/in.)_\infty$ for a wide range of Mach numbers (M_∞). The Re_t data exhibit an increase with increasing unit Reynolds number. This trend is as expected and has been previously reported, e.g., see Refs. 23 and 138. The data in Figs. 73 and 74 show that the variation of Re_t with unit Reynolds number is similar over a wide range of Mach numbers and tunnel sizes.

The variations of Re_t data with Mach number for several different size tunnels are shown in Figs. 75 and 76 for planar models and sharp cone models, respectively. Variation in Re_t with M_∞ is not strongly influenced by tunnel size for either planar or cone models. These data also indicate that the changes in Re_t data with changing M_∞ is significantly greater for planar models than sharp-cone models. The estimated values of Re_t obtained from the computer code[50] are in good agreement with the experimental data except for the AEDC-VKF Tunnel D cone data at $M_\infty \approx 4$. A contributing factor to this discrepancy between the experimental data and computed values at $M_\infty \approx 4$ is the disagreement between the measured tunnel wall δ^* and the theoretical value of δ^* used in the computer code (see Appendix B of Ref. 50).

Additional comparisons between Eqs. (2) and (3) and experimental data can be found in Ref. 50. It is obvious from the results presented in Figs. 75 and 76 that transition data from different sizes of supersonic-hypersonic wind tunnels cannot be used to establish Mach number trends.

Figure 77 presents $(Re_t)_\delta$ data as a function of cone local Mach number for a free-stream Mach number of eight. The data for the 7.5- and 15.8-deg cones were first published by Stainback (1967).[127] All of the data shown in Fig. 77 were later published by Stainback (1969).[34] For a given free-stream Mach number, there are two cone angles that produce equivalent local unit Reynolds numbers but significantly different local sone surface Mach numbers (see Ref. 27 or Fig. C-1 in Appendix C of Ref. 50). Figure 77 shows that when the local Mach number was changed from approximately 4 to 7 for constant free-stream conditions [constant M_∞, constant $(Re/in.)_\infty$], there was no significant change (upward trend) with Mach number except at the lowest $(Re/in.)_\infty$ value. Recent data published by Owen, Horstman, Stainback (1976)[105] using the same approach confirm the invariance of $(Re_t)_\delta$ with M_∞ as shown in Fig. 78.

The experimental data presented in Figs. 77 and 78 are particularly significant to the transition-aerodynamic noise dominance theory prepared by Pate (1967, 1971, 1974, 1977).[26-28,50,128] The aerodynamic-noise-transition hypothesis formulated by Pate and the resulting empirical equation developed [Eqs. (2) and (3)] predict no change in $(Re_t)_\delta$ with changing M_∞, provided the free-stream conditions M_∞ and $(Re/in.)_\infty$ do not change. Predictions from the aerodynamic-noise-transition computer code [Eq. (3) and Appendix C of Ref. 50] are presented in Fig. 78, and the agreement with the data is considered good. Note that the computer code predicted the slight increase in $(Re_t)_\delta$ with increasing M_∞ that is evident in the data. This is a result of the θ_c values not being selected to provide a constant $(Re/in.)_\delta$ value as was the case for data shown in Fig. 77.

It should be pointed out that the 5- and 20-deg cone angles produce equivalent local unit Reynolds numbers as do the 7.5- and 15.8-deg cones for $M_\infty = 8$ (see Fig. 77) (see Fig. C-1 of Ref. 50). However, for the local unit Reynolds number conditions to have been equivalent for both sets of cone data as listed in Fig. 77, there would necessarily have been a 10 to 15% difference in $(Re/in.)_\infty$. A 15% difference in $(Re/in.)_\infty$ would produce a maximum change in Re_t of approximately 10%, and this is well within the scatter of the data shown in Fig. 77. Consequently, it seems justified to compare the four sets of data directly.

The results shown in Figs. 73 through 78 show that a large part of Re_t variation with unit Reynolds number and Mach number in wind tunnels is related to the presence of free-stream aerodynamic noise disturbances. Pate[27,50] developed the following empirical equation for the ratio of cone to planar transition Reynolds numbers:

$$\frac{(Re_t)_{\delta,\ cone}}{(Re_t)_{\delta,\ planar}} = \frac{\text{Eq. (3)}}{\text{Eq. (2)}} = 3880\ (C_F)^{1.15}\ \frac{(\bar{c})_{cone}}{(\bar{c})_{flat\text{-}plate}} \qquad (4)$$

Computed transition ratios using Eq. (4) are presented in Fig. 79 for a large range of tunnel sizes, Mach numbers, and $(Re/in.)_\infty$ values. There is reasonable agreement between Eq. (4) results and the experimental data. The data also show a decrease in the transition ratio with an increase in tunnel size. Additional data and discussion can be found in Ref. 50.

Many investigators have referenced the analytical analysis and minimum critical Reynolds number criteria of Tetervin[129,130] and Battin and Lin[131] when attempting to explain the cone-planar $(Re_t)_\delta$ ratios of approximately three that have been observed experimentally. Note that the cone/flat plate Re_t ratio varies from ≈ 2.5 at $M_\infty = 3$ to ≈ 1 at $M_\infty \approx 8$ to 10. Note that the correlation of Harvey,[47] Fig. 69, indicated equivalent Re_t values for cones and flat plates at low disturbance levels, i.e. high Mach ~~number~~.

Presented in Fig. 80 is a summary plot of the measured versus the computed Re_t values for the 262 data points used by Pate (1977)[50] in developing the transition-aerodynamic-noise correlations and empirical equations, Eqs. (2) and (3), shown in Fig. 70. The standard deviation (σ) was 11.6% as determined from the 262 data points. Two other transition studies have published standard deviation values for empirical prediction methods. Deem, et al. (1965)[39] found a standard deviation of 33% based on 291 data points as was shown in Fig. 57. Beckwith and Bertran (1972)[33] found $\sigma \approx 29$ to 41% (see Fig. 58) for empirical equations developed at NASA-LRC. Based on a direct comparison of the standard deviation values, the method of Pate (1977)[50] provided a considerably improved method for predicting transition locations on planar and sharp cone models in wind tunnels for $M_\infty > 3$.

7.0 Concluding Remarks

Effects of free-stream disturbances on boundary-layer transition on sharp flat plates and sharp

slender cones in conventional supersonic-hypersonic wind tunnels, can be summarized as follows:

1. Experimental studies have shown that free-stream disturbance intensities present in subsonic-transonic-supersonic-hypersonic wind tunnels have a dominating effect on boundary-layer transition on simple geometries (flat plates and sharp cones). Free-stream disturbances also have a measurable effect on other boundary-layer characteristics.

2. At subsonic speeds the dominant disturbance is turbulence (velocity fluctuation, $\tilde{u}/U_\infty$) and/or acoustic sound ($\tilde{p}/q_\infty$). At transonic speeds the dominant disturbance is acoustic noise ($\tilde{p}/q_\infty$) generated by the test section porous or slotted walls. At supersonic-hypersonic Mach numbers radiated noise ($\tilde{p}$) from the turbulent boundary layer on the tunnel walls is the dominant source of disturbance.

3. Model transition Reynolds number data have been shown to correlate with the free-stream disturbance intensities levels. At subsonic speeds the correlating parameter is $\tilde{u}/U_\infty$ and at transonic-supersonic-hypersonic speeds it is $\tilde{p}/q_\infty$.

4. Transition Reynolds numbers measured in supersonic-hypersonic tunnels are strongly dependent on tunnel size. Data obtained in supersonic wind tunnels ($M_\infty \gtrsim 3$) having test section heights from 0.5 to 16 ft have demonstrated a significant and monatonic increase in transition Reynolds numbers with increasing tunnel size. Free-stream radiated noise measurements have shown that the intensity levels decrease with increasing tunnel size.

5. Correlations of transition Reynolds numbers as a function of the radiated noise parameters [tunnel wall C_F and δ^* values and tunnel circumference (c)] have been successfully developed for $3 \lesssim M_\infty \lesssim 20$. The resulting empirical equations, $Re_t = f(C_F, \delta^*, c)$, math model, and FORTRAN IV digital computer code will accurately predict transition locations on sharp flat plates and cones in all sizes of conventional supersonic-hypersonic wind tunnels. The standard deviation (σ) between measured and computed Re_t values as determined from 262 data points was 11.6%

6. The ratio of cone transition Reynolds numbers to flat-plate values does not have a constant value of three, as often assumed. The ratio will vary from a value of near three at $M_\infty = 3$ to near one at $M_\infty = 8$. The exact value is unit Reynolds number and tunnel size dependent. The aerodynamic-noise-transition empirical equations (above) predict that for $M_\infty \gtrsim 10$ and $(Re/in.) \gtrsim 0.4 \times 10^6$, the ratio will be less than one.

7. Radiated noise dominance of the transition process offers an explanation for the unit Reynolds number effect in conventional supersonic-hypersonic wind tunnels.

8. The effect of tunnel size on transition Reynolds numbers must be considered in the development of data correlations, in the evaluation of theoretical math models and in the analysis of transition-sensitive aerodynamic data.

9. Variation of Re_t with Mach number effect cannot be determined from data obtained in various size conventional supersonic-hypersonic wind tunnels because of the adverse effect of radiated noise.

10. The boundary-layer trip correlation developed by van Driest and Blumer (wherein the effective transition location "knee" can be predicted) has been shown to be valid for different sizes of wind tunnels and is not dependent on the free-stream radiated noise levels.

References

[1] Morkovin, M. V., "On the Many Faces of Transition," Reprinted from Viscous Drag Reduction, Plenum Press, 1969.

[2] Morkovin, M. V., "Critical Evaluation of Transition from Laminar to Turbulent Shear Layers with Emphasis on Hypervelocity Traveling Bodies," AFFDL-TR-68-149, March 1969.

[3] Reshotko, E., "Stability Theory as a Guide to the Evaluation of Transition Data," AIAA Journal, Vol. 7, No. 6, June 1969, pp. 1086-1091.

[4] Kendall, J. M., "Wind Tunnel Experiments Relating to Supersonic and Hypersonic Boundary-Layer Transition," AIAA Journal, Vol. 13, No. 3, March 1975, pp. 290-299.

[5] Mack, L. M., "Linear Stability Theory and the Problem of Supersonic Boundary-Layer Transition," AIAA Journal, Vol. 13, No. 3, March 1975, pp. 278-289.

[6] Jaffe, N. A., Okamura, T. T., and Smith, A. M. O., "The Determination of Spatial Amplification Factors and Their Application to Predicting Transition," AIAA Paper No. 69-10, 7th Aerospace Sciences Meeting. January 1969.

[7] Emmons, H. W., "The Laminar-Turbulent Transition in a Boundary Layer," Part I, Journal of the Aeronautical Sciences, Vol. 18, No. 7, July 1951, pp. 490-498.

[8] Schubauer, G. B. and Skranstad, H. K., "Laminar-Boundary-Layer Oscillations and Transition on a Flat Plate," NACA Report 909, 1948.

[9] Gazley, C. Jr., "Boundary-Layer Stability and Transition in Subsonic and Supersonic Flow," Journal of the Aeronautical Sciences, Vol. 20, No. 1, January 1953, pp. 19-28.

[10] Czarnecki, K. R. and Sinclair, A. R., "Factors Affecting Transition at Supersonic Speeds," NACA RM L53I18a, November 1953.

[11]Laufer, J. and Marte, J. E., "Results and a Critical Discussion of Transition-Reynolds Numbers Measurements on Insulated Cones and Flat Plates in Supersonic Wind Tunnels," JPL Report No. 20-96, November 1965.

[12]Brinich, P. F. and Sands, N., "Effect of Bluntness on Transition for a Cone and a Hollow Cylinder at Mach 3.1," NACA TN 3979, May 1957.

[13]Brinich, P. F., "Recovery Temperature Transition and Heat-Transfer Measurements at Mach 5," NASA TN D-1047, August 1961.

[14]Owen, P. R. and Randall, D. G., "Boundary-Layer Transition on a Swept-Back Wing," RAE Tech. Memo Aero. 277, June 1952.

[15]Dryden, H. L., "Review of Published Data on the Effect of Roughness on Transition from Laminar to Turbulent Flow," Journal of the Aeronautical Sciences, July 1953, pp. 477-482.

[16]van Driest, E. R. and Boison, J. C., "Experiments on Boundary-Layer Transition at Supersonic Speeds," Journal of the Aeronautical Sciences, Vol. 24, No. 12, December 1957, pp. 885-899.

[17]van Driest, E. R. and Blumer, C. B., "Boundary-Layer Transition: Free-Stream Turbulence and Pressure Gradient Effects," AIAA Journal, Vol. 1, No. 6, June 1963, pp. 1303-1306.

[18]van Driest, E. R. and Blumer, C. B., "Boundary-Layer Transition at Supersonic Speeds: Roughness Effects with Heat Transfer," AIAA Journal, Vol. 6, No. 4, April 1968, pp. 603-607.

[19]Wisniewski, R. J. and Jack, J. R., "Recent Studies on the Effect of Cooling on Boundary-Layer Transition at Mach 4," Journal of the Aeronautical Sciences, Vol. 28, No. 25, 1961.

[20]Richards, B. E. and Stollery, J. L., "Further Experiments on Transition Reversal at Hypersonic Speeds," AIAA Journal, Vol. 4, No. 12, December 1966, pp. 2224-2226.

[21]Potter, J. L., "Boundary-Layer Transition on Supersonic Cones in an Aeroballistic Range," AIAA Journal, Vol. 13, No. 3, March 1975, pp. 270-277.

[22]Whitehead, A. H., Jr., "Flow-Field and Drag Characteristics of Several Boundary-Layer Tripping Elements in Hypersonic Flow," NASA TN D-5454, October 1969.

[23]Potter, J. L. and Whitfield, J. D., "Effects of Slight Nose Bluntness and Roughness on Boundary-Layer Transition in Supersonic Flow," Journal of Fluid Mechanics, Vol. 12, Pt. 4, April 1962.

[24]Chapman, G. T., "Some Effects of Leading-Edge Sweep on Boundary-Layer Transition at Supersonic Speeds," NASA TN D-1075, September 1961.

[25]Pate, S. R., "Experimental and Analytical Investigation at Boundary-Layer Transition on Swept Wings at Mach Numbers 2.5 to 5," Thesis Master of Science Degree, University of Tennessee Space Institute, March 1965.

[26]Pate, S. R. and Schueler, C. J., "Radiated Aerodynamic Noise Effects on Boundary-Layer Transition in Supersonic and Hypersonic Wind Tunnels," AIAA Journal, Vol. 7, No. 3, March 1969, pp. 450-457; also AEDC-TR-67-236.

[27]Pate, S. R., "Measurements and Correlations of Transition Reynolds Numbers on Sharp Slender Cones at High Speeds," AIAA Journal, Vol. 9, No. 6, June 1971, pp. 1082-1090; also AEDC-TR-69-172.

[28]Pate, S. R., "Supersonic Boundary-Layer Transition -- Effects of Roughness and Free-Stream Disturbances," AIAA Journal, Vol. 9, No. 5, May 1971, pp. 797-803.

[29]Kendall, J. M., Jr., "Supersonic Boundary-Layer Transition Studies," JPL Space Programs Summary 37-62, Vol. III, 1970.

[30]Kendall, J. M., Jr., "Wind Tunnel Experiments Relating to Supersonic and Hypersonic Boundary-Layer Transition," AIAA Paper No. 74-133.

[31]Owen, F. K., "Transition Experiments on a Flat Plate at Subsonic and Supersonic Speeds," AIAA Paper No. 69-9, 7th Aerospace Sciences Meeting, January 1969.

[32]Richards, B. E., "Transition and Turbulent Boundary Layers on a Cold Flat Plate in Hypersonic Flow," The Aeronautical Quarterly, Vol. XVIII, August 1967, pp. 237-258.

[33]Beckwith, I. E. and Bertram, M. H., "A Survey of NASA Langley Studies on High-Speed Transition and the Quiet Tunnel," NASA TM X-2566, July 1972.

[34]Stainback, C. P., "Effect of Unit Reynolds Number, Nose Bluntness, Angle of Attack, and Roughness on Transition on a 5° Half-Angle Cone at Mach 8," NASA TN D-4961, January 1969.

[35]Dougherty, N. S. and Steinle, F. W., Jr., "Transition Reynolds Number Comparisons in Several Major Transonic Tunnels," AIAA Paper No. 74-627, 1974.

[36]Dougherty, N. S., Jr. and Fisher, D. F., "Boundary-Layer Transition on a 10-Degree Cone: Wind Tunnel/Flight Data Correlation," AIAA Paper No. 80-0154, AIAA 18th Aerospace Sciences Meeting, January 1980.

[37]Stetson, K. F., "Effect of Bluntness and Angle of Attack on Boundary Layer Transition on Cones and Biconic Configurations," AIAA Paper No. 79-0269, 17th Aerospace Sciences Meeting, January 1979.

[38]Fehrman, A. L. and Masek, R. U., "Study of Uncertainties of Predicting Space Shuttle Thermal Environment," MDC E0639, June 1972.

[39]Deem, R. E., Erickson, C. R., and Murphy, J. S., "Flat-Plate Boundary-Layer Transition at Hypersonic Speeds," FDL-TDR-64-129, October 1964; also AIAA Paper No. 65-128.

[40]Granville, P. S., "The Prediction of Transition from Laminar to Turbulent Flow in Boundary Layers on Bodies of Revolution," Report No. 3900 (AD787060), September 1974.

[41]Smith, A. M. O. and Gamberoni, N., "Transition, Pressure Gradient and Stability Theory," Douglas Aircraft Report No. ES26388, August 1956.

[42]Michel, R., "Determination du Point de Transition de Calcul de la Trainee des Profils en Incompressible," La Recherche Aeronautique, No. 24, 1951.

[43]Adams, J. C., Jr., "Three-Dimensional Laminar Boundary-Layer Analysis of Upwash Patterns on Sharp Cones at Angle of Attack," AEDC-TR-71-215 (AD736880), December 1971.

[44]Adams, J. C., Jr. and Martindale, W. R., "Hypersonic Lifting Body Boundary-Layer Analysis at High Angles of Incidence," Journal of Spacecraft and Rockets, Vol. II, No. 10, October 1974, pp. 721-727; also AEDC-TR-73-2, February 1973.

[45]Wells, C. S., Jr., "Effects of Free-Stream Turbulence on Boundary-Layer Transition," AIAA Journal, Vol. 5, No. 1, January 1967, pp. 172-174.

[46]Mack, L. M., "Transition and Laminar Instability," JPL Publication 77-15, May 1977.

[47]Harvey, W. D., "Influence of Free-Stream Disturbances on Boundary-Layer Transition," NASA Technical Memorandum 78635, April 1978.

[48]Hall, D. J. and Gibbings, J. C., "Influence of Stream Turbulence and Pressure Gradient upon Boundary Layer Transition," Journal Mechanical Engineering Science, Vol. 14, No. 2, 1972, pp. 124-146.

[49]Shamroth, S. J. and McDonald, H., "Assessment of a Transition Boundary-Layer Theory at Low Hypersonic Mach Numbers," NASA CR-2131, Langley

[50]Pate, S. R., "Dominance of Radiated Aerodynamic Noise on Boundary-Layer Transition in Supersonic-Hypersonic Wind Tunnels - Theory and Application," AEDC-TR-77-107, March 1978; also PhD Dissertation, University of Tennessee, March 1977.

[51]Smith, A. M. O., Review of "The M&M Tapes," an AIAA Recorded Lecture Series Review: "High Speed Boundary Layer Stability and Transition," Astronautics and Aeronautics, April 1972.

[52]Kovasznay, L. S. G., "Turbulence in Supersonic Flow," Journal of the Aeronautical Sciences, Vol. 20, No. 10, October 1953, pp. 657-674.

[53]Dryden, H. L., "Air Flow in the Boundary Layer near a Plate," NACA Report No. 562, 1936.

[54]Hall, A. and Hislop, G. S., "Experiments on the Transition of the Laminar Boundary Layer on a Flat Plate," R&M 1843, 1938, British Aeronautical Research Committee.

[55]Boltz, F. W., Kenyon, G. C., and Allen, C. Q., "The Boundary-Layer Transition Characteristics of Two Bodies of Revolution, A Flat Plate, and an Unswept Wing in a Low-Turbulence Wind Tunnel," NASA Tec-nical Note D-309.

[56]Spangler, J. G. and Wells, C. S., Jr., "Effects of Free-Stream Disturbances on Boundary-Layer Transition," AIAA Journal, March 1968, pp. 543-545.

[57]Uberoi, M. S., "Effect of Wind-Tunnel Contraction on Free-Stream Turbulence," Journal of the Aeronautical Sciences, August 1956, pp. 754-764.

[58]Varner, M. O., "Noise Generation in Transonic Tunnels," AIAA Journal, Vol. 13, No. 11, November 1975, pp. 1417-1418; also AIAA Paper No. 74-633, Bethesda, MD., 1974; also AEDC-TR-74-126, April 1975, AEDC.

[59]Credle, O. P. and Carleton, W. E., "Determination of Transition Reynolds Number in the Transonic Mach Number Range," AEDC-TR-70-218 (AD875995), October 1970.

[60]Credle, O. P., "Perforated Wall Noise in the AEDC-PWT 16-ft and 4-ft Transonic Tunnels," AEDC-TR-71-216 (AD888561L), October 1971.

[61]Owen, F. K., "Evaluation of Flow Quality in Two NASA Transonic Wind Tunnels," Paper No. 79-1532, AIAA 12th Fluid and Plasma Dynamics Conference, July 1979.

[62]Mabey, D. G., "Boundary Layer Transition Measurements on the AEDC 10° Cone in Three RAE Wind Tunnels and their Implications," Royal Aircraft Establishment Technical Report 76077, June 1976.

[63]Morkovin, M. V., "On Transition Experiments at Moderate Supersonic Speeds," Journal of the Aeronautical Sciences, Vol. 24, No. 7, July 1957, pp. 480-486.

[64]Morkovin, M. V., "On Supersonic Wind Tunnels with Low Free-Stream Disturbances," Journal of Applied Mechanics, Tran. ASME, Vol. 26, Series E, June 1959, pp. 319-324.

[65]Laufer, J., "Sound Radiation from a Turbulent Boundary Layer," Jet Propulsion Laboratory Report JPL/CIT TR-32-119, November 1961.

[66]Donaldson, J. C. and Wallace, J. P., "Flow Fluctuation Measurements at Mach Number 4 in the Test Section of the 12-Inch Supersonic Tunnel D," AEDC-TR-71-143 (AD723630), August 1971.

[67]Brinich, P. F., "Effect of Leading-Edge Geometry on Boundary-Layer Transition at $M_\infty = 3.1$," NACA TN 3659, 1956.

[68]Ross, R., "Influence of Total Temperature on Transition in Supersonic Flow," AIAA Journal, Vol. 11, No. 4, April 1973, pp. 563-565.

[69]Laufer, J., "Aerodynamic Noise in Supersonic Wind Tunnels," JPL Progress Report No. 20-378, February 1959; also Journal of the Aerospace Sciences, Vol. 28, No. 9, September 1961, pp. 685-692.

[70]Jet Propulsion Research Summary No. 36-6, Vol. II, January 1961.

[71]Kistler, A. L. and Chen, W. S., "Fluctuating Pressure Field in a Supersonic Turbulent Boundary Layer," Journal of Fluid Mechanics, Vol. 16, Part I, May 1963, pp. 41-64.

[72]Laufer, J., "Some Statistical Properties of the Pressure Field Radiated by a Turbulent Boundary," Physics of Fluids, Vol. 7, No. 8, August 1964, pp. 1191-1197.

[73]Phillips, O. M., "On the Generation of Sound by Supersonic Turbulent Shear Layers," Journal of Fluid Mechanics, Vol. 9, Part 1, September 1960, pp. 1-28.

[74]Williams, J. E. F. and Maidanik, G., "The Mach Wave Field Radiated by Supersonic Turbulent Shear Flows," Journal of Fluid Mechanics, Vol. 21, Part 4, 1965, pp. 641-657.

[75]Morkovin, M. V., "Fluctuation and Hot-Wire Anemometry in Compressible Flows," AGARDograph 24, North Atlantic Treaty Organization Advisory Group for Aeronautical Research and Development, Paris, France, November 1956.

[76]Bell, D. R., "Boundary-Layer Characteristics at Mach Numbers 2 through 5 in the Test Section of the 12-Inch Supersonic Tunnel (D)," AEDC-TDR-63-192 (AD418711), September 1963.

[77]Donaldson, J. C., "The Development of Hot-Wire Anemometry Test Capabilities for $M_\infty = 8$ Applications," AEDC-TR-76-88 (AD-A029570), September 1976.

[78]Demetriades, A., "New Experiments on Hypersonic Boundary Layer Stability Including Wall Temperature Effects," reprinted from Proceedings of the 1978 Heat Transfer and Fluid Mechanics Institute, Clayton T. Crowe and W. L. Grosshandler, Editors, Stanford University Press, 1978.

[79]Wagner, R. D., Maddalon, D. V., Weinstein, L. M., "Influence of Measured Free-Stream Disturbances on Hypersonic Boundary Layer Transition," AIAA Paper No. 69-704, AIAA Fluid and Plasma Dynamics Conference, June 1969.

[80]Wagner, R. D., Maddalon, D. V., and Weinstein, L. M., "Influence of Measured Free-Stream Disturbances on Hypersonic Boundary-Layer Transition," AIAA Journal, Vol. 8, No. 9, September, 1976.

[81]Fischer, M. C. and Wagner, R. D., "Transition and Hot-Wire Measurements in Hypersonic Flow," AIAA Journal, Vol. 10, No. 10, October 1972, pp. 1326-1332; also AIAA Paper No. 72-181, January 1972 by Stainback, Fischer, and Wagner.

[82]Stainback, P. C. and Wagner, R. D., Jr., "A Comparison of Measured Wind-Tunnel Disturbance Levels Measured with a Hot-Wire Anemometer and Pitot Pressure Probe," AIAA Paper No. 72-1002, September 1972.

[83]Stainback, P. C., "Part I: Measurement of Transition Reynolds Numbers and Surface Fluctuating Pressures at a Local Mach Number of 5," and "Part II: Transition and Hot-Wire Measurements Up to a Local Mach Number of 16 in Helium," by M. C. Fischer and R. D. Wagner, Effects of Wind-Tunnel Disturbances on Hypersonic Boundary-Layer Transition, AIAA Paper No. 72-181, AIAA 19th Aerospace Sciences Meeting, January 1972.

[84]Beckwith, I. E., "Development of a High Reynolds Number Quiet Tunnel for Transition Research," AIAA Journal, Vol. 13, No. 3, March 1975, pp. 300-306.

[85]Harvey, W. D., Stainback, P. C., Anders, J. B., and Cary, A. M., "Nozzle Wall Boundary-Layer Transition and Freestream Disturbances at Mach 5," AIAA Journal, Vol. 13, No. 3, pp. 307-314, March 1975.

[86]Harvey, W. D., Berger, M. H., and Stainback, P. C., "Experimental and Theoretical Investigation of a Slotted Noise Shield Model for Wind Tunnel Walls," AIAA Paper No. 74-624, AIAA 8th Aerodynamic Testing Conference, July 1974.

[87]Stainback, P. C. and Anders, J. B., "Part I: Disturbance Measurements in a Mach 5 Wind Tunnel," and "Part II: Measurements and Calculations of Laminar, Transitional, and Turbulent Boundary Layers on the Wall of a Mach 5 Nozzle," by Harvey, W. D., Cary, A. M., and Harris, J. E., An Investigation of Boundary-Layer Transition on the Wall of a Mach 5 Nozzle, AIAA Paper No. 74-136, AIAA 12th Aerospace Sciences Meeting, January-February 1974.

[88]Anders, J. B., Stainback, P. C., and Beckwith, I. E., "New Technique for Reducing Test Section Noise in Supersonic Wind Tunnels," AIAA Journal, Vol. 18, No. 1, January 1980, pp. 5-6.

[89]Michel, R., "Effects of Turbulence and Noise on Aerodynamic Phenomena and the Result of a Wind Tunnel Test," AGARD-R-615, ONERA, Toulouse, France, November 1973.

[90]Mabey, D. G., "The Influence of Flow Unsteadiness on Wind Tunnel Measurements at Transonic Speeds," Royal Aircraft Establishment, LaWs Paper No 38, April 1972.

[91]Green, J. E., "On the Influence of Free Stream Turbulence on a Turbulent Boundary Layer, as it Relates to Wind Tunnel Testing at Subsonic Speeds," Royal Aircraft Establishment TR 72201, October 1972.

[92]Meier, H. U., "The Response of Turbulent Boundary Layers to Small Turbulence Levels in the External Free Stream," ICAS Paper No. 76-05, The Tenth Congress of the International Council of the Aeronautical Sciences, Ottawa, Canada, October 1976.

[93]Meier, H. U., "The Effect of Velocity Fluctuations and Nonuniformities in the Free Stream on the Boundary Layer Development," presented at the Symposium on turbulent shear flows, April 18-20, 1977, University Park, Pennsylvania.

[94]Meier, H. U. and Kreplin, H. P., "The Influence of Turbulent Velocity Fluctuations and Integral Length Scales of Low Speed Wind Tunnel Flow on the Boundary Layer Development," AIAA Paper No. 78-800, AIAA 10th Aerodynamic Testing Conference, San Diego, California, April 1978.

[95]Meier, H. U. and Kreplin, H. P., "Influence of Freestream Turbulence on Boundary-Layer Development," AIAA Journal, Vol. 18, No. 1, January 1980.

[96]Benek, J. A., "Effects of Acoustic and Vortical Disturbances on the Turbulent Boundary Layer at Free-Stream Mach Number 0.5," AEDC-TR-77-73, December 1977.

[97]Werle, M. J., Mook, D. T., and Tang, H., "Effect of Free-Stream Vorticity on Boundary-Layer Stability," Virginia Polytechnica Institute Report No. VPI-E-72-2, February 1972.

[98]Vrebalovich, T., Discussion on "Supersonic Wind Tunnels with Low Free-Stream Disturbances," by M. V. Morkovin, Journal of Applied Mechanics, Trans. ASME, June 1960, pp. 362-364.

[99]Bergstron, E. R. and Raghunathan, S., "Aerodynamic Noise and Boundary-Layer Transition Measurements in Supersonic Test Facilities," AIAA Journal, Vol. 10, No. 11, November 1972, pp. 1531-1532.

[100]Ross, R., "Boundary-Layer Transition on the Same Model in Two Supersonic Wind Tunnels," AIAA Journal, Vol. 12, No. 7, July 1974, pp. 992-993.

[101]LaGraff, J. E., "Experimental Studies of Hypersonic Boundary Layer Transition," Oxford University, Rept. No. 1104/70, May 1970.

[102]Struminskiy, V. V., Kharitonov, A. M., and Chernykh, V. V., "Experimental Study of the Transitions of a Laminar Boundary Layer into a Turbulent Layer at Supersonic Velocities," FTD-45-23-1793-72.

[103]Kharitonov, A. M. and Chernykh, V. V. "Nature of the Influence of the Unit Reynolds Number on Supersonic Boundary Layer Transition," NASA Tech. Translation, NASA-TT-F-16, 146, August 1974, (translated from Russian, January 1975).

[104]Bergstrom, E. R., et al., "Flat Plate Boundary Layer Transition in the LUT Gun Tunnel: A Transition-Radiated Aerodynamic Noise Correlation for Gun Tunnel and Convention Wind Tunnel Data at Supersonic Hypersonic Mach Numbers," N72 12161, August 1971, Loughborough University of Technology, Leicestershire, England.

[105]Owen, F. K., Horstman, C. C., Stainback, P. C., and Wagner, R. D., "Comparison of Wind Tunnel Transition and Freestream Disturbance Measurements," AIAA Journal, Vol. 13, No. 3, March 1975, pp. 266-269; also NASA TN D-7453, 1976.

[106]Potter, J. L. and Whitfield, J. D., "Boundary-Layer Transition under Hypersonic Conditions," AGARD Specialists Mtg. on Recent Developments in Boundary Layer Research, AGARDograph 97, Part III; also AEDC-TR-65-99 (AD462716), 1965.

[107]Donaldson, J. C., "Personal Communication," February 1980.

[108]Kistler, E. L., "Boundary-Layer Transition: A Review of Theory, Experiment, and Related Phenomena," NASA-CR-128450, February 1971 (Lockheed Electronics Co., Houston, Texas).

[109]Tetervin, N., "Am Empirical Equation for Predicting of Transition Location on Cones in Supersonic-Hypersonic Flight," NOLTR-73-127, June 1973.

[110]Reshotko, E. L., "Boundary Layer Stability and Transition," Conference on Boundary Layer Concepts in Fluid Mechanics, University of Massachusetts, July 1969.

[111]Hanner, O. M, Jr. and Schmitt, D. A., "A Review of Boundary-Layer Transition with Emphasis upon Space Shuttle Design Considerations," in "Space Systems and Thermal Technology for the 70's," ASME 70 HT/SPT-18, June 1970.

[112]White, F. M., Viscous Fluid Flow, McGraw-Hill, New York, 1974.

[113]Schlichting, H., Boundary Layer Theory, 4th Edition, McGraw-Hill, 1960.

[114]van Driest, E. R. and McCauley, W. D., "The Effect of Controlled Three-Dimensional Roughness on Boundary-Layer Transition at Supersonic Speeds," Journal of the Aeronautical Sciences, Vol. 27, No. 4, April 1960, pp. 261-271.

[115]van Driest, E. R. and Blumer, C. B., "Boundary-Layer Transition at Supersonic Speeds -- Three-Dimensional Roughness Effects (Spheres)," Journal of the Aeronautical Sciences, Vol. 29, No. 8, August 1962, pp. 909-916.

[116]Whitfield, J. D. and Iannuzzi, F. A., "Experiments on Roughness Effects on Cone Boundary-Layer Transition up to Mach 16," AIAA Journal, Vol. 7, No. 3, March 1969, pp. 465-470.

[117]Pate, S. R. and Eaves, R. H., Jr., "Sensitivity of Boundary-Layer Transition to Surface Irregularities for Space Shuttle Application," Journal of Spacecraft and Rockets, Vol. 10, No. 12, December 1973, pp. 813-814.

[118]Stalmach, C. J., Jr. and Goodrich, W. D., "Aeroheating Model Advancements Featuring Electroless Metallic Plating," Proceedings of AIAA 9th Aerodynamic Testing Conference, Arlington, Texas, June 1976.

[119]Hopkins, E. J., Jillie, D. W., and Sorensen, Virginia L., "Charts for Estimating Boundary Layer Transition on Flat Plates," NASA TN-D-5846, June 1970.

[120]Boudreau, A. H., "Artificially Induced Boundary Layer Transition on Blunt-Slender-Cones Using Distributed Roughness and Spherical Type Tripping Devices at Hypersonic Speeds," AIAA Paper No. 78-1127, AIAA 11th Fluid and Plasma Dynamics Conference, Seattle, Washington, July 1978.

[121]Reda, D. C. and Raper, R. M., "Measurements of Transition-Front Asymmetries on Ablating Graphite Nosetips in Hypersonic Flight," AIAA Paper No. 79-0268R, reprinted from AIAA Journal, Vol. 17, No. 11, November 1979, p. 1201.

[122]Whitfield, J. D. and Dougherty, N. S., Jr., "A Survey of Transition Research at AEDC," Paper No. 25, AGARD Fluid Dynamics Panel Symposium on Laminar-Turbulent Transition, Lyngby, Denmark, May 2-4, 1977, AGARD CP No. 224, October 1977; also AEDC-TR-77-52 (AD-A041740, July 1977.

[123]van Driest, E. R., "The Problem of Aerodynamic Heating," Aeronautical Engineering Review, Vol. 15, No. 10, October 1956, pp. 26-41.

[124]Rhudy, J. P., "Effects of Uncooled Leading-Edge on Cooled-Wall Hypersonic Flat Plate Boundary-Layer Transition," AIAA Journal, Vol. 8, No. 3, March 1970, pp. 576-577.

[125] Nagel, A. L., Savage, R. T., and Wanner, R., "Investigation of Boundary Layer Transition in Hypersonic Flow at Angle of Attack," AFFDL-TR-66-122, August 1966.

[126] Whitfield, J. D. and Potter, J. L., "The Influence of Slight Leading-Edge Bluntness on Boundary-Layer Transition at a Mach Number of Eight," AEDC-TDR-64-18 (AD431533), March 1964.

[127] Stainback, P. C., "Some Effects of Roughness and Variable Entropy on Transition at a Mach Number of 8," AIAA Paper No. 67-132, January 1967.

[128] Pate, S. R., "Comparison of NASA Helium Tunnel Transition Data with Noise-Transition Correlation," reprinted from AIAA Journal, Vol. 12, No. 11, November 1974, pp. 1615.

[129] Tetervin, N., "A Discussion of Cone and Flat-Plate Reynolds Numbers for Equal Ratios of the Laminar Shear to the Shear Caused by Small Velocity Fluctuations in a Laminar Boundary Layer," NACA TN 4078, August 1957.

[130] Tetervin, N., "An Estimate of the Minimum Reynolds Number for Transition from Laminar to Turbulent Flow by Means of Energy Considerations," Journal of the Aerospace Sciences, Vol. 28, No. 2, February 1961, pp. 160-161; also NAVORD Report 6854 (AD437345), January 1961.

[131] Battin, R. H. and Lin, C. C., "On the Stability of the Boundary Layer over a Cone," Journal of the Aeronautical Sciences, Vol. 17, No. 7, July 1950, pp. 453-454.

[132] Coles, D., "Measurements of Turbulent Friction on a Smooth Flat Plate in Supersonic Flow," Journal of the Aeronautical Sciences, Vol. 21, No. 7, July 1954, pp. 433-448.

[133] Rogers, Ruth H., "Boundary Layer Development in Supersonic Shear Flow," AGARD Report 269, April 1960.

[134] Lees, L. and Lin, C. C., "Investigation of the Stability of the Laminar Boundary Layer in a Compressible Fluid," NACA TN 1115, September 1946.

[135] Laufer, J. and Vrebalovich, T., "Stability and Transition of a Supersonic Laminar Boundary Layer on an Insulated Flat Plate," Journal of Fluid Mechanics, Vol. 9, 1960, pp. 257-299.

[136] Liepman, Hans W., "Investigation of Laminar Boundary-Layer Stability and Transition on Curved Boundaries," NACA ACR 3H30, August 1943.

[137] Benek, J. A. and High, M. D., "A Method for the Prediction of the Effects of Free-Stream Disturbances on Boundary-Layer Transition," AEDC-TR-73-158, October 1973; also AIAA Journal, Vol. 12, No. 10, pp. 1425-1427, October 1974.

[138] Potter, J. L., "The Unit Reynolds Number Effect on Boundary Layer Transition," PhD Dissertation, Vanderbilt University, Nashville, Tennessee, May 1974.

[139] McCauley, W. D., Saydah, A. R., and Bueche, J. F., "Effect of Spherical Roughness on Hypersonic Boundary-Layer Transition," AIAA Journal, Vol. 4, No. 12, December 1966, pp. 2142-2148.

[140] Everhart, P. E. and Hamilton, H. H., "Experimental Investigation of Boundary-Layer Transition on a Cooled 7.5° Total-Angle Cone at Mach 10," NASA TN-D-4188, October 1957.

[141] Sanator, R. J., DeCarlo, J. P., and Torillo, D. T., "Hypersonic Boundary-Layer Transition Data for a Cold-Wall Slender Cone," AIAA Journal, Vol. 3, No. 4, April 1965, pp. 758-760.

Nomenclature

b	Model leading-edge thickness at a specific location
$\bar{b}$	Average value of model leading-edge thickness
C	Tunnel test section circumference
C_1	Tunnel test section circumference of 12- x 12-in. tunnel ($C_1 = 48$ in.)
$C_{F_{II}}$	Mean turbulent skin-friction coefficient calculated using method of van Driest-II
$\tilde{e}$	Root-mean-square of the hot-wire voltage fluctuation
$G(f)$	Normalized energy density distribution function, $(Hz)^{-1}$
f	Frequency, cycles/sec
H, h	Enthalpy
k	Diameter of roughness element
$\bar{k}$	Total height of roughness element above model surface (sphere diameter plus band thickness)
ℓ_m	Axial distance from tunnel throat to model nose
M	Mach number
$\tilde{m}$	Root-mean-square of the mass flow fluctuation
$\bar{m}$	Mean mass flow value
p, $\bar{p}$	Static pressure
$\tilde{p}$, $\tilde{p}_{RMS}$	Root-mean-square value of radiated pressure fluctuation $\sqrt{(p')^2}$
p'	Instantaneous fluctuation pressure
p_o	Tunnel stilling chamber total pressure
p_∞	Free-stream static pressure
q_∞	Free-stream dynamic pressure, psia $q_\infty = \frac{1}{2} \rho_\infty U_\infty^2 = \frac{\gamma}{2} p_\infty M_\infty^2$
R_D	Reynolds number, $R_D = \frac{p_e U_e D}{\mu_e}$ D = cone base diam
Re	Reynolds number
$Re/in.$, Re_∞, $(Re/in.)_\infty$	Free-stream Reynolds number, per in. $(\rho_\infty U_\infty/\mu_\infty)$
$Re_{e,\theta}$, $(Re_\theta)_t$, $Re_{\theta tr}$	Reynolds number based on edge conditions and momentum thickness at the transition location, x_t

Re_k — Trip Reynolds number $\left(Re_k = \frac{\rho_\infty U_\infty k}{\mu_\infty}\right)$

$Re_{\bar{k}}'$ — Potter-Whitfield trip correlation Reynolds number

$$Re_{\bar{k}}' = \left(\frac{U_{\bar{k}} \bar{k}}{\nu_{\bar{k}}} \frac{T_{\bar{k}}}{T_e}\right)^{0.5+\omega}$$

For adiabatic wall

$$Re_{\bar{k}}' = \bar{k} \left(\frac{U_\delta}{\nu_\delta}\right)\left(\frac{M_{\bar{k}}}{M_\delta}\right) X \left[1 + \tfrac{1}{2} (\gamma - 1)\, \eta_r\, M_\delta^2\right]^{-1.26}$$

Re_t, $R_{e,tr}$, R_t, $R_{1,tr}$ — Flat plate or hollow-cylinder transition Reynolds number based on free-stream conditions,

$$Re_t = (Re/in.)_\infty (X_t) = \frac{U_\infty X_t}{\nu_\infty}$$

$(Re_t)_\delta$ — Cone transition Reynolds number (based on local conditions),

$$(Re_t)_\delta = (Re/in.)_\delta (X_t) = \frac{U_\delta X_t}{\nu_\delta}$$

Re_{x_k} — Trip position Reynolds number, $Re_{x_x} = \rho_\delta U_\infty X_k / \mu_\delta$

$Re_{\delta^*,t}$ — Reynolds number based on the boundary-layer displacement thickness at the transition location, x_t

T — Temperature

T_{aw} — Adiabatic wall temperature, $T_{aw} = T_\infty \left(1 + \frac{\gamma - 1}{2} r M_\infty^2\right)$

$\tilde{T}$ — Root-mean-square of the temperature fluctuation

$\bar{T}_T$, $\bar{T}_o$ — Mean total temperature value

U_∞, $\bar{U}_\infty$ — Free-stream velocity

$\tilde{u}$ — Root-mean-square velocity fluctuation

X_t — Surface distance location of boundary-layer transition

X_{t_o} — Transition location on smooth body

x — Surface distance from model nose

γ — Ratio of specific heats

ΔC_p, $\Delta C_{p_{rms}}$ — Dynamic pressure coefficient, $\Delta C_p = \tilde{p}/q_\infty$

δ^* — Boundary-layer displacement thickness

η_r, r — Temperature recovery factor $(T_{aw} - T_\delta / T_o - T_\delta)$

θ_c — Cone half-angle

μ — Absolute viscosity

ν — Kinematic viscosity, $\nu = \mu/\rho$

ρ, $\bar{\rho}$ — Density

τ_w — Wall local shear stress

Subscripts

Beg. — Beginning of transition location

End — End of transition location

e — Boundary-layer edge conditions

o — Stagnation conditions

s — Cone surface

w — Wall

δ — Local inviscid flow properties at edge of boundary layer

∞ — Free stream

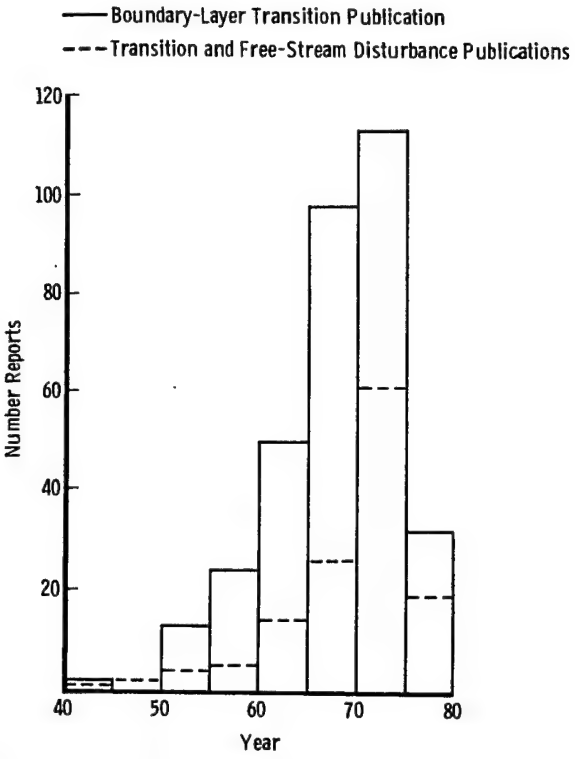

Fig. 1. Trends in transition publications.

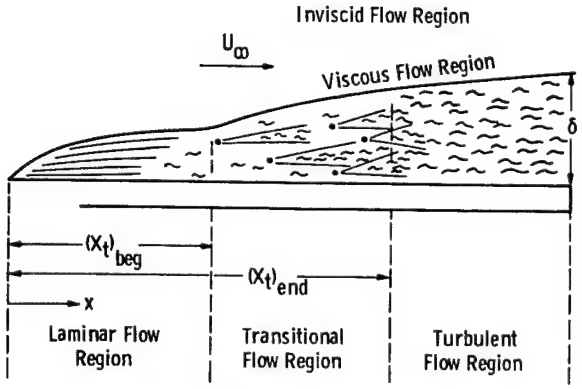

a. Boundary-layer development.

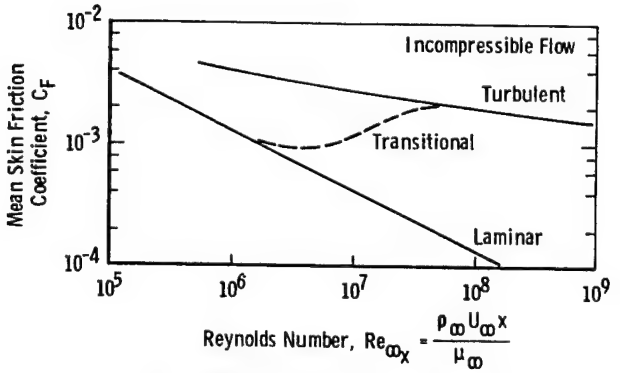

b. Skin-friction coefficient.

Fig. 2. Schematic illustration of a laminar, translational, and turbulent boundary layer.

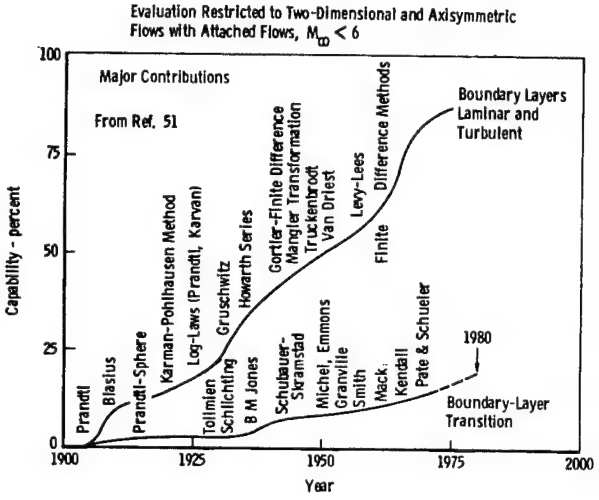

Fig. 3. Capability for analyzing and predicting boundary layers and transition (Smith 1972).

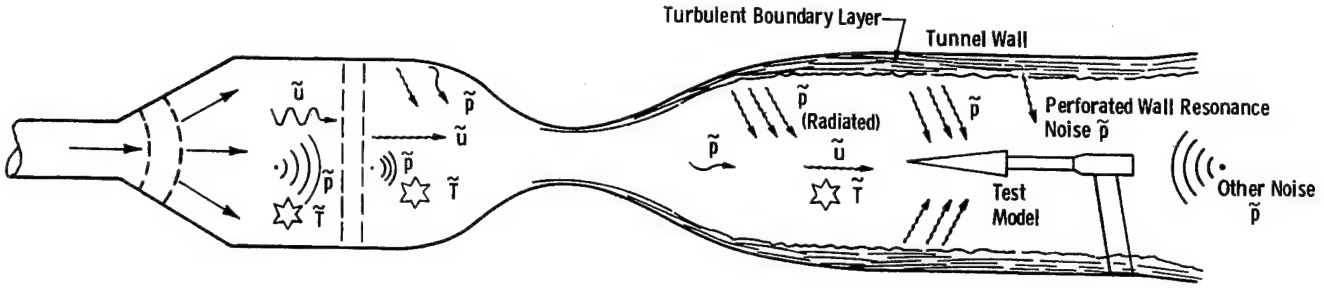

Vorticity (Turbulence - Velocity Fluctuations), $\tilde{u}$
Acoustic Sound (Pressure Fluctuations), $\tilde{p}$
Entropy Fluctuations (Temperature Spottyness), $\tilde{T}$

Mach Number Range	Type Disturbance		Effect on Transition
Subsonic $M_\infty \lesssim 0.6$	Velocity Fluctuations,	$\tilde{u}$	* Usually Dominant
	Acoustic Noise,	$\tilde{p}$	* Can be Dominant
	Temperature Fluctuations,	$\tilde{T}$	Negligible
Transonic $0.6 \lesssim M_\infty \lesssim 1.3$	Velocity Fluctuations,	$\tilde{u}$	* Can be Dominant
	Acoustic Noise,	$\tilde{p}$	* Usually Dominant
	Temperature Fluctuations,	$\tilde{T}$	Negligible
Supersonic $1.3 \lesssim M_\infty \lesssim 6$	Velocity Fluctuations,	$\tilde{u}$	Usually Negligible
	Radiated Noise,	$\tilde{p}$	* Usually Dominant
	Temperature Fluctuations	$\tilde{T}$	Usually Negligible
Hypersonic $6 \lesssim M_\infty \lesssim 15$	Velocity Fluctuations,	$\tilde{u}$	Usually Negligible
	Radiated Noise,	$\tilde{p}$	* Usually Dominant
	Temperature Fluctuations,	$\tilde{T}$	Could be Significant

Fig. 4. Flow disturbances in wind tunnels.

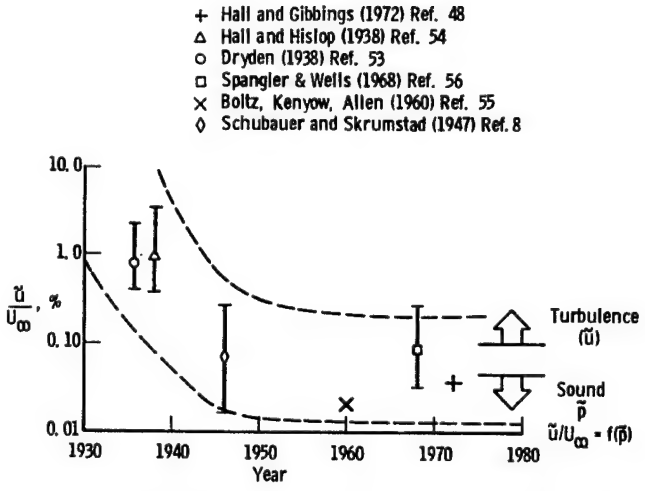

Fig. 5. Free-stream turbulence and acoustic disturbance levels in subsonic tunnels.

U_0 (fps)	$\frac{u'}{U_0}$ (percent)	$\frac{v'}{U_0}$ (percent)	$\frac{w'}{U_0}$ (percent)	$\frac{\sqrt{\frac{1}{3}(u'^2+v'^2+w'^2)}}{U_0}$ $\tilde{u}$, (percent)
30	0.019	0.011	0.012	0.0145
40	.021	.020	.019	.0200
50	.024	.023	.020	.0224
60	.027	.026	.021	.0248
70	.030	.030	.026	.0287
80	.033	.035	.032	.0334 ←
90	.035	.039	.037	.0371
100	.037	.042	.041	.0401
110	.040	.044	.045	.0430
120	.045	.046	.047	.0459

$\frac{\tilde{u}}{U_\infty}$ = 0.352; 1/2 in. Rope with 6 in. x 6 in. mesh, located downstream of screens

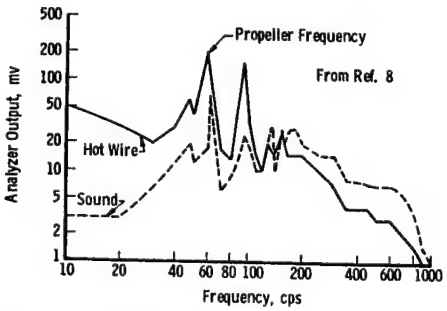

Fig. 6. Subsonic free-stream disturbance intensity and spectra (Schubauer & Skramstad 1947).

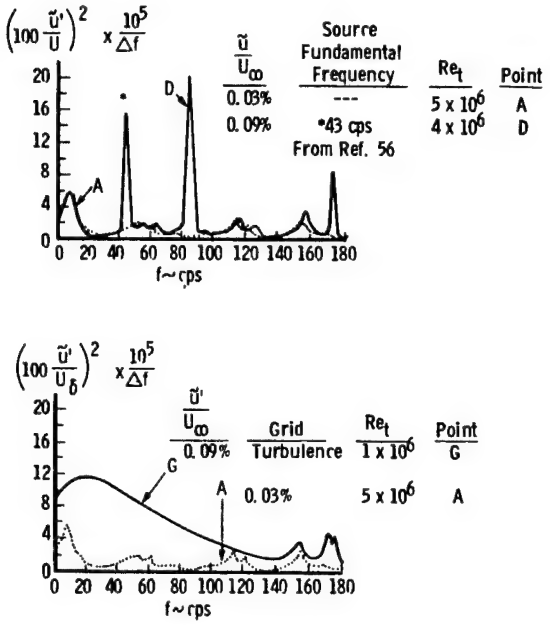

Fig. 7. Subsonic free-stream turbulence ($\tilde{u}$ and acoustic sound, $\tilde{u} = F(\tilde{p})$, spectra (Spangler and Wells 1968).

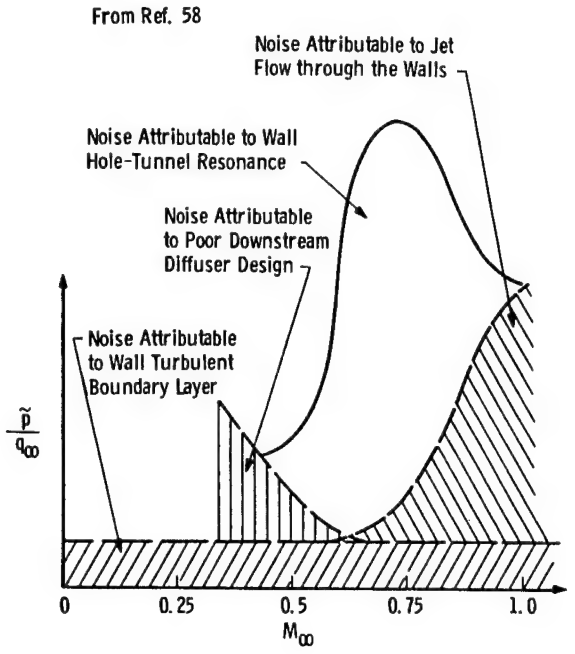

Fig. 9. Possible noise-generating mechanisms (Varner 1975).

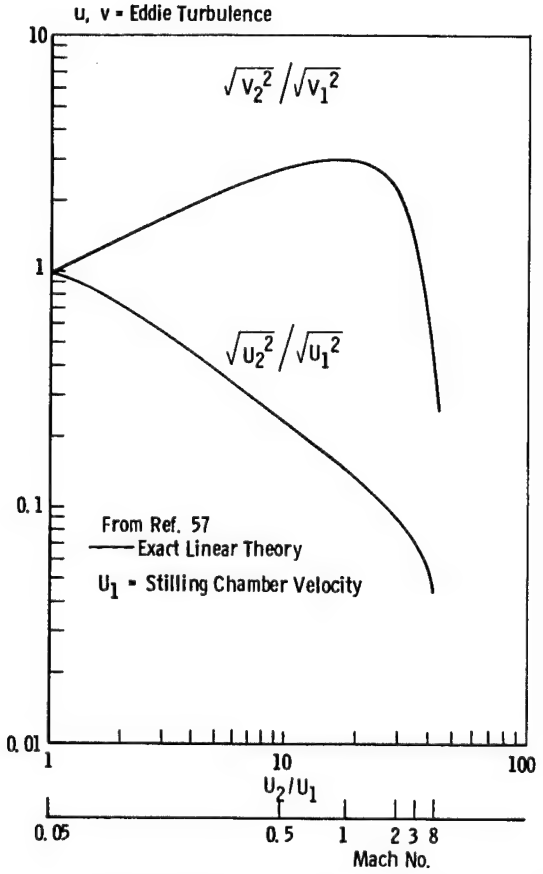

Fig. 8. Effect of supersonic nozzle on eddy turbulence; solid line, exact linear theory (Uberoi 1956).

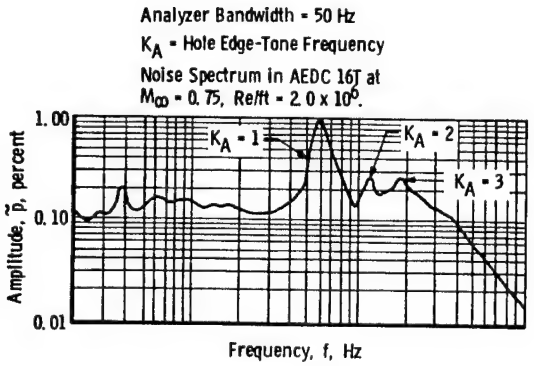

a. Acoustic noise spectra.

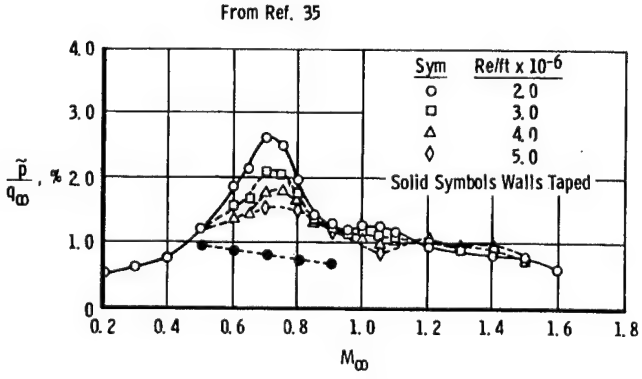

b. Noise intensity variation in AEDC 16T.

Fig. 10. Acoustic disturbance spectra and intensity in the AEDC Transonic Tunnel 16T (porous walls) (Dougherty and Steinle 1974).

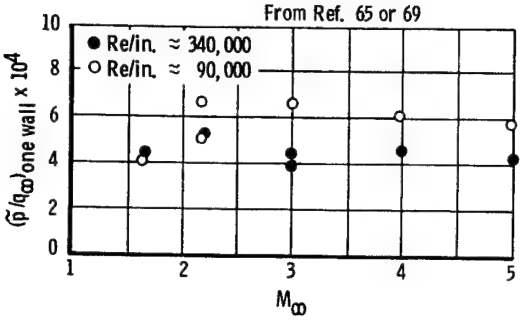

Fig. 11. Variation of free-stream pressure fluctuations with tunnel Mach number (Laufer 1961).

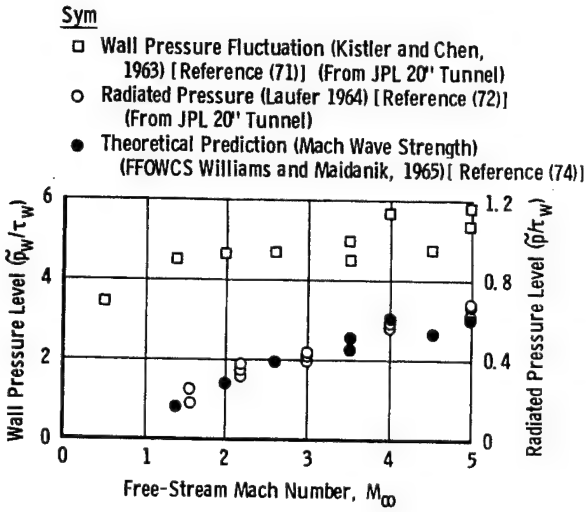

Fig. 12. Comparison of measured and predicted radiated pressure levels in supersonic tunnel (Williams & Maidanik 1965).

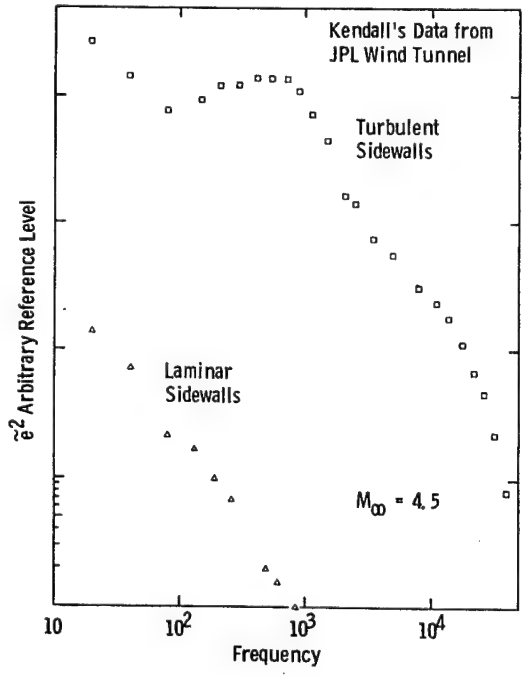

Fig. 13. Spectra of free-stream fluctuation at M_∞ = 4.5 with and without turbulence generated sound (from Ref. 2).

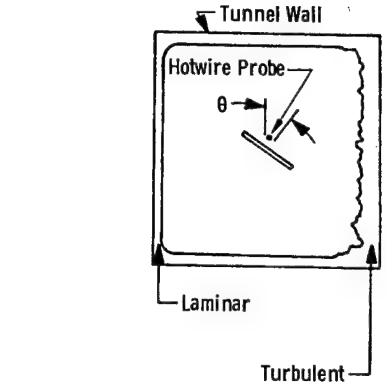

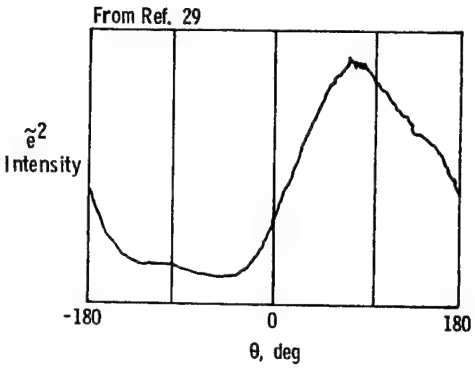

Fig. 14. Supersonic free-stream radiated noise fluctuations, directionality, and intensity, M_∞ = 4.5 (Kendall 1970).

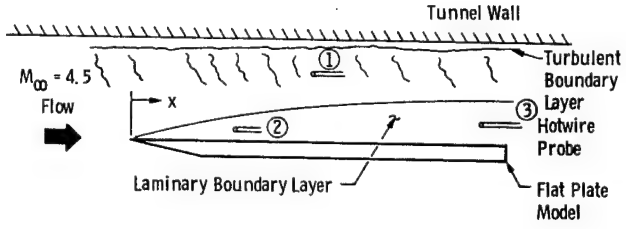

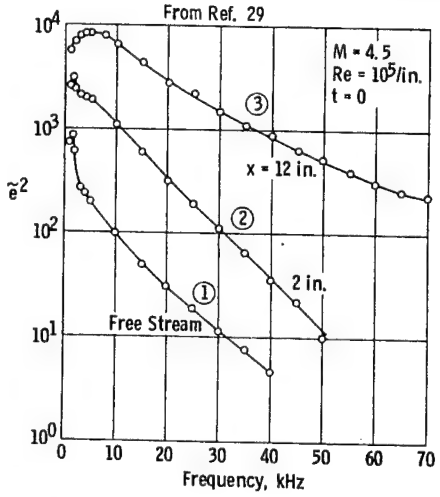

Fig. 15. Supersonic energy spectra (Kendall 1970).

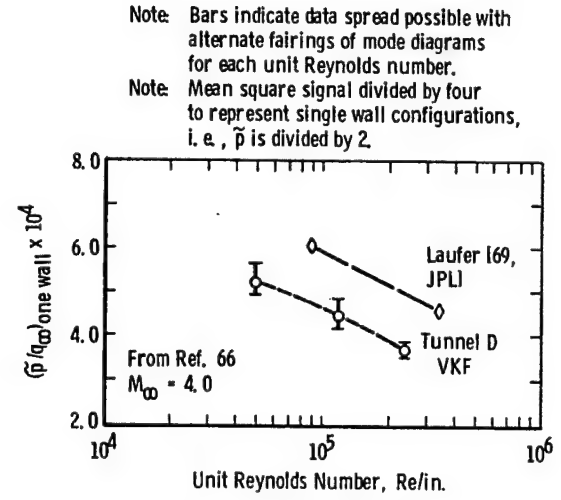

Fig. 16. Variation of RMS pressure fluctuations (normalized by dynamic pressure with unit Reynolds number (Donaldson & Wallace 1971).

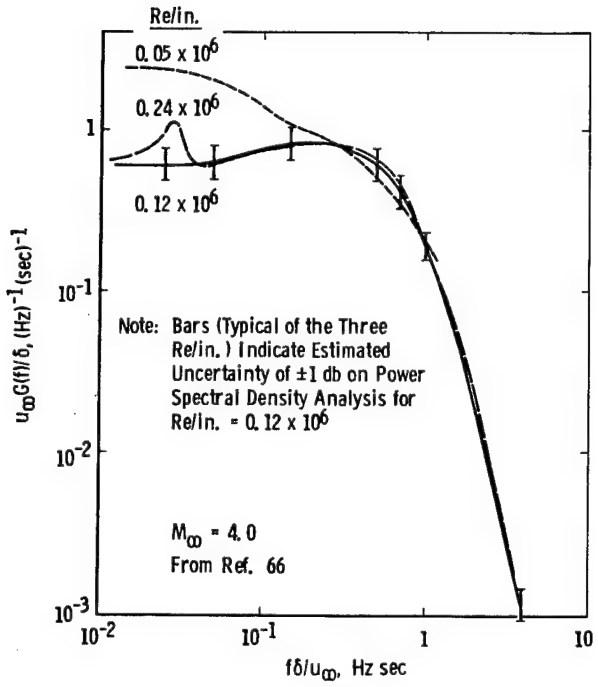

Fig. 17. Hot-wire signal spectra for wire overheat of $a_w' = 0.4$ (Donaldson & Wallace 1971).

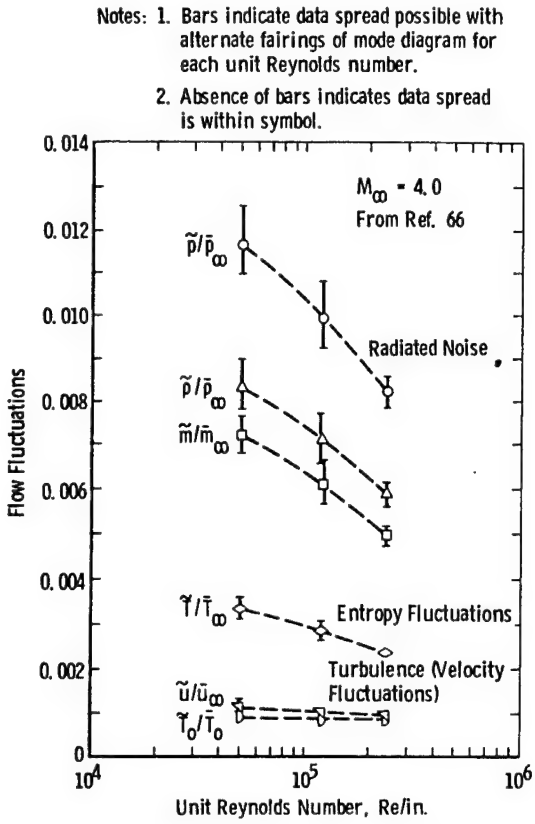

Fig. 18. Variation of flow fluctuations with unit Reynolds number (Donaldson & Wallace 1971).

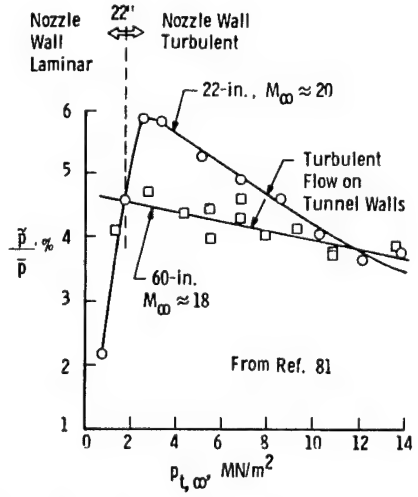

Fig. 19 Disturbance levels at $M_\infty \approx 20$ (Fischer and Wagner 1972).

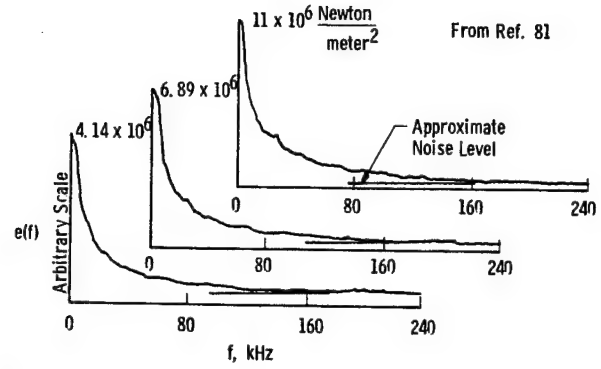

Fig. 20 Free-Stream Disturbance Spectra $M_\infty \approx 20$ (Fischer and Wagner (1972).

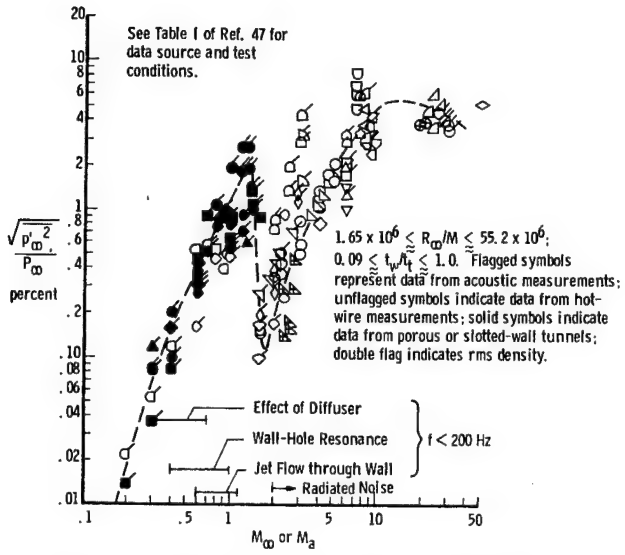

a. Free-stream rms pressure fluctuations divided by mean static pressure.

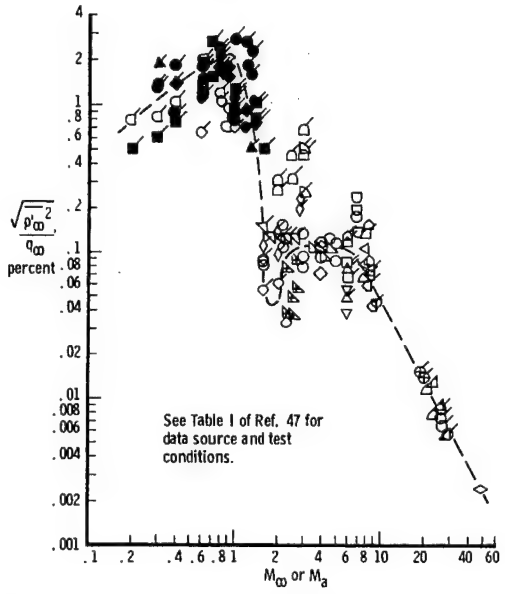

b. Free-stream rms pressure fluctuations divided by dynamic pressure.

Fig. 21. Typical free-stream pressure fluctuations in wind tunnels (Harvey 1978).

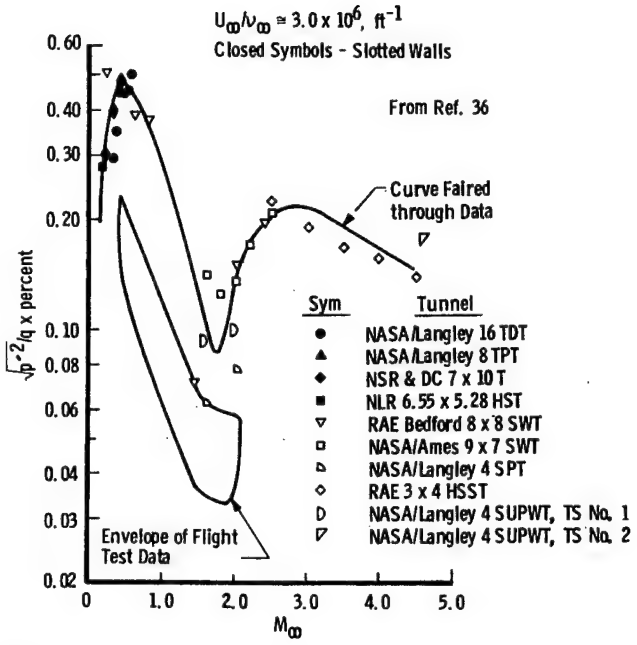

Fig. 22. Comparison of lowest disturbance levels measured in wind tunnels with disturbances in flight (Dougherty 1980).

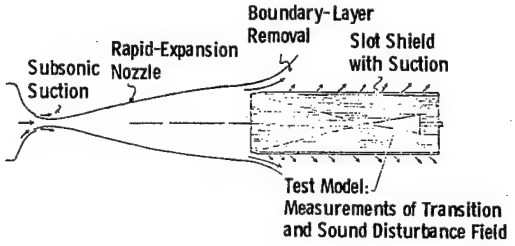

a. Sound shield concept.

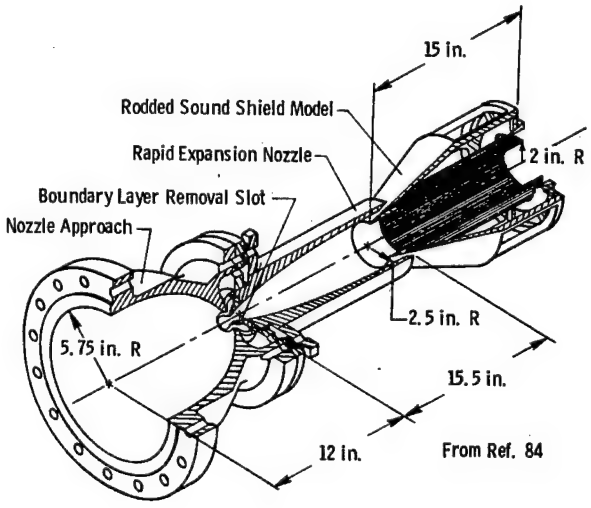

b. Nozzle details.

Fig. 23. NASA-Langley $M_\infty = 5$ quiet tunnel concept (Beckwith 1975).

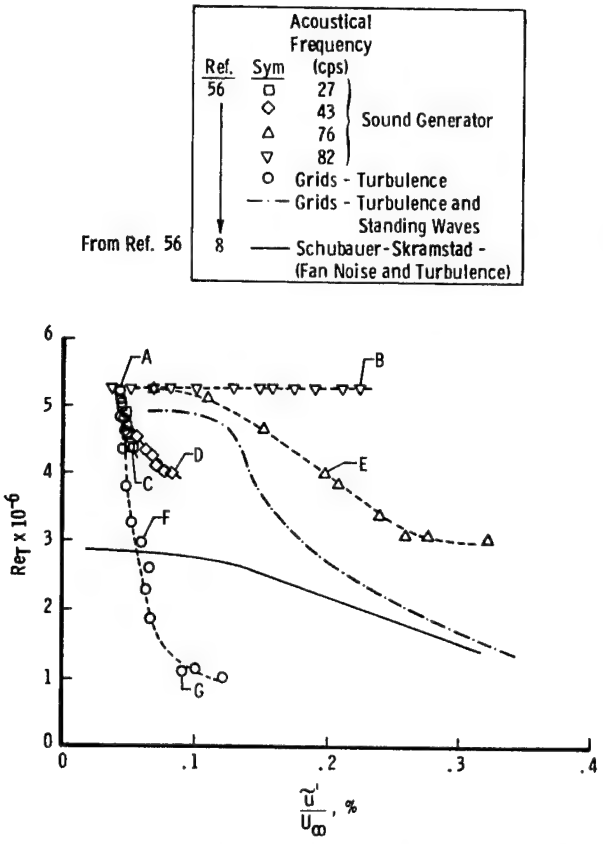

Fig. 24. Effects of free-stream disturbances on boundary-layer transition (Schubauer & Skramstad 1947; Spangler & Wells 1968).

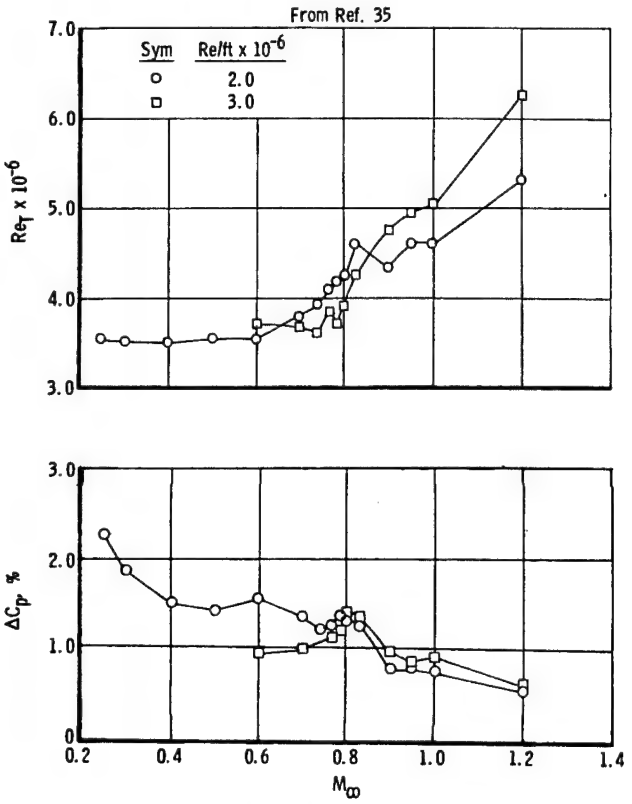

Fig. 26. Noise and Re_T variation in NASA/LRC 8 TPT (Dougherty and Steinle 1974).

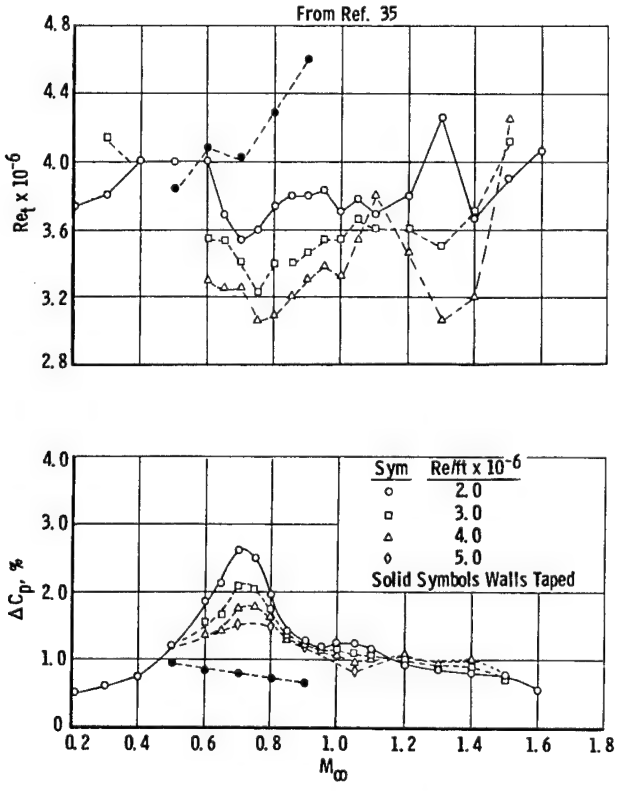

Fig. 25. Noise and Re_T variation in AEDC 16T (Dougherty and Steinle 1974).

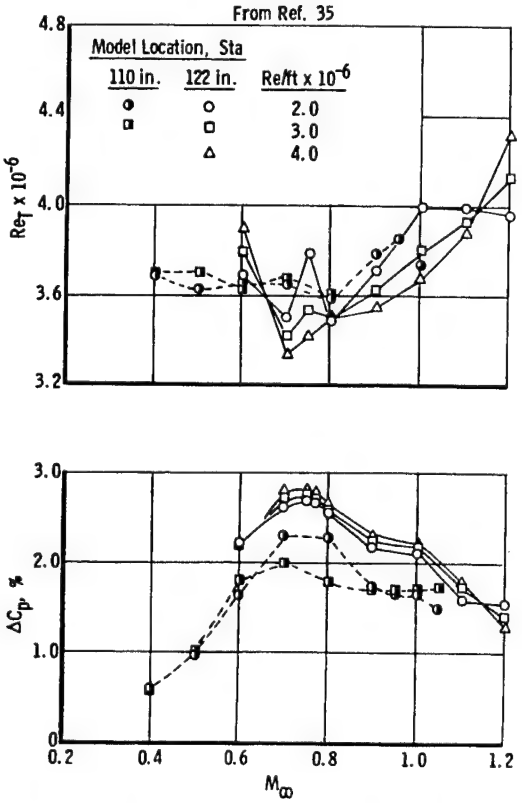

Fig. 27. Noise and Re_T variation in NASA/ARC 11 TPT (Dougherty and Steinle 1974).

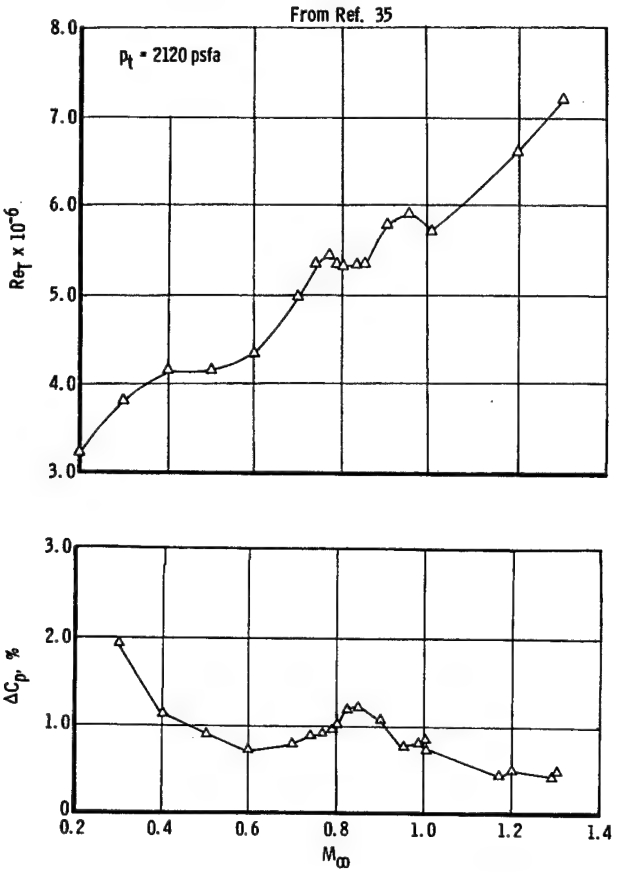

Fig. 28. Noise and Re_T variation in NASA/LRC 16 TT (Dougherty and Steinle 1974).

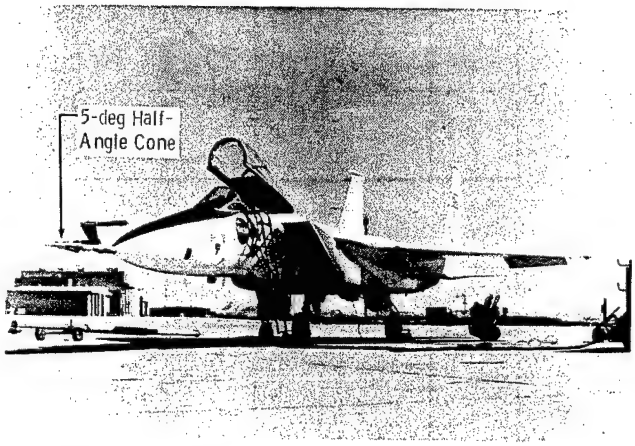

Fig. 29. 5-deg cone mated to the test F-15 aircraft (Dougherty 1980).

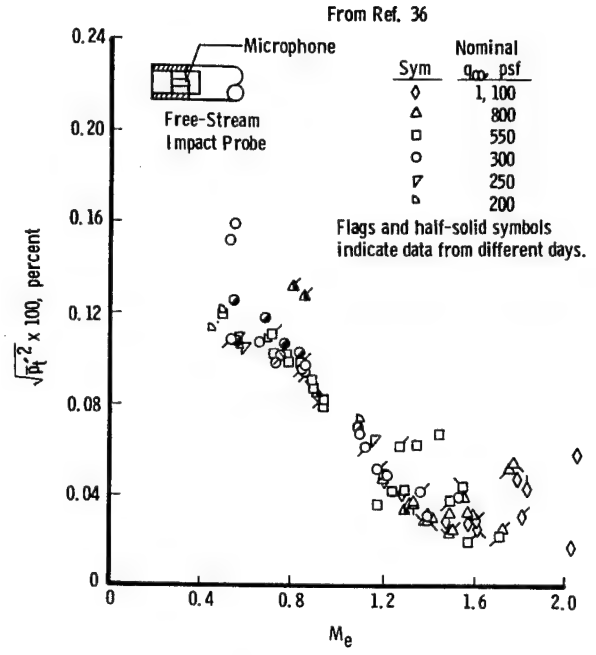

Fig. 30 Free-stream impact pressure fluctuations (Dougherty and Fisher 1980).

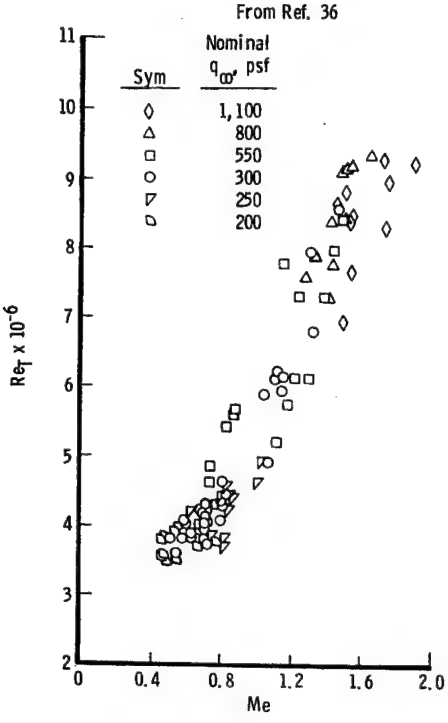

Fig. 31. In-flight transition Reynolds numbers as a function of M_3 (Dougherty and Fisher 1980).

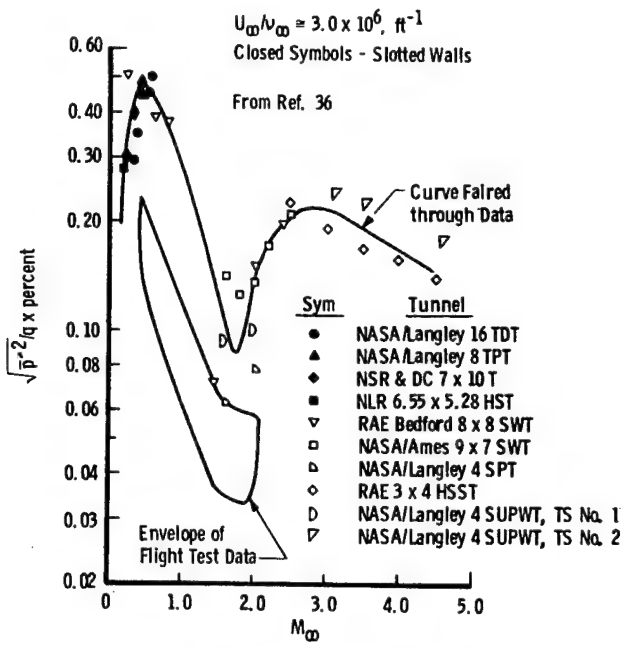

Fig. 32. Comparison of lowest disturbance levels measured in wind tunnels with disturbances in flight (Dougherty and Fisher 1980).

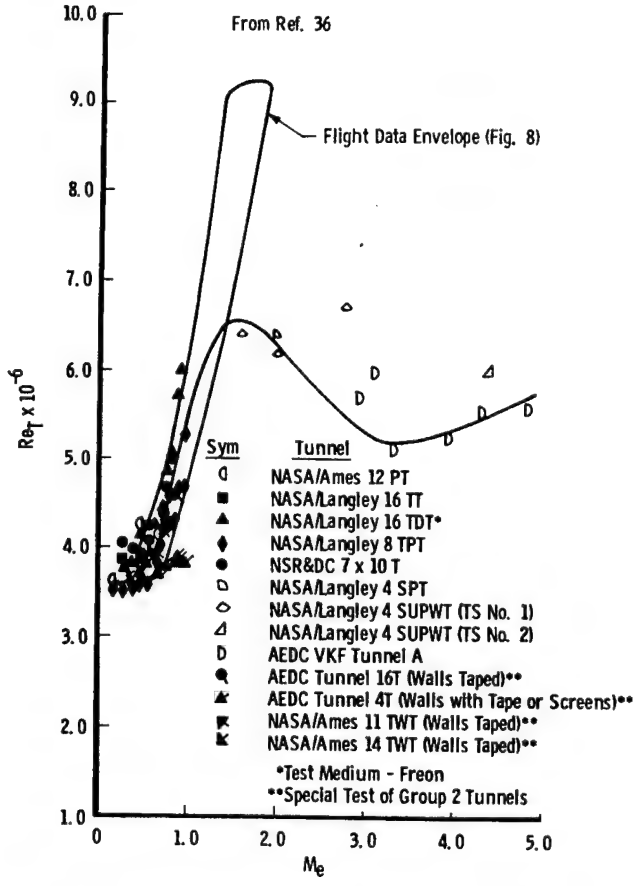

Fig. 33. Transition Reynolds numbers in lower-disturbance-level wind tunnels (Dougherty and Fisher 1980).

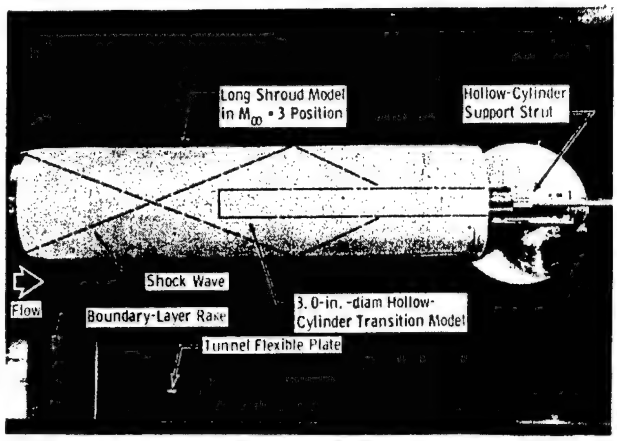

a. Long shroud installation in the AEDC-VKF Tunnel A.

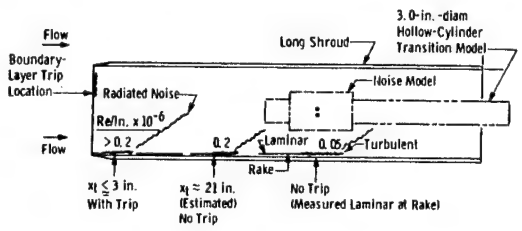

b. Boundary-layer development inside long shroud.

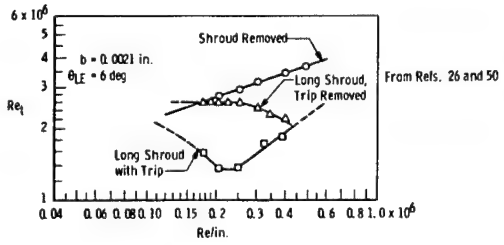

c. Transition Reynolds numbers on the 3.0-in.-diam hollow-cylinder model.

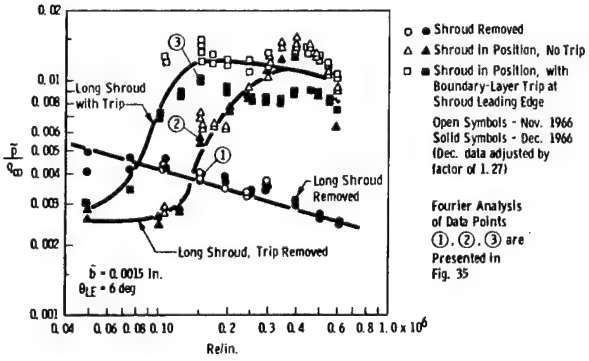

d. Root-mean-square radiated pressure fluctuations.

Fig. 34. Comparisons of transition Reynolds numbers and root-mean-square radiated pressure fluctuations at M_∞ = 3.0 (Pate and Schueler 1967).

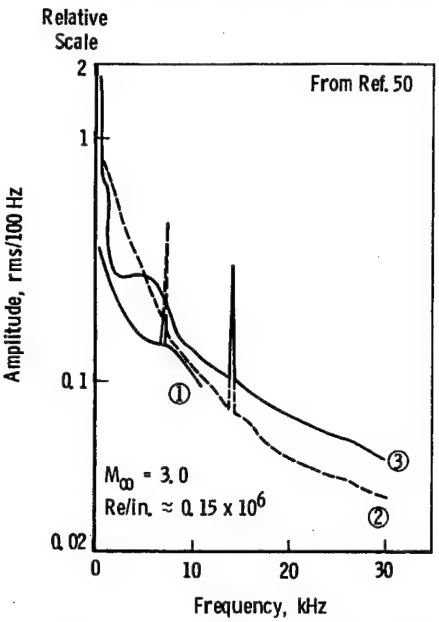

Fig. 35. Fourier analysis of selected data points from Fig. 34 (Pate 1977).

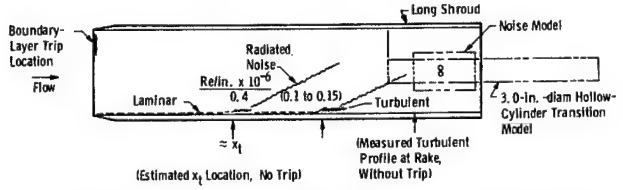

a. Boundary-layer development inside long shroud.

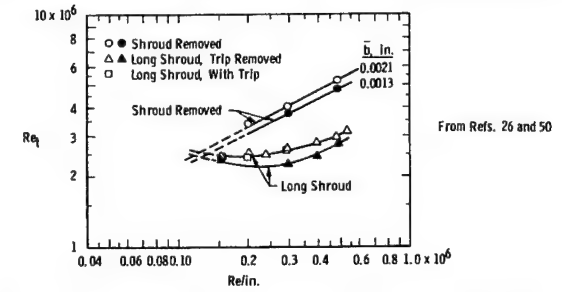

b. Transition Reynolds numbers on the 3.0-in.-diam hollow-cylinder model.

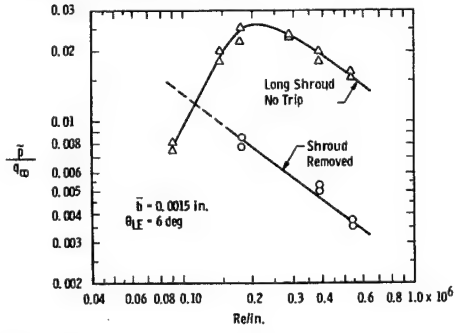

c. Root-mean-square radiated pressure fluctuations.

Fig. 36. Comparisons of transition Reynolds numbers and root-mean-square radiated pressure fluctuations at M_∞ = 5.0 Pate & Schueler 1967).

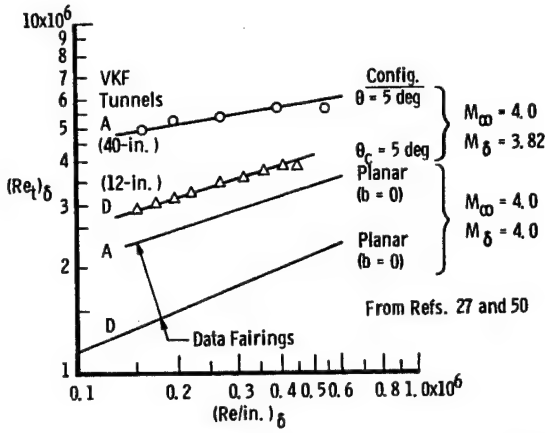

Fig. 37. Variation of transition Reynolds numbers with tunnel size, M_∞ = 4.0 (Pate 1971).

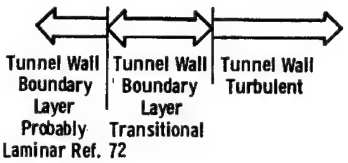

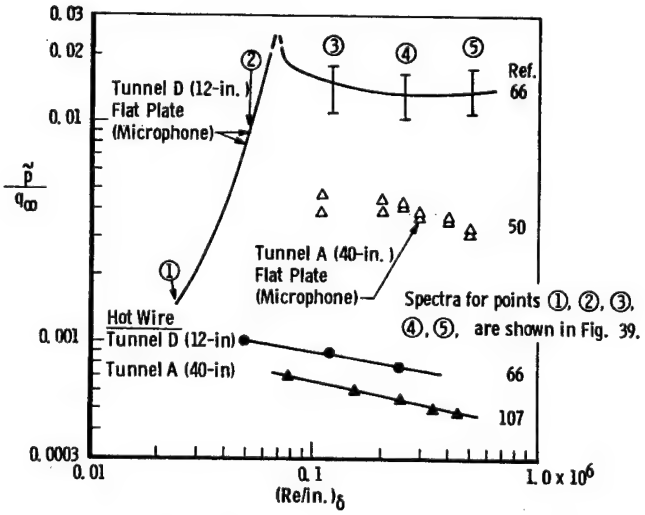

Fig. 38. Free-stream pressure fluctuation measurements, AEDC-VKF Tunnels A and D, M_∞ = 4.0.

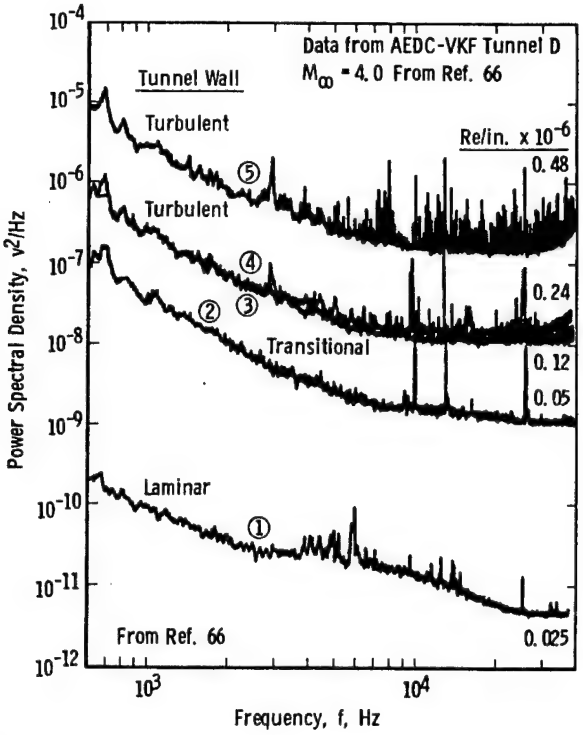

Fig. 39. Comparison of power spectra of microphone output for various unit Reynolds numbers (Dougherty & Wallace 1971).

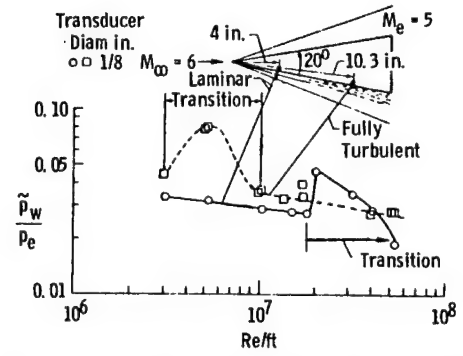

a. Variation of overall rms pressure with unit Reynolds number.

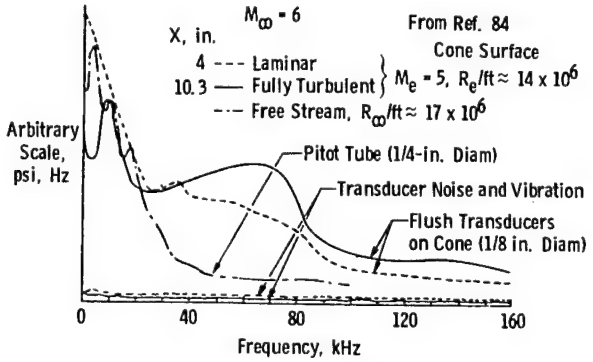

b. Spectra of pressure fluctuations with ΔF = 200 Hz.

Fig. 40. Measurements of fluctuating pressures under laminar and turbulent boundary layers on a sharp cone in Mach 6 high Reynolds number tunnel at NASA Langley (Beckwith 1975).

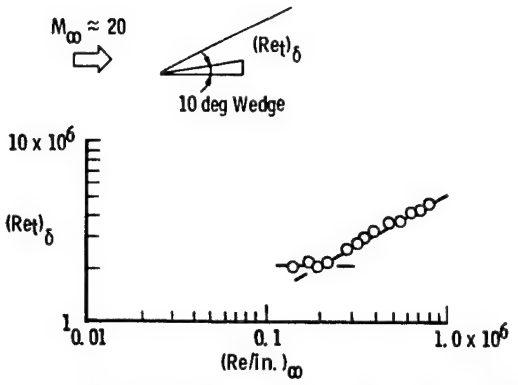

a. 10-deg wedge transition Reynolds numbers.

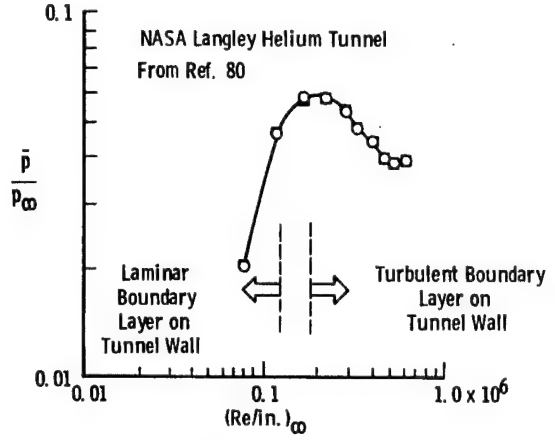

b. Free-stream pressure fluctuations.

Fig. 41. Effect of free-stream disturbances on wedge model transition, $M_\infty \approx 20$ (Wagner, Maddalor, Weinstein (1969).

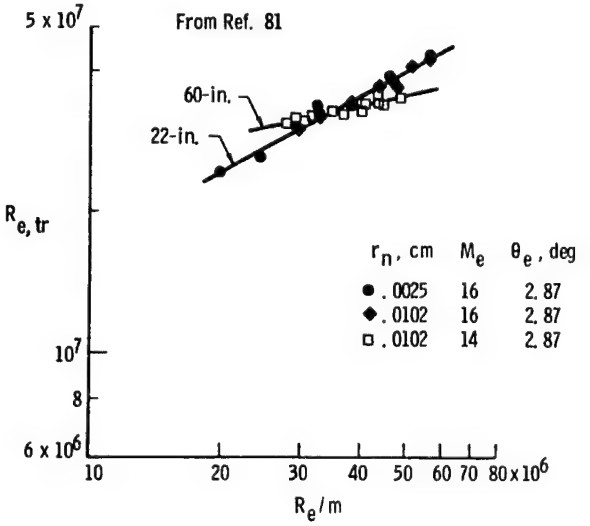

a. Transition Reynolds number vs unit Reynolds numbers.

Fig. 42. Transition and free-stream disturbance measurement at $M_\infty \approx 20$.

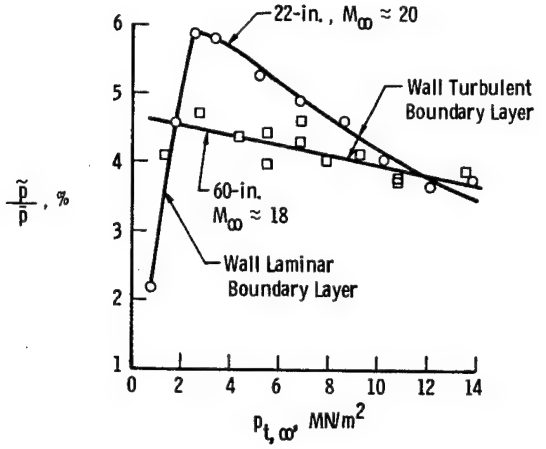

b. Free-stream disturbances.

Fig. 42. Concluded.

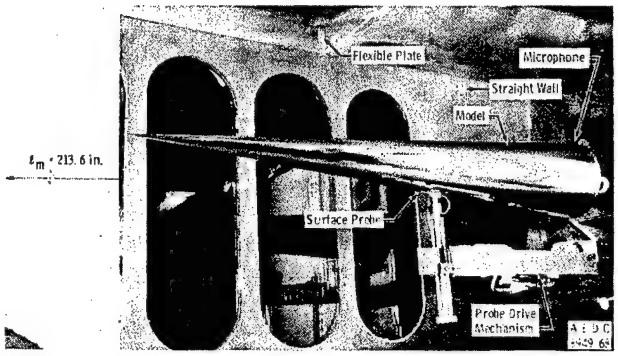

Fig. 43. Installation of the 5-deg cone transition model installed in the AEDC-VKF Tunnel A (40- x 40-in.).

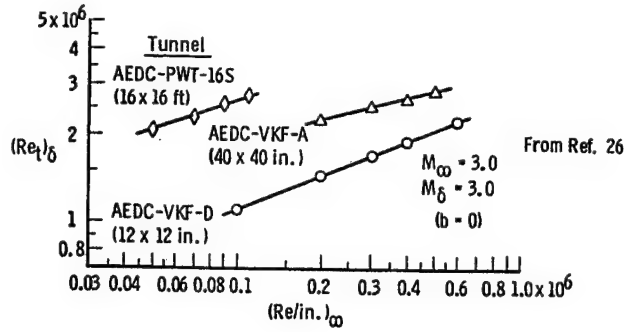

a. Planar (hollow cylinder) model.

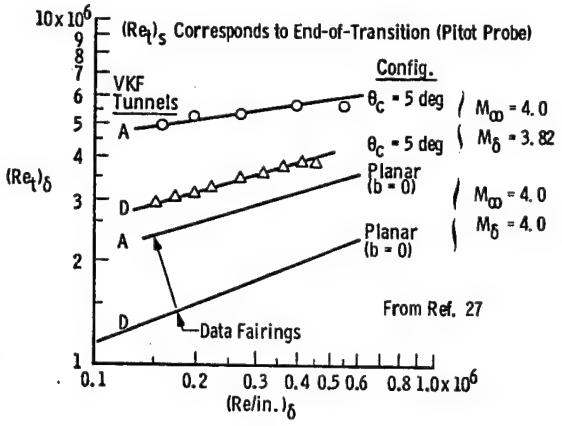

b. Cone model.

Fig. 44. Variation of transition Reynolds numbers with tunnel size (Pate 1967, 1971).

Sym	M_∞	Tunnel	Test Section Size	ℓ_m, in.
○	3.6	CSST	10.6 x 10.6 in.	48
△	3.6	SST	47.2 x 47.2 in.	213

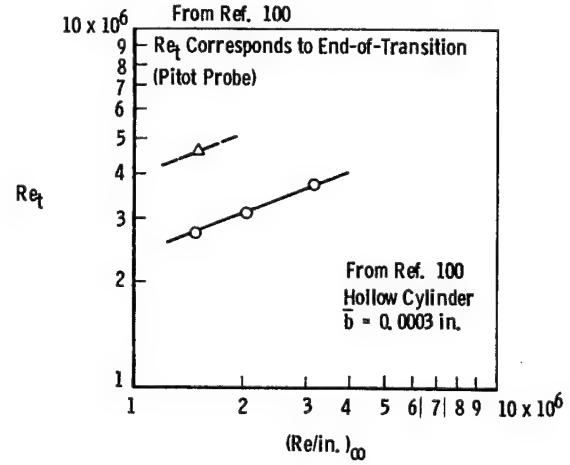

Fig. 45. Effect of tunnel size on Re_t data from Netherland tunnels (Ross 1974).

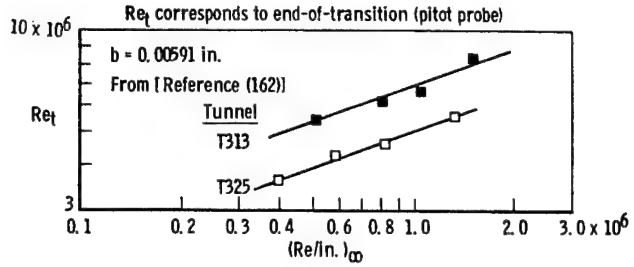

a. $M_\infty = 4.0$.

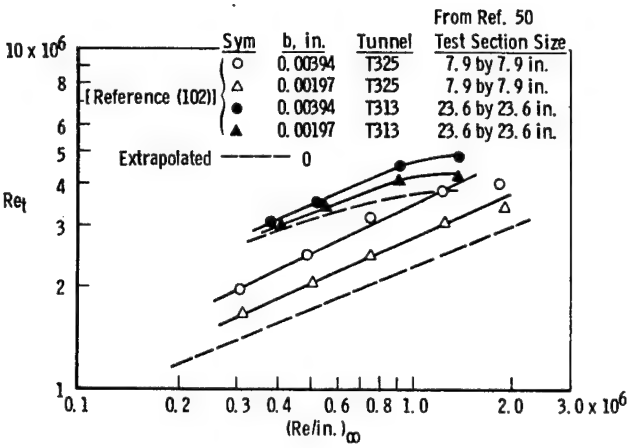

b. $M_\infty = 3.0$.

Fig. 46. Effect of tunnel size on flat-plate transition Reynolds numbers (Struminsky, Kharitonov, Chernykh, 1972 - USSR).

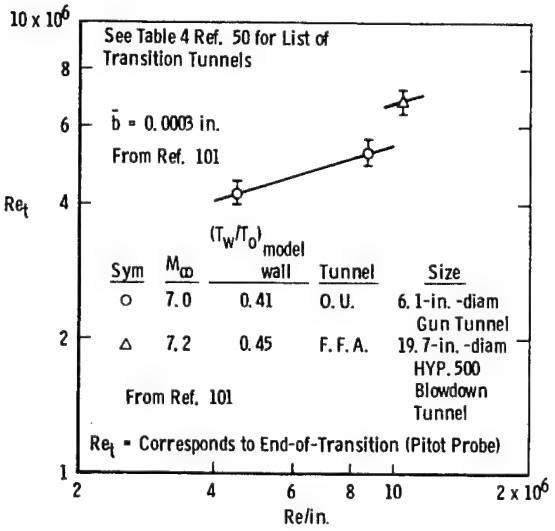

Fig. 47. Hollow-cylinder transition data (Great Britain - Sweden).

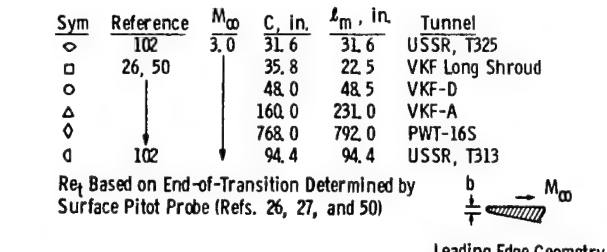

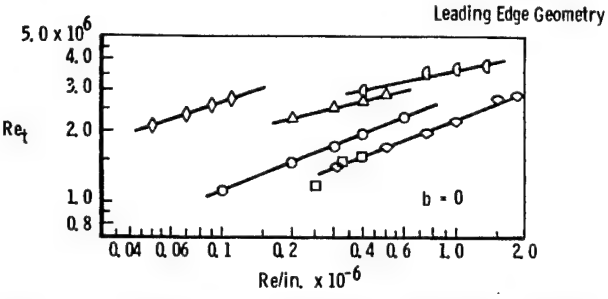

Fig. 48. Variation of transition Reynolds numbers with tunnel size and $M_\infty = 3.0$, sharp-leading-edge flat-plate/hollow-cylinder models.

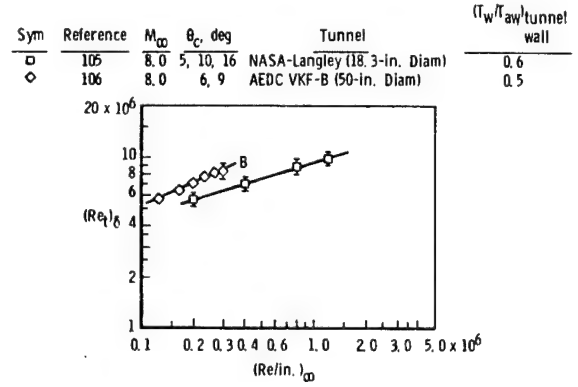

Fig. 49. Variation of sharp-cone transition Reynolds numbers with tunnel size at $M_\infty \approx 8$.

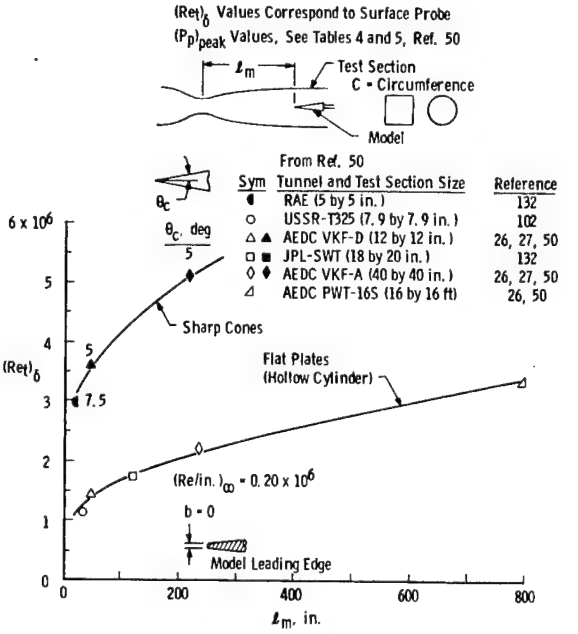

Fig. 50. Effect of tunnel size on transition Reynolds numbers at $M_\infty \approx 3.0$, flat plates and sharp cones (Pate 1977).

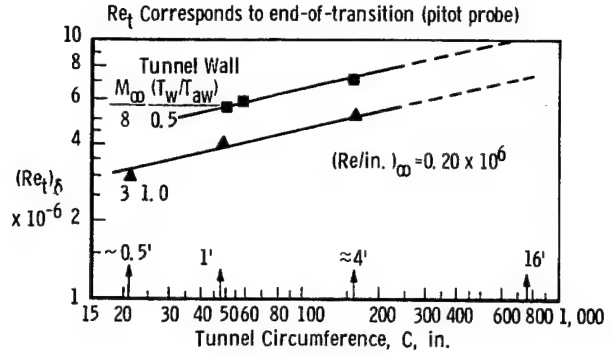

Fig. 51. Effect of wind tunnel size on sharp-cone transition Reynolds numbers for various Mach numbers (Pate 1977).

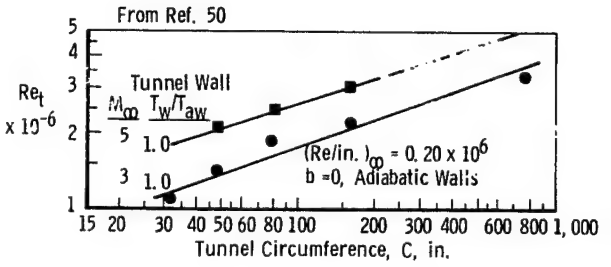

Fig. 52. Effect of wind tunnel size on planar model transition Reynolds numbers for various Mach numbers (Pate 1977).

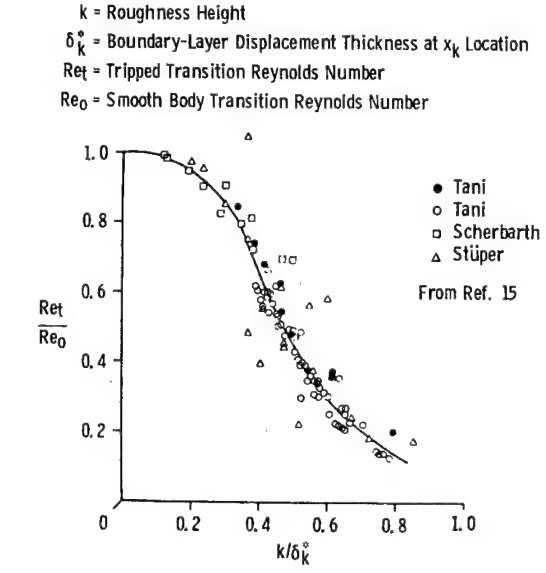

Fig. 53. Ratio of transition Reynolds number of rough plate to that of smooth plate and ratio of height of roughness element to boundary-layer displacement thickness at element, single cylindrical (circle and square symbols) and flat-strip elements (triangular symbols) (Dryden 1953).

Facility	Sym	M_δ	Source
JPL	o	1.90 to 3.67	Adiabatic and Wall Cooling References (18)
AEDC-VKF D	●	2.89	Ref. 28, Adiabatic Wall, k = 0.010
	▲	2.89	Ref. 28, Adiabatic Wall, k = 0.015
	■	3.82	Ref. 28, Adiabatic Wall, k = 0.015
AEDC-VKF A	◗	2.89	Ref. 28, Adiabatic Wall, k = 0.010

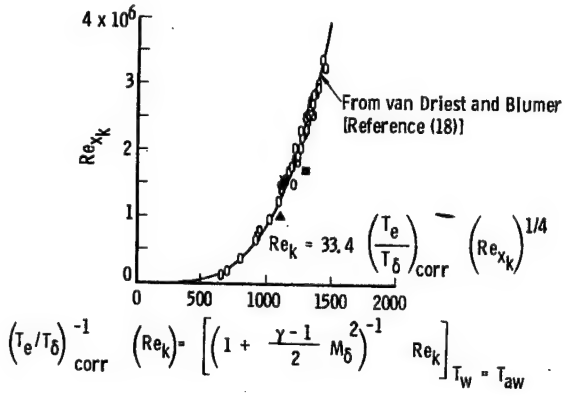

a. Correlation of effective trip location.

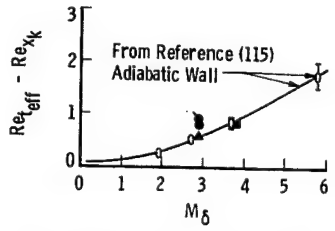

b. Interval between effective point and trip location Reynolds numbers.

Fig. 54. Correlation of tripped results using the methods of van Driest-Blumer (1968).

Sym	M_δ	Roughness	AEDC Tunnel	Model	Reference
o σ	2.89	Spheres	D	Cone	28
σ	3.82	Spheres	D	Cone	28
●	2.89	Spheres	A	Cone	28
▨	0-5	(Spheres, Wires, Grit)	-	(Cone, Cyl., Plate)	23

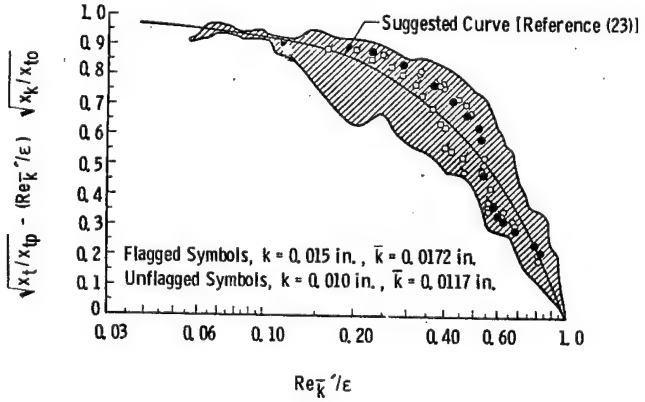

Fig. 55. Correlation of tripped results using the method of Potter-Whitfield (Pate 1977).

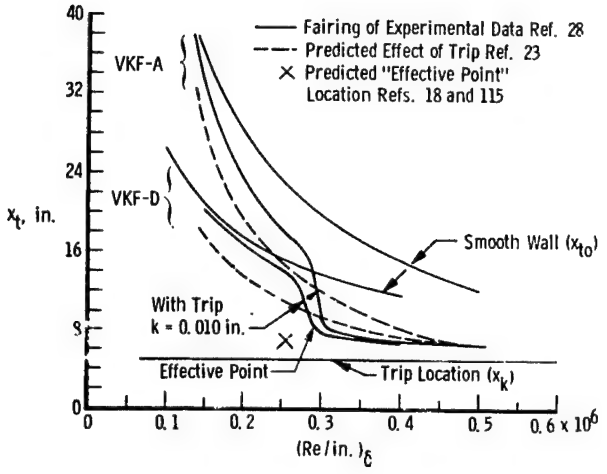

a. $M_\infty = 2.89$, k = 0.010 in., $\bar{k} = 0.0117$ in., $x_k = 4.9$ in.

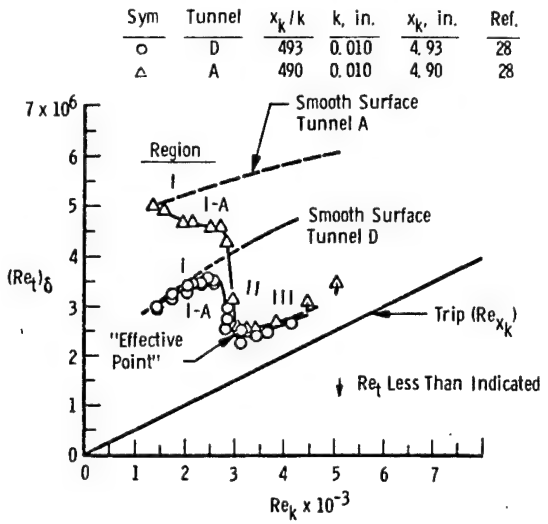

b. $M_\delta = 3.89$

Fig. 56. Combined effects of trips and free-stream disturbances (radiated noise) on transition (Pate 1977).

General Eq. $F_2 = \sum_{i=0}^{k} \left[\left(\sum_{j=0}^{k} a_{ij} M_e^j \right) \left(\frac{h_w}{h_e} \right)^i \right]$

For Wind Tunnel Data:

$$F_2 = 1.6002 + 0.14207\, M_e + 0.27641 \left(\frac{h_w}{h_e}\right) - 0.032828\, M_e \left(\frac{h_w}{h_e}\right) - 0.042888 \left(\frac{h_w}{h_e}\right)^2 + 0.0054027\, M_e \left(\frac{h_w}{h_e}\right)^2$$

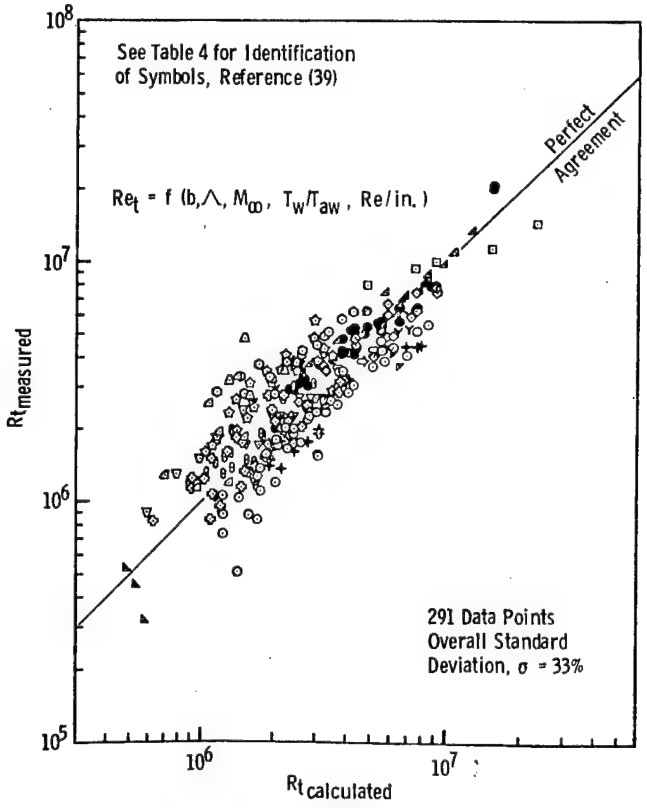

Fig. 57. Comparison of measured and predicted transition Reynolds numbers (Deem et al. 1965).

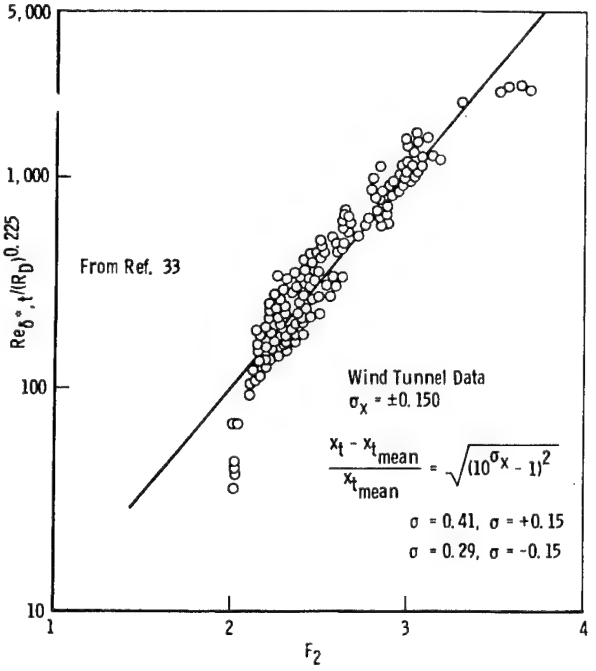

Fig. 58. Correlation of sharp cone transition Reynolds numbers at supersonic-hypersonic conditions and zero angle of attack (Beckwith and Bertrum 1972).

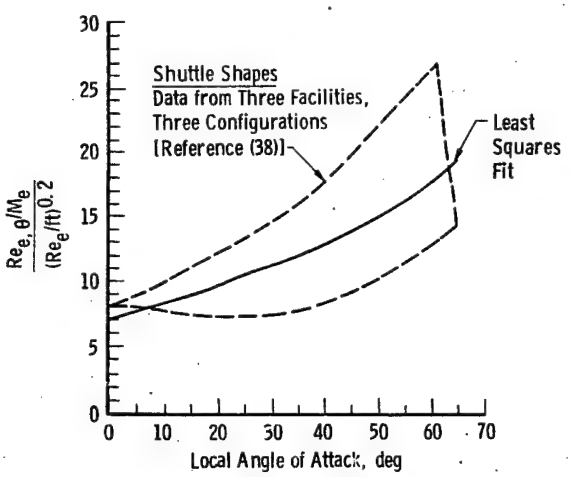

Fig. 59 Correlation of space shuttle wind surface centerline transition Reynolds number data (Fehrman and Masek 1972).

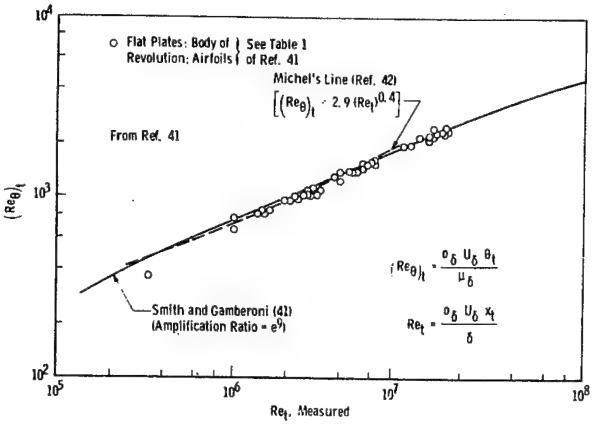

Fig. 61. Correlation and prediction of incompressible flow transition Reynolds numbers (Smith 1956).

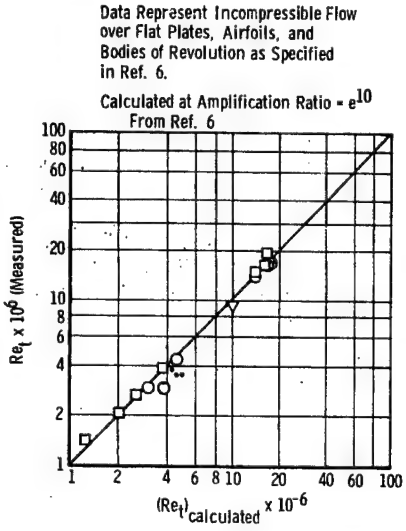

Fig. 62 Overall correlation of transition data (Jaffe, Okamura, Smith 1969).

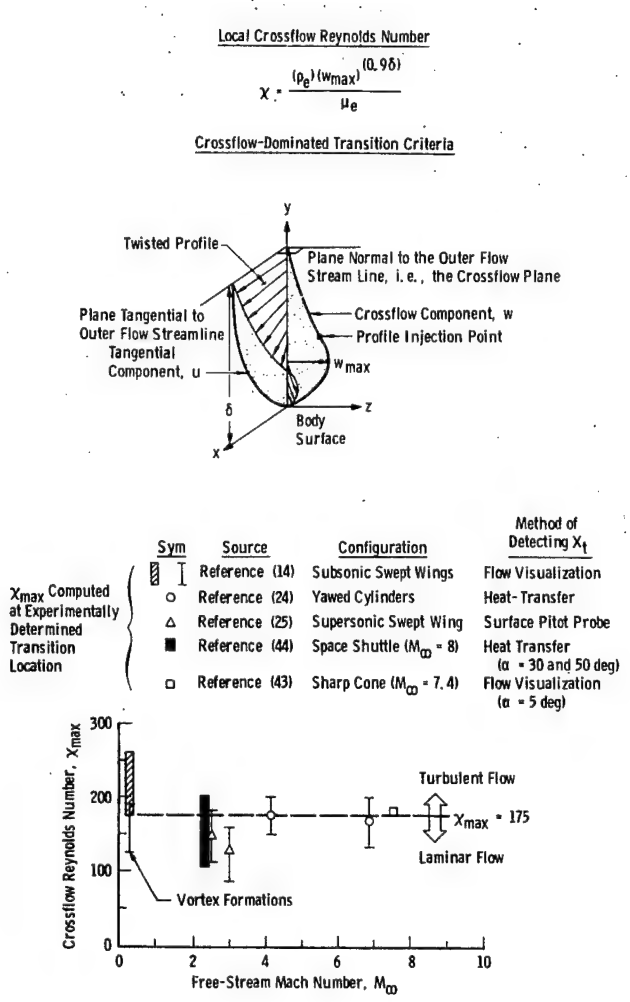

Fig. 60. Correlation of transition and cross-flow Reynolds number.

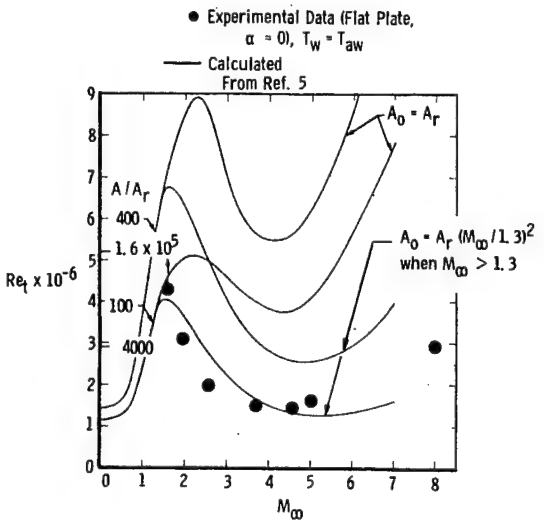

Fig. 63 Theoretical calculations of effect of Mach number on transition for two A/A_r and two assumptions about initial disturbance amplitude (Mack 1975).

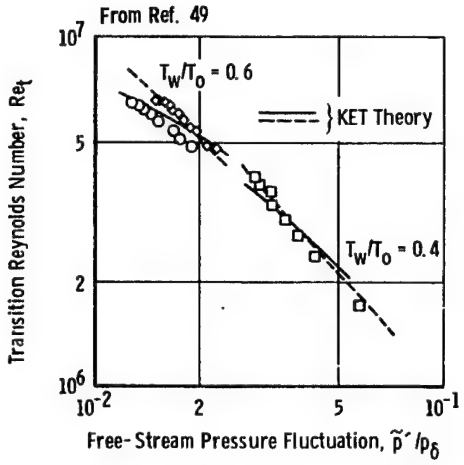

a. Effect of free-stream fluctuating pressure on boundary-layer transition location on sharp cones at M_e = 5.

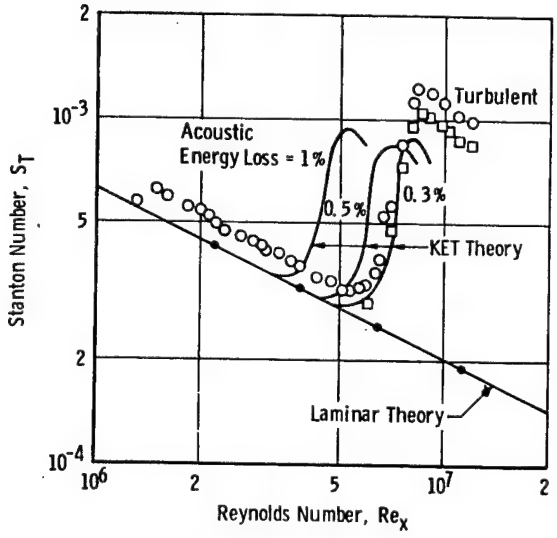

b. Heat-transfer distributions.

Fig. 64 Comparison between measured and predicted transitional heat transfer with transition triggered from pressure-velocity fluctuation (Shamroth and McDonald 1972).

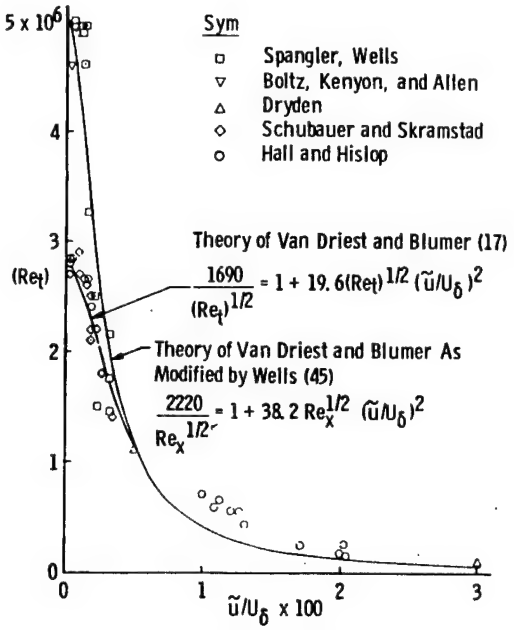

Fig. 65. Effect of free-stream turbulence on boundary-layer transition (Wells 1967).

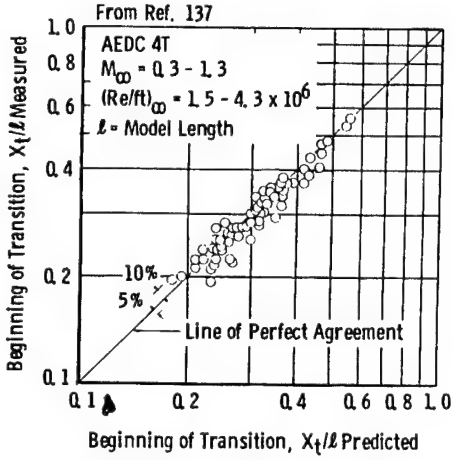

a. Comparison of predicted and measured transition locations.

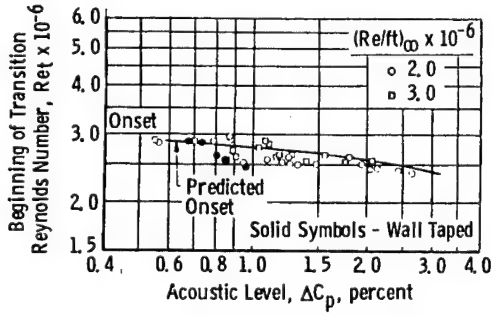

b. Transition Reynolds number as a function of acoustic level in the AEDC-PWT 16T. Comparison with Prediction 66.

Fig. 66. Comparisons of Benek-High method for predicting transition with experimental sharp cone data, $M_\infty \approx 0.4$-1.3 (Benek and High 1974).

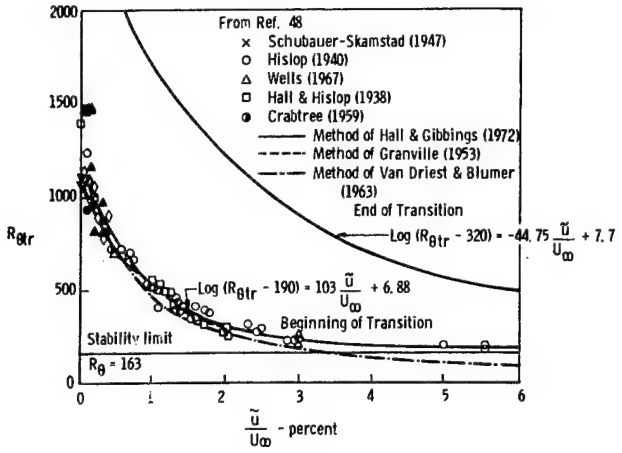

Fig. 67. Effect of free-stream turbulence upon transition (Hall and Gibbings 1972).

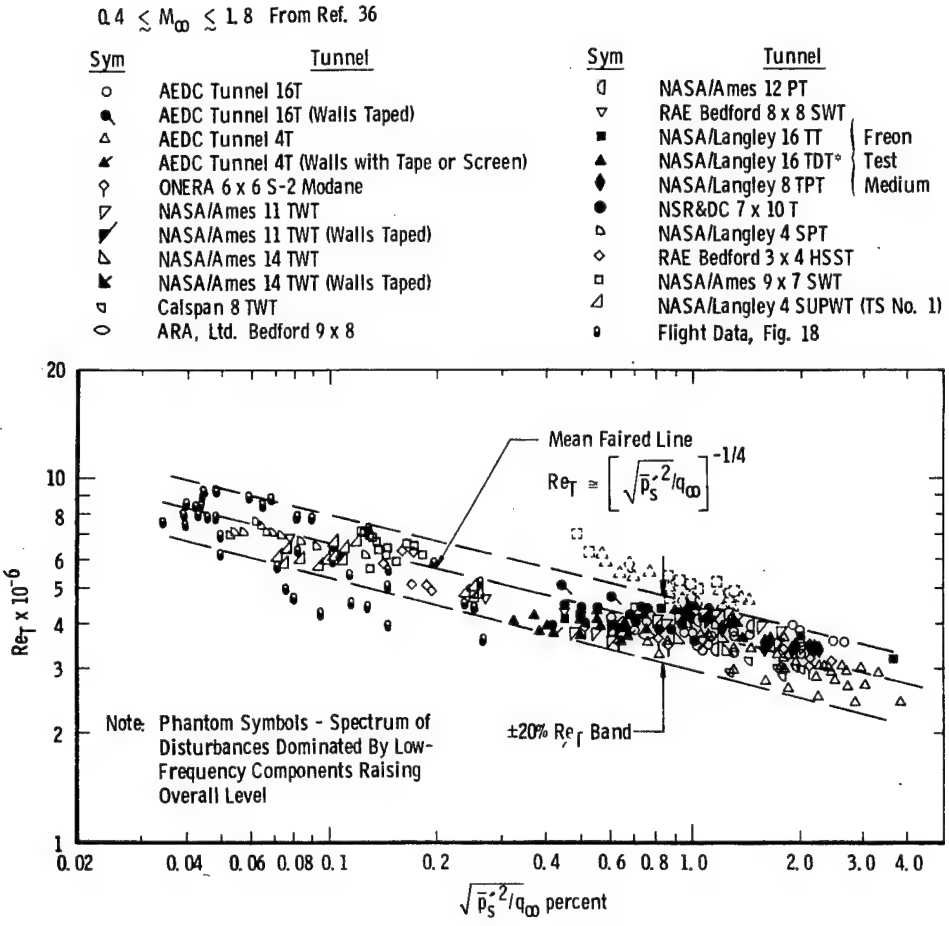

Fig. 68. Correlation of transonic wind tunnel and flight data (Dougherty 1980).

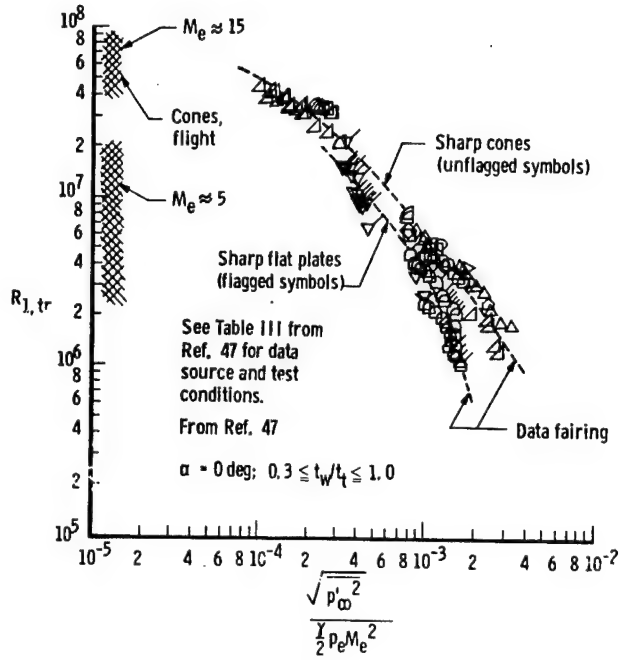

a. $4 \leq M_\infty \leq 23$.

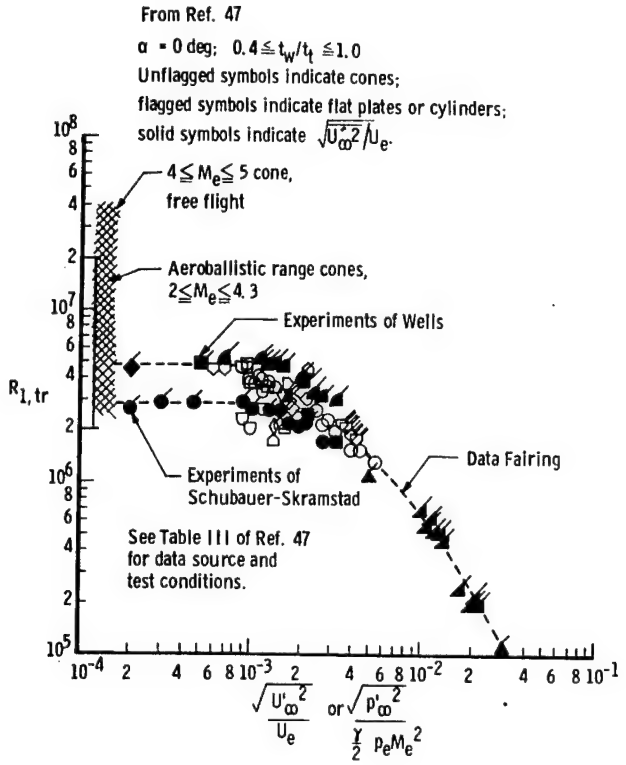

b. $0 \leq M_\infty \leq 4$.

Fig. 69. Influence of free-stream disturbance level on transition for cones, cylinders, and flat plates (Harvey 1978).

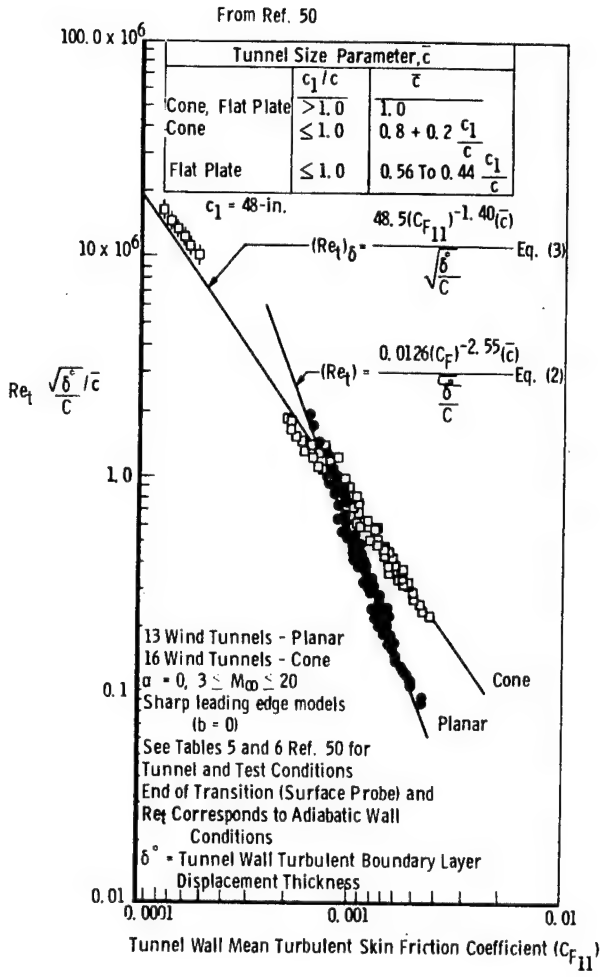

Fig. 70. Correlation of planar model and sharp-cone transition Reynolds numbers (Pate 1977).

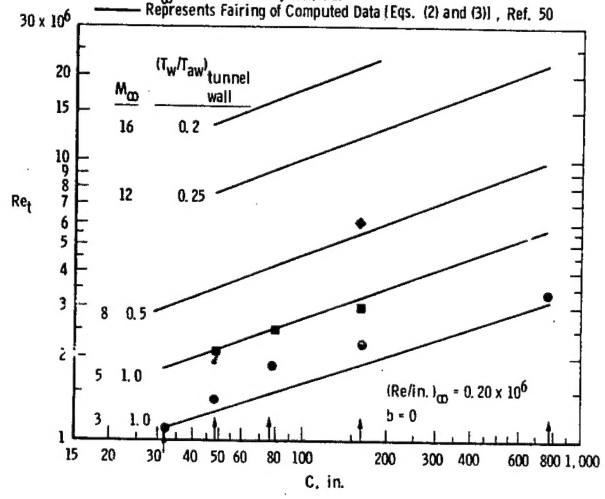

a. Planar model.

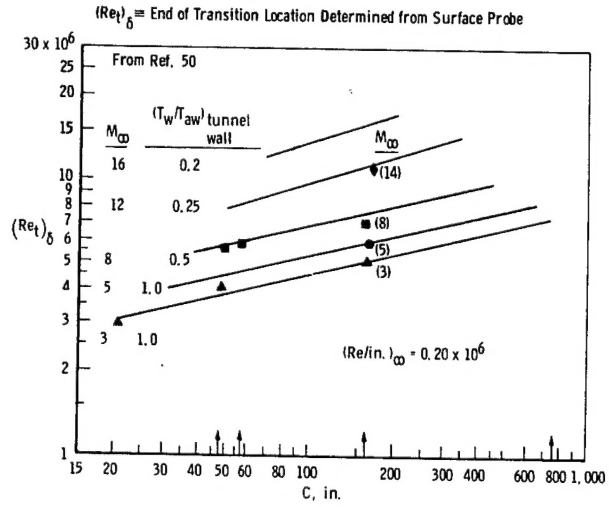

b. Sharp cone.

Fig. 71. Effect of wind tunnel size on transition Reynolds numbers for various Mach numbers (Pate 1977).

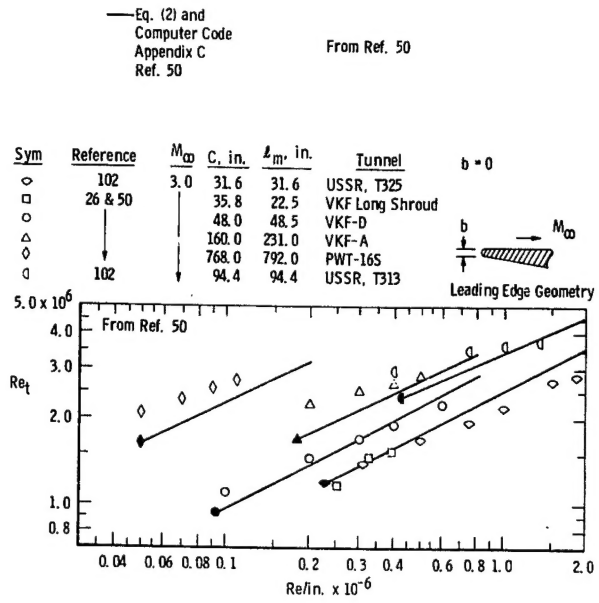

a. Flat plates, $M_\infty = 3.0$.

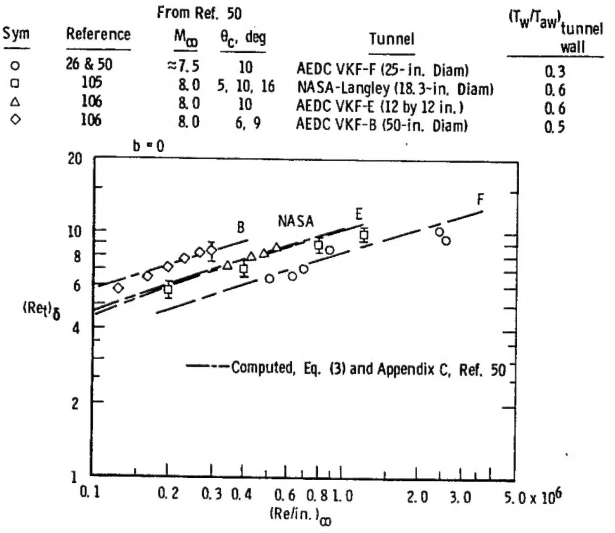

b. Sharp cones, $M_\infty \approx 8$.

Fig. 72. Variation of transition Reynolds numbers with tunnel size (Pate 1977).

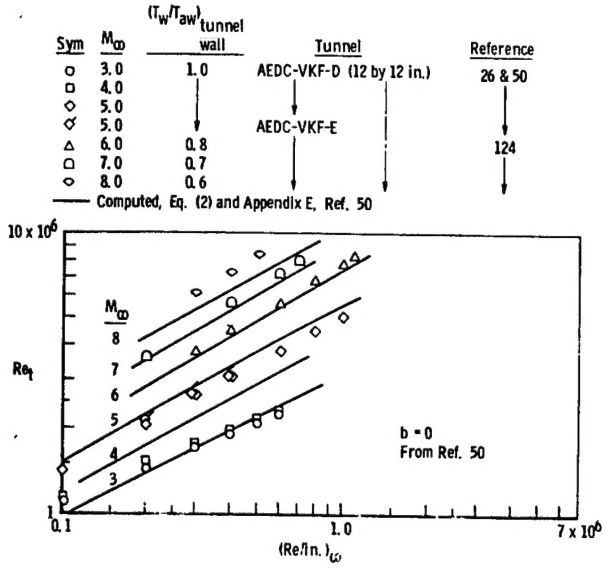

a. Small size tunnels.

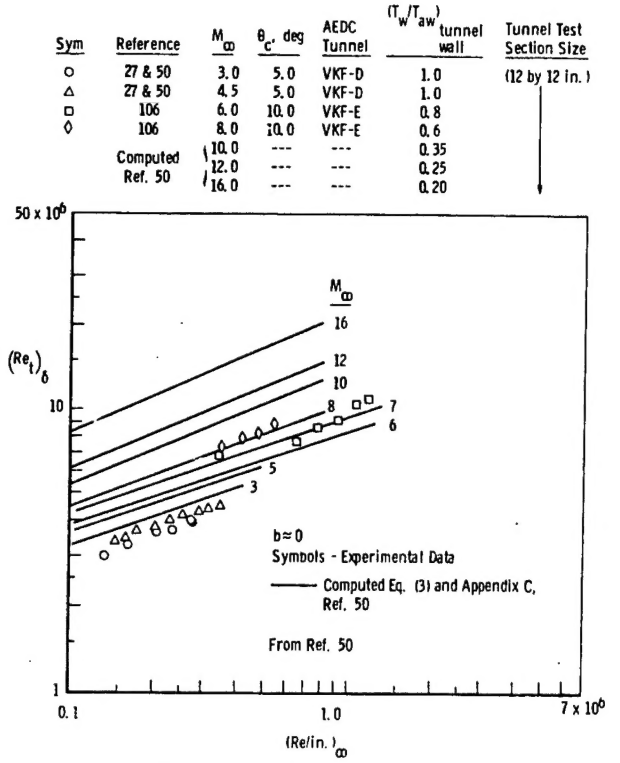

a. Small size tunnels.

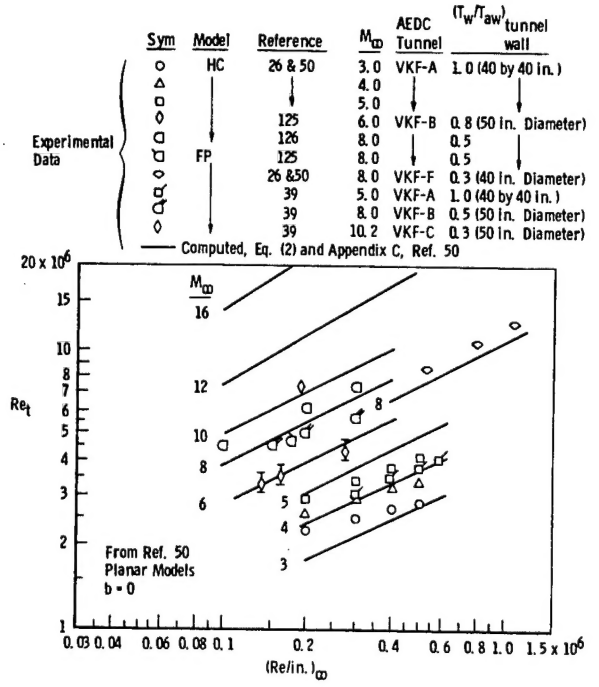

b. Large size tunnels.

Fig. 73. Effect of Mach number and unit Reynolds number on planar model transition data (Pate 1977).

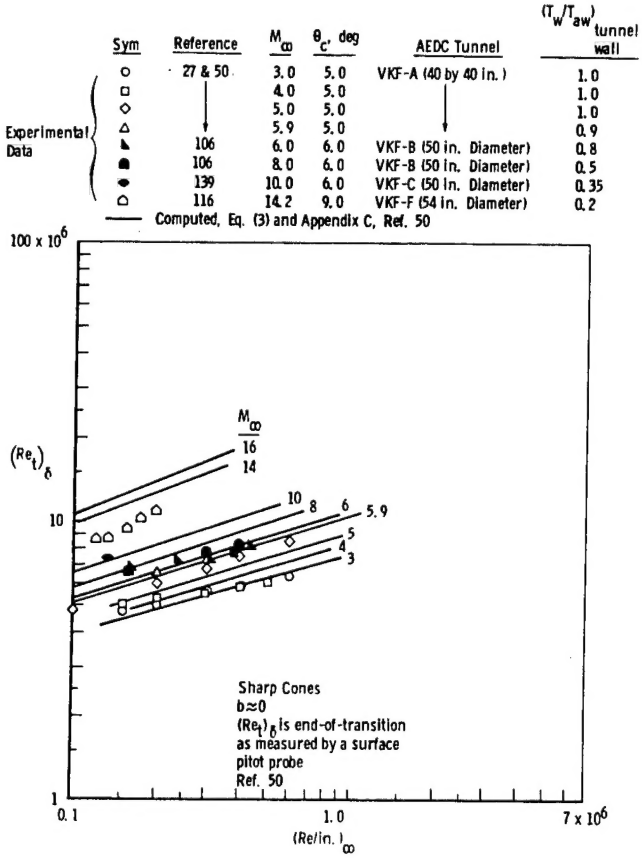

b. Large size tunnels.

Fig. 74. Effect of Mach number and unit Reynolds number on sharp-cone transition data (Pate 1977).

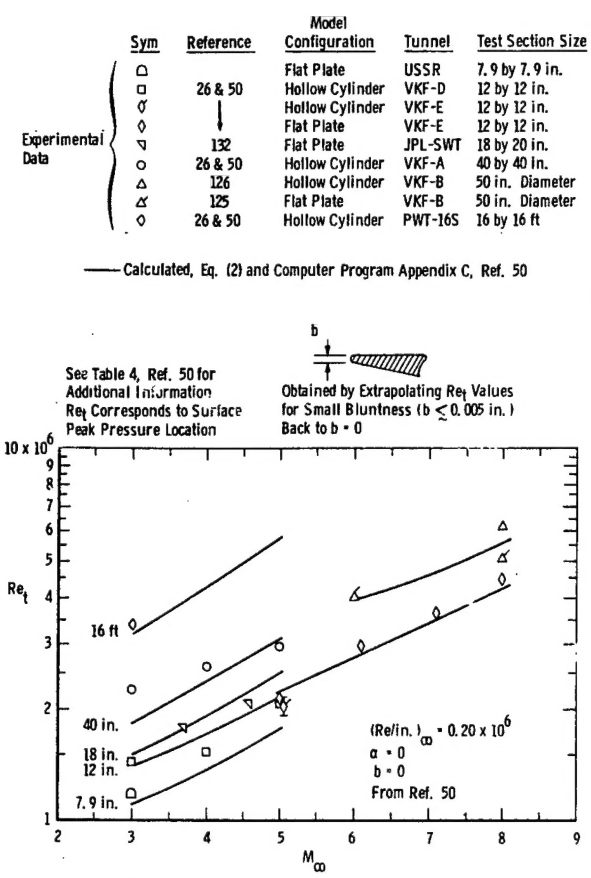

Fig. 75. Variation of planar model transition Reynolds numbers with tunnel size and Mach number (Pate 1977).

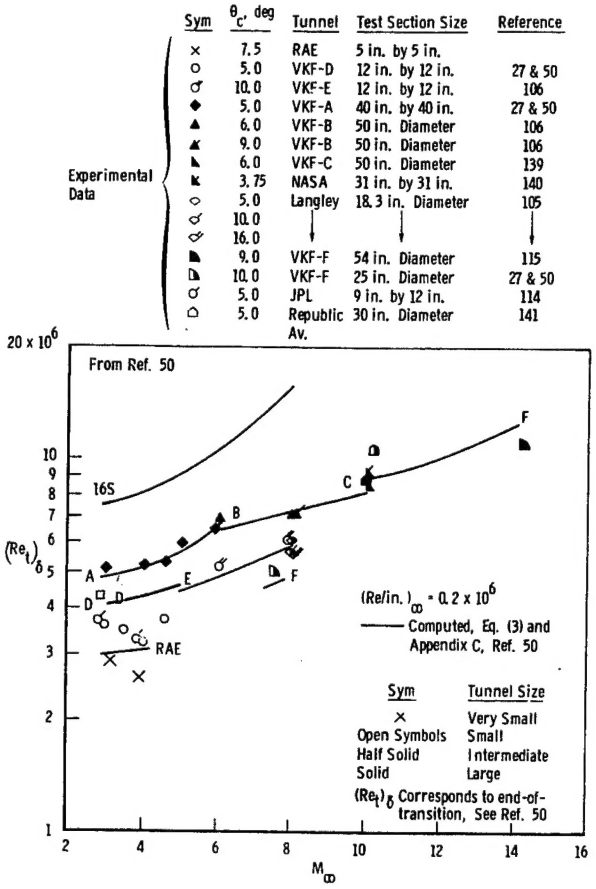

Fig. 76. Variation of sharp-cone transition Reynolds numbers with tunnel size and Mach number (Pate 1977).

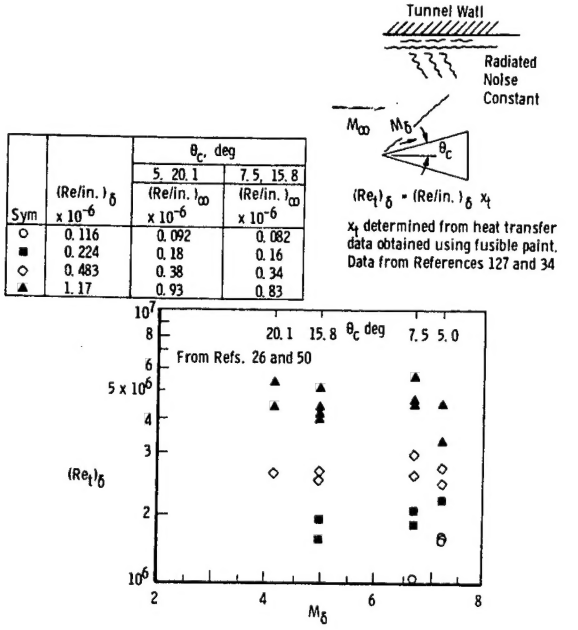

Fig. 77. Transition Reynolds number as a function of local Mach number for sharp cones, $M_\infty = 8$.

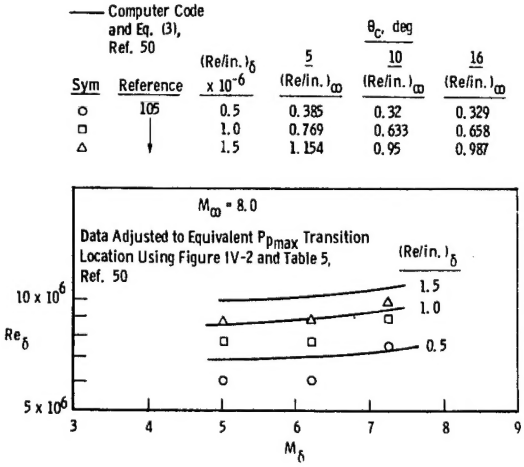

Fig. 78. Comparisons of predicted and measured $(Re_t)_\delta$ values.

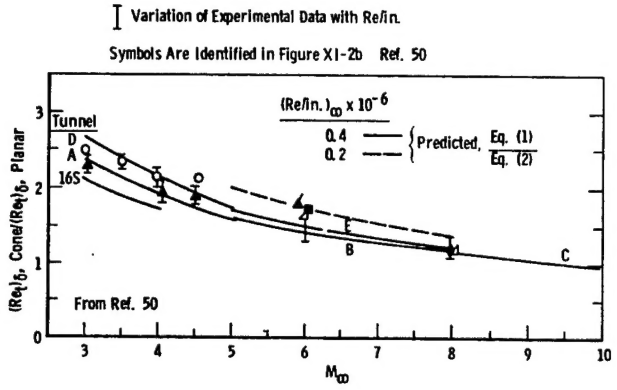

Fig. 79. Comparison of predicted and measured cone planar transition ratios (Pate 1977).

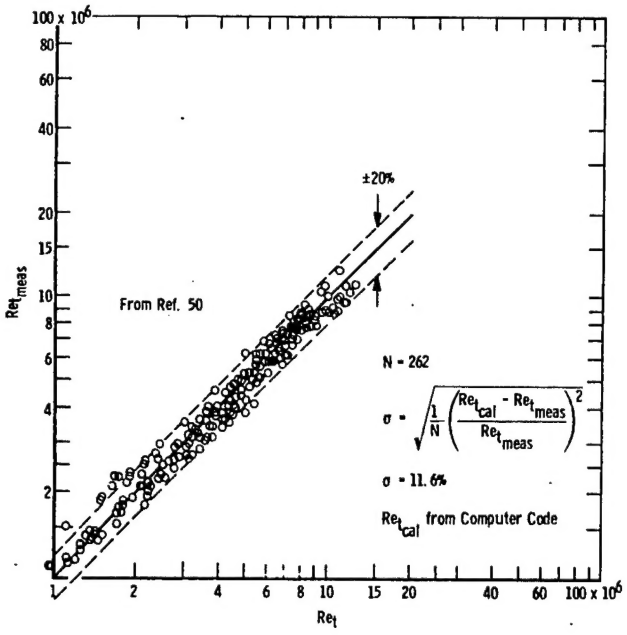

Fig. 80. Comparison of predicted and measured transition Reynolds number from Fortran Computer Program (Pate 1977).